

## ABSTRACT

Title of dissertation:                   ROLE OF SALT BRIDGES IN GROEL  
ALLOSTERY

Dong Yang, Doctor of Philosophy, 2014

Dissertation directed by:           Professor George H. Lorimer  
Department of Chemistry and Biochemistry

Chaperonin GroEL facilitates protein folding with two stacked back-to-back, identical rings and the “lid”, co-chaperonin GroES. The mis-folded/unfolded substrate protein (SP) adjusts the chaperonin cycling from an asymmetric to a symmetric cycle by catalyzing the release of ADP from the *trans* ring of GroEL, thus promoting the **R** to **T** allosteric transition. ATP binding to the SP bound ring promotes the association of a second GroES and subsequently a GroEL-GroES<sub>2</sub> “football” complex is formed as the folding functional form. However, ADP does release spontaneously, albeit at very slow rate, in the absence of SPs.

The intrinsic mechanism by which GroEL relaxes to the lower potential energy **T** state remains poorly understood. A network of salt bridges forms and breaks during the allosteric transitions of GroEL. Residue D83 in the equatorial domain forms an intra-subunit salt bridge with K327 in the apical domain, and R197 in the

apical domain forms an inter-subunit salt bridge with E386 in the intermediate domain. These two salt bridges stabilize the **T** state and break during the **T** to **R** state transition. Removal of these salt bridges by mutation destabilizes the **T** state and favors the **R** state of GroEL. These mutations do not alter the intrinsic ATPase activity of GroEL. However, the affinity for nucleotides becomes enhanced and ADP release is hindered such that SP cannot displace the equilibrium to the **T** state, as normally it does in the wild type. The exchange of ADP to ATP and association of a second GroES is compromised with the following GroEL-GroES<sub>2</sub> “football” formation is hindered. These mutations do not completely eliminate the **T** state, in the absence of nucleotide, as shown biochemically and by crystal structures. The biased allosteric equilibrium hampers the formation of folding active “football” complex as the mutant GroEL’s incompetency to revisit **T** state in the presence of nucleotide, but not due to the elimination of its **T** state. This study revealed the critical role of salt bridges in regulating the allosteric transitions of GroEL and conjugated formation of the “football” complex.

ROLE OF SALT BRIDGES IN GROEL ALLOSTERY

By

Dong Yang

Dissertation submitted to the Faculty of the Graduate School of the  
University of Maryland, College Park in partial fulfillment  
of the requirements for the degree of  
Doctor of Philosophy  
2014

Advisory Committee:  
Professor George H. Lorimer, Chair  
Professor Dorothy Beckett  
Professor David Fushman  
Professor Nicole LaRonde-LeBlanc  
Professor Edward Eisenstein

© Copyright by  
Dong Yang  
2014

## **DEDICATION**

This dissertation is dedicated to my family for forgiving my absence and supporting me for the past years!

## ACKNOWLEDGEMENTS

The first and most important person I would like to thank to, but never be able to express how grateful I am to my advisor, Dr. George Lorimer. Answered my phone call from the other side of the Pacific Ocean six years ago, he trusted me and admitted me as a graduate student in his lab. Only with his patience, enlightening, and encouragement that I could survive from the NMR class, the candidacy exam and all the rest of the adventure. He is always there, accessible, cheer leading the lab, and taking us to the Pasta Plus. It is my great honor to work with him as a graduate student, and all these made a wonderful memory as part of my life!

Dr. Dorothy Beckett, who is both physically and mentally strong, has always been my role model and helped me a lot in the sedimentation and ITC experiment. I deeply appreciate her help and criticism over the past.

Dr. Seth Thomas, the first taught me how to say “pipette”, and many other graduate students and post docs in this building had helped me on learning how to use all the instruments and experiment procedures and tricks. I would not achieve anything I get without your help! Dr. Irene Kiburu, Dr. Tinoush Moulaei, Dr. Maria Ingaramo, Dr. Poorni Adikaram, Chris Eginton, William Cressman, Dr. Yiling Luo, Dr. Bin Chen, Dr. Luigi Alvarado, Dr. Daoning Zhang and many others.

Charles Muller for always helps me in my English, from the first class notes, my proposal writing, till my dissertation editorial work! I won't survive in this foreign country without you! My lab members for all your help: technical support and intelligent discussion!

My advisory committee for taking their time to read my dissertation and guidance over the past years!

Finally to my family and friends here and back in China, for not complaining about my absence on many weddings including my only, dearest sister.

## TABLE OF CONTENTS

LIST OF FIGURES .....	viii
LIST OF TABLES .....	xi
LIST OF ABBREVIATIONS.....	xii
Chapter 1 Introduction and Specific Aims.....	1
1.1 The Physiological Importance of GroEL.....	1
1.2 The GroEL Architecture .....	2
1.3 The Asymmetric and Symmetric Chaperonin Cycle .....	5
1.4 The Nested Allostery and Allosteric Ligands.....	8
1.5 Two Folding Theories.....	10
1.5.1 Active Unfolding Mechanism.....	10
1.5.2 Passive Folding Mechanism .....	11
1.6 The Physiological Significance of A Double Ring Structure .....	12
1.7 Specific Aims.....	13
Chapter 2 General methods and experimental procedures .....	16
2.1 Site Directed Mutagenesis of GroEL.....	16
2.2 Protein Purification .....	17
2.3 The Modification of GroEL and GroES .....	18
2.4 Characterization of the FRET Pair.....	20
2.5 FRET Efficiency Study of GroELS Stoichiometry .....	25
2.6 Stop Flow FRET Kinetics.....	28
2.7 Steady-State FRET Kinetics .....	29
2.8 ATPase assay .....	30
2.8.1 Steady state ATPase Assay.....	30
2.8.2 Pre-steady State ATPase Assay .....	30
2.9 Pre-steady State ADP Release Assay .....	34
2.10 Electron Microscopy .....	36
2.11 MDH Activity and Encapsulation Measurement.....	37
2.12 Isothermal Titration Calorimetry Study of ADP Binding to GroEL .....	40
2.13 <i>In vivo</i> Study of GroEL and Its Variants in Supplementing Cell Growth .....	41
Chapter 3 Characterization of GroEL <sup>DM</sup> mutant.....	43
3.1 Introduction.....	43
3.1.1 Allosteric Transitions during the Complete Chaperonin Cycle.....	43
3.1.2 Allosteric Effectors during the Complete Chaperonin Cycle .....	45
3.2 Structural Characterization of GroEL <sup>DM</sup> Mutant .....	48
3.2.1 Native-PAGE Analysis of GroEL Oligomeric State .....	49
3.2.2 Electron Microscopy Study.....	50
3.2.3 Analytical Ultracentrifugation .....	51
3.2.4 Mass Spectrometry.....	54
3.3 Steady State ATPase Assay .....	56



3.3.1 Steady State ATPase Assay as of [ATP] under Standard Condition .....	56
3.3.2 Steady State ATPase Assay as of [ATP] at Altered Condition .....	59
3.3.3 Steady State ATPase Assay as of [SP] .....	62
3.4 Pre-steady state ATPase Analysis.....	64
3.4.1 Measurement of Pi release from GroEL-GroES <sub>1</sub> complex.....	65
3.4.2 Measurement of ADP Release from GroEL-GroES <sub>1</sub> Complex.....	66
3.5 GroES dissociation kinetics from GroEL <sup>WT</sup> and GroEL <sup>DM</sup> .....	69
Chapter 4 Characterization of “Football” Complex-its Formation and Allosteric Regulation .....	74
4.1 Introduction.....	74
4.2 Calibration of FRET Based System to Determine GroELS Stoichiometry .....	76
4.3 FRET Efficiency Study of GroELS Complex .....	79
4.3.1 FRET Efficiency of GroELS Complex in the Presence of ATP/ADP·BeF <sub>x</sub> .....	79
4.3.2 Titration of GroELS Complex by SPs .....	80
4.3.3 Titration of GroELS Complex by Potassium Ions.....	82
4.4 The Mechanism of Formation of “Football” Complex.....	85
4.4.1 The Association of GroES to apo-GroEL.....	85
4.4.2 The Hydrolysis of ATP during the GroES Association to apo-GroEL <sup>WT</sup> .	87
4.4.3 The Association of GroES to GroELS Resting State Complex .....	88
4.4.4 The Association of GroES to GroELS Acceptor State Complex .....	90
Chapter 5 The “Football” Dynamics and Its Role in Chaperonin Assisted Protein Folding .....	94
5.1 Substrate Case I-Rubisco .....	95
5.1.1 The Interaction between Rubisco and GroEL.....	95
5.1.2 The Interaction between Rubisco and “Football” Complex .....	99
5.2 Substrate Case II-Malate Dehydrogenase.....	100
5.2.1 The Refolding of MDH by GroELS Complex.....	100
5.2.2 The Encapsulation of MDH by GroELS Complex .....	101
5.2.3 The Interaction between MDH and “Football” Complex .....	102
5.3 Substrate Case III- $\alpha$ -LA.....	104
5.4 The Dynamics of “Football” Complex .....	106
5.4.1 The “Football” GroES is Exchanging with Others.....	106
5.4.2 The SP Encapsulated in “Football” is Exchanging with Others .....	107
Chapter 6 The Role of Salt Bridges in The Formation of the “Football” Complex .	112
6.1 The Failure of SP Induced “Football” Complex Formation .....	112
6.1.1 Starting from apo- GroEL <sup>DM</sup> : EM Analysis .....	112
6.1.2 Analysis Starting from apo-GroEL <sup>DM</sup> : .....	114
6.1.3 Starting from GroEL <sup>DM</sup> -GroES <sub>1</sub> Complex .....	117
6.2 The Decreased Binding towards SP.....	118
6.3 The Decreased Rate of Refolding SP.....	121
6.4 The Decreased Encapsulation of SP .....	123
6.5 The Altered Binding of ADP to GroEL.....	124

Chapter 7 <i>In vivo</i> Study of GroEL in Supplementary Cell Growth.....	127
7.1 The <i>in vivo</i> Study of GroEL <sup>DM</sup> and GroEL <sup>D398A</sup> .....	128
7.2 The <i>in vivo</i> Study of GroEL <sup>K105A</sup> .....	130
Chapter 8 Summary .....	132
8.1 GroEL-GroES <sub>2</sub> Symmetric “Football” Complex is the Folding Functional Form .....	134
8.2 Salt Bridges as an Intrinsic Resetting Mechanism in the Chaperonin Cycle..	137
REFERENCES .....	141

## LIST OF FIGURES

Figure 1-1 Architecture of GroEL-GroES <sub>2</sub> “Football” Complex. ....	3
Figure 1-2 The Asymmetric and Symmetric Chaperonin.....	6
Figure 1-3 Allosteric Ligands of GroEL.....	9
Figure 2-1 Quantification of F5M labelled GroES with SDS-PAGE.....	19
Figure 2-2 FRET spectrum of IAEDANS and F5M.....	20
Figure 2-3 The Architecture of GroEL-GroES <sub>1</sub> Complex and Its Labelling Positions. .....	21
Figure 2-4 Fluorescence Spectrum between GroEL and GroES. ....	23
Figure 2-5 Fluorescence Change upon Mixing with Different GroEL and GroES. ...	25
Figure 2-6 FRET titration of GroES <sup>F5M</sup> to GroEL <sup>IAEDANS</sup> .....	26
Figure 2-7 Characterization of the Dynamics of PBP <sup>MDCC</sup> .....	32
Figure 2-8 Characterization of the Kinetics of PBP <sup>MDCC</sup> .....	33
Figure 2-9 Characterization of the Coupling Enzyme System. ....	35
Figure 2-10 Measurement of MDH Encapsulation during Its Refolding by GroEL. .	40
.....	44
Figure 3-1 Pre-steady State Assay with the Acceptor State Complex.....	44
Figure 3-2 Salt bridges D83-K327 and R197-E386 Involved in the T to R transition of GroEL. ....	47
Figure 3-3 Native PAGE Evaluation of GroEL.....	50
Figure 3-4 Negative Stain Electron Microscopic of GroEL.....	50
Figure 3-5 Sedimentation Equilibrium Analysis of GroEL.....	52
Figure 3-6 Sedimentation Velocity Analysis of GroEL <sup>WT</sup> .....	53

Figure 3-7 Mass Spectrometry Analysis of GroEL <sup>WT</sup> . .....	55
Figure 3-8 Steady State ATPase of GroEL <sup>WT</sup> and GroEL <sup>DM</sup> . .....	58
Figure 3-9 Steady State ATPase of GroEL <sup>DM</sup> at Lower Subunit Concentration. ....	60
Figure 3-10 Steady State ATPase of GroEL <sup>DM</sup> at Lower K <sup>+</sup> Concentration. ....	61
Figure 3-11 Steady State ATPase of GroEL <sup>DM</sup> and GroEL <sup>WT</sup> as function of [SP]. ...	63
Figure 3-12 Pre-steady State ATPase activity of GroEL <sup>WT</sup> and GroEL <sup>DM</sup> . .....	66
Figure 3-13 Pre-steady State ADP Release from GroEL <sup>WT</sup> and GroEL <sup>DM</sup> . .....	67
Figure 3-14 Dissociation of GroES from the GroELS Complex. ....	71
Figure 4-1 Electron Microscopy of GroELS Complexes. ....	77
Figure 4-2 Steady State FRET Titration of GroES <sup>F5M</sup> to GroEL <sup>WT-IAEDANS</sup> . .....	79
Figure 4-3 Steady State FRET Titration of SP to GroELS complex. ....	81
Figure 4-4 Steady State FRET Titration of K <sup>+</sup> to GroELS complex. ....	83
Figure 4-5 Pre-Steady State FRET Formation of GroELS Complex. ....	86
Figure 4-6 Pre-Steady State ATP Hydrolysis during GroELS Complex Formation. .	87
Figure 4-7 GroELS Complex Formation of from the Resting State Complex. ....	89
Figure 4-8 GroELS Complex Formation of from the Acceptor State Complex. ....	91
Figure 4-9 SP Switches The Chaperonin from Asymmetric to Symmetric Cycling. .	92
Figure 5-1 FRET Spectrum between Trp on Rubisco and IAEDANS on GroEL. ....	96
Figure 5-2 FRET Indicating Interaction between Rubisco and GroEL <sup>IAEDANS</sup> during Its Refolding. ....	98
Figure 5-3 MDH Activity and Encapsulation during Its Refolding by GroEL. ....	101
Figure 5-4 MDH Stimulated “Football” Complex during Its Refolding by GroEL. .	102
Figure 5-5 $\alpha$ -LA Switched Asymmetric Cycle to Symmetric Cycle. ....	105

Figure 5-6 Dynamics of GroES in The “Football” Cycle. ....	107
Figure 5-7 FRET between $\alpha$ -LA <sup>IAEDANS</sup> and GroEL <sup>F5M</sup> . ....	108
Figure 5-8 Dynamics of SP in The “Football” Cycle. ....	109
Figure 5-9 SP Dissociation from The “Football” at Different Temperature. ....	110
Figure 6-1 Electron Microscopy of GroEL <sup>DM</sup> -GroES Complexes. ....	113
Figure 6-2 Steady State FRET Titration of GroES <sup>F5M</sup> to GroEL <sup>DM-IAEDANS</sup> . ....	114
Figure 6-3 Pre-Steady State GroEL <sup>DM</sup> -GroES Complex Formation and ATP Hydrolysis. ....	116
Figure 6-4 FRET Spectrum between Trp on $\alpha$ -LA and IAEDANS on GroEL. ....	119
Figure 6-5 FRET Titration of $\alpha$ -LA to GroEL <sup>IAEDANS</sup> at Various ADP Concentration. .....	120
Figure 6-6 MDH Activity during Its Refolding by GroEL <sup>DM</sup> . ....	122
Figure 6-7 Measurement of MDH Encapsulation during Its Refolding by GroEL <sup>DM</sup> . .....	123
Figure 6-8 ITC Measurement of ADP Binding to GroEL. ....	125
Figure 7-1 Map of Plasmid pTrc99A. ....	127
Figure 7-2 Complementary Growth of GroEL Variant at Different Temperature. ..	128
Figure 7-3 Complementary Growth of GroEL <sup>K105A</sup> at Different Temperature. ....	130

## LIST OF TABLES

Table 2-1 Mutation Primers and Sequencing Primers Used. ....	17
Table 3-1 Parameters in Sedimentation Equilibrium Analysis. ....	52
Table 3-2 Half-Life of GroES Dissociation from the “Bullet” Complex. ....	72
Table 6-1 The Binding Constant Derived of $\alpha$ -LA to GroEL. ....	120
Table 6-2 The Binding Constant of ADP to GroEL Derived from ITC. ....	125

## LIST OF ABBREVIATIONS

Å	angstroms
ADP	Adenosine diphosphate
Amp	Ampicillin
AMP-PNP	5'-adenylyimidodiphosphate
ATP	Adenosine triphosphate
DEAE	diethylaminoethyl
DM	double mutant of D38A and R197A on GroEL
DMSO	dimethylsulfoxide
DNA	deoxyribonucleic acid
DTT	dithiothreitol
<i>E. coli</i>	<i>Escherichia coli</i>
EDTA	ethylenediaminetetraacetic acid
EL	GroEL protein
ES	GroES protein
F5M	fluorescein-5-maleimide
FRET	förster resonance energy transfer
IAEDANS	5-((((2-iodoacetyl)amino)ethyl)amino)naphthalene-1-sulfonic acid
IPTG	isopropyl-β-D-thiogalactopyranoside
kDa	Kilodaltons
KNF	Koshland-Nemethy-Filmer
LB	Luria-Bertani broth

LDH	lactate dehydrogenase (bovine)
MDCC	7-Diethylamino-3-(((2-aleimidyl)ethyl)amino)carbonyl)coumarin
MDH	malate dehydrogenase (pig heart mitochondrial)
ms	milliseconds
MW	molecular weight
MWC	Monod-Wyman-Changeux
NADH	Nicotinamide adenine dinucleotide
Ni-NTA	nickel-nitrilotriacetic acid
nm	nanometers
NMR	nuclear magnetic resonance
PAGE	polyacrylamide gel electrophoresis
PBP	phosphate binding protein
PCR	polymerase chain reaction
PEP	Phosphoenol pyruvate
PK	Pyruvate kinase (bovine)
<b>R</b>	Relaxed state
Rubisco	Ribulose biphosphate carboxylase
SDS	Sodium dodecyl sulfate
SP	Substrate protein
SR1	SR1 protein, or plasmid coding this SR1 protein
<b>T</b>	Tense state
TEMED	N,N,N',N'-tetramethylethylenediamine
Tet	tetracycline



Tris	Tris (hydroxymethyl) aminomethane
U	units of enzyme activity
wt/WT	Wild type

## Chapter 1 Introduction and Specific Aims

In a living organism, the genetic information transcribed from DNA into RNA has to be translated into proteins in order to fulfill its biological function. Many studies regarding the function of the ribosome demonstrate that the synthesis of a polypeptide chain is a chemically streamlined process with high fidelity. The product of ribosomal synthesis is a linear, one-dimensional polymer with its pre-defined spatial, three-dimensional structure inherited from its gene sequence<sup>1</sup>. With or without modification, the nascent polypeptides have to rotate each bond and form hydrogen bonds<sup>2</sup> as well as salt bridges in between its amino acid residues before it reaches the marginally stable structure<sup>3</sup>. Even though the destination of the final structure is clear and thermodynamically favored, the journey is full of traps and energy minima<sup>4,5</sup>. If a nascent polypeptide forms an improper fold it still has the opportunity to be refolded by chaperones before proteolysis, allowing the cell to avoid an otherwise energy wasting process<sup>5</sup>.

### 1.1 The Physiological Importance of GroEL

There are many types of chaperones in the cytosol that help fold nascent peptides<sup>6,7</sup>. GroEL, from *Escherichia coli* (*E. coli*), is one of the most well studied type I molecular chaperones which mediates the folding of many proteins including ribulose-1,5-bisphosphate oxygenase-carboxylase<sup>8,9</sup>, malate dehydrogenase<sup>10</sup>, rhodanese<sup>11</sup>, citrate synthase<sup>12</sup>,  $\alpha$ -glucosidase<sup>13</sup> and glutamine synthase<sup>14</sup>. When new polypeptides are synthesized at high cellular concentrations they are at risk for aberrant folding and aggregation<sup>15</sup>. The folding mechanism of many proteins is

described by an energy landscape profile, where there are many energy minima, and the most profound one is the properly folded-native state<sup>16</sup>. Some mis-folded proteins might escape the traps by thermal energy fluctuations provided that the local minima are not too deep<sup>4</sup>. However, if they are unable to escape on their own and GroEL is absent most mis-folded proteins will remain in the local minima. Such a scenario can lead to either hazardous aggregation, which has is associated with many neural degenerative diseases in both humans and animals<sup>17</sup>, or ubiquitin mediated proteolysis which ends up as a waste of biological energy<sup>18</sup>. GroEL apparently assists mis-folded proteins change the folding landscape of its SPs, not by lowering the energy barrier of the folding intermediate, but by providing energy to the trapped proteins<sup>5,19,20</sup>. Details of this process will be discussed in the folding mechanism section later in this section.

## **1.2 The GroEL Architecture**

GroEL is composed of two back-to-back stacked heptamer rings, where each contains seven identical monomers of 57 kDa<sup>21</sup>. GroES, which is the co-chaperonin of GroEL, is a dome like heptamer of seven identical monomers of 10 kDa (figure 1-1, A). GroES binds on top of the GroEL ring, forming a cavity (the so called Anfinsen Cage) where the SPs can fold<sup>22,23</sup>.

In each of the GroEL monomers, there are three domains functioning differently while inherently connected, as shown in Figure 1-1. The large  $\alpha$ -helical equatorial domain (E domain, residues 6 to 133 and 409 to 523) is the base from which the intermediate domain (I domain, residues 134 to 190 and 376 to 408) and apical domain (A domain, residues 191 to 375) extend<sup>22,24</sup>. The equatorial domain is

also the site where inter-ring communication takes place<sup>25,26</sup>. Among all the conformational changes, the equatorial domain exhibits the least conformational change<sup>24</sup>. The stacking interactions that keep the two equatorial domains together are accomplished by several amino acid residuals in the E domain<sup>27</sup> (figure 1-1, B). Disrupting these amino acids compromises the stability of the whole chaperonin and causes it to break apart into two single rings<sup>27</sup>. Other important amino acid residues (Arg13, Ala126 and possibly Asp115) in the E domain help transmit the inter-ring signals, and mutations at these positions alter the allosteric behavior of the chaperonin<sup>26</sup>.

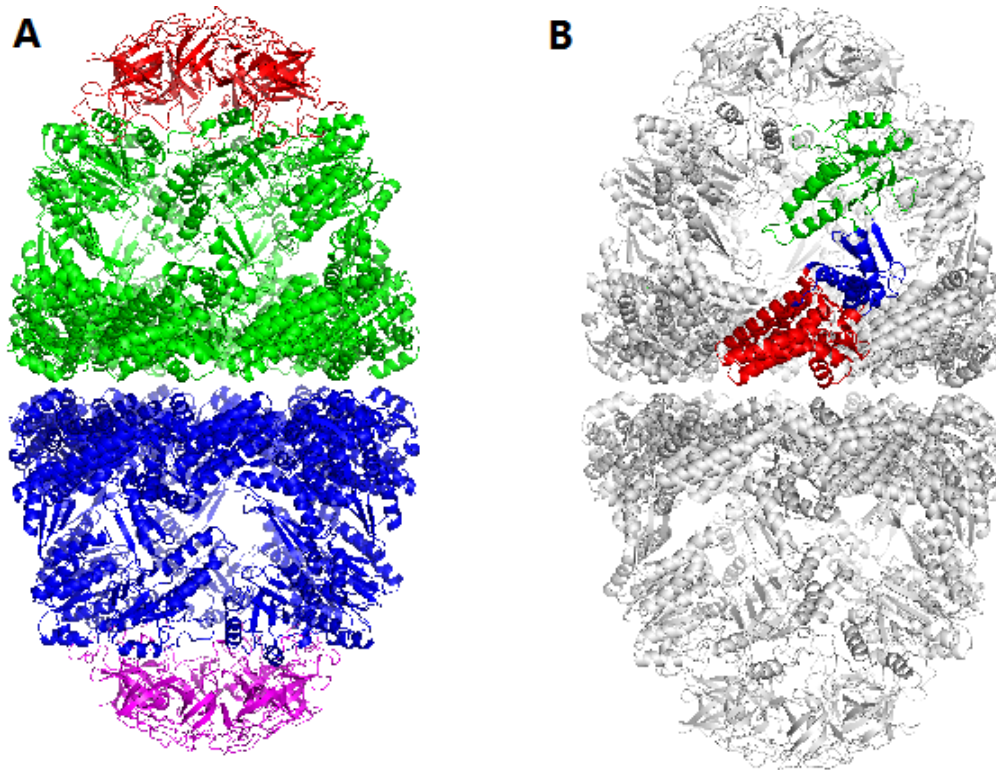


**Figure 1-1 Architecture of GroEL-GroES<sub>2</sub> "Football" Complex.** **A)** The symmetric GroEL-GroES<sub>2</sub> complex is composed of two GroES (red and magentas) molecule with one GroEL molecule where the two rings of GroEL (green and blue) are identical. **B)** Each subunit in one GroEL is composed of three domains: apical domain (green), intermediate (blue) and equatorial domain (red). This figure is made from a PDB file that has not published yet<sup>28</sup>.

The opening of the central cavity is formed by the apical domain (residues 191 to 376). This domain offers hydrophobic sites (a groove between two central helices H and I, figure 1-1, B) where SP<sup>29,30</sup> and the mobile loop of GroES can bind<sup>31</sup>. This apical surface can recognize a range of local structures such as  $\alpha$ -helices, extended strands, and  $\beta$ -hairpins<sup>29,32</sup>. Seven of these sites from one ring offer a smooth, hydrophobic surface that can bind to exposed hydrophobic regions in the SP in a multivalent fashion that are normally buried in their native folded state.<sup>33</sup>

The intermediate domain (residues 134 to 190 and 377 to 408, figure 1-1 B) is formed by three connected  $\alpha$ -helices and three  $\beta$ -strands which connect the E domain and A domain respectively. Within this domain seven subunits in one ring interact with each other via salt bridges (E386 with R197 forming inter-subunit, inter-domain salt bridge, E386 and K80 forming intra-subunit, inter-domain salt bridge) which are responsible for the concerted movement of all subunits in one ring<sup>34-36</sup>. Through hinge movement at its top and bottom, the intermediate domain is able to rotate down into the nucleotide binding pocket at the E domain, which brings the base D398 close enough to allow for ATP hydrolysis<sup>37</sup>. At its top, the rotation brings the opening of the A domain, where the distance of helix H and I between neighboring subunits is markedly increased<sup>24</sup>.

GroES, also called the co-chaperonin, is a heptamer of identical subunits. Each of the subunits is composed of a core  $\beta$ -barrel and two hairpin loops with a MW of 10 kDa. These seven monomers form a lid like structure that fits the apical domain of GroEL after its binding with nucleotide. GroES binds with GroEL via its mobile loop interaction with helix H and I of apical domain, and considered to compete with

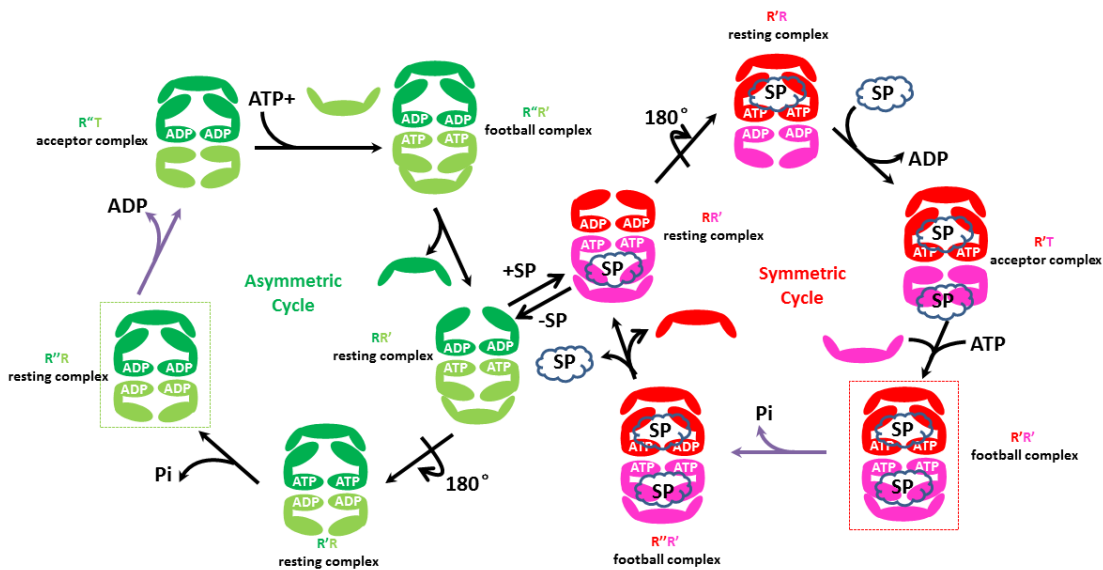
SP for binding to GroEL since these two helices are also the SP binding site<sup>38</sup>. Vectorial displacement of SP by GroES causes the release of SP into the central cavity of GroEL.

### 1.3 The Asymmetric and Symmetric Chaperonin Cycle

During the chaperonin cycle GroEL undergoes large rigid body, conformational changes driven by ATP<sup>24</sup>. When there is no nucleotide bound to GroEL, both of the heptamer rings are in the “closed” (**T**) state, usually designated as **TT** for two rings (figure 1-2). This state is the SP acceptor state. After the binding of SP via multivalent hydrophobic interactions, seven nucleotides cooperatively bind to one ring following the binding of GroES<sup>39</sup>, which is then referred to as the *cis* ring while the opposite one is *trans* ring. Association of ATP drives the conformational change of these subunits to the ‘open’ (**R**) state, forming an **RT** state of the *cis/trans* ring. This **T** to **R** transition exposes the hydrophobic residues at the apical domain of the *cis* ring outward, which offers a binding site for GroES (competing with the SP for these sites), and eventually promotes the dissociation of the SP from the binding site and into the “Anfinsen cage”<sup>30</sup>. Once the SP is encapsulated into the cylindrical cavity of GroEL, the binding of GroES on the *cis* ring introduces a conformational change from **RT** to **R'T**. ATP binding further drives the conformation from **R'T** to **R''T**. Binding of ATP to the *trans* ring triggers the release of GroES from the *cis* ring and the disassembly of the GroES<sup>cis</sup>-[ADP]<sub>7</sub>- [GroES] complex (square here indicate the ADP/GroES, or Mg<sup>2+</sup>, is not free to exchange)<sup>22,40</sup>. The newly ATP bound ring becomes a *cis* ring and the opposite one becomes the *trans* ring (**R''T** to **TR**), starting a new chaperonin cycle<sup>41</sup>. These two rings are acting almost in phase with each

other in the presence of SP<sup>42,43</sup>. In the absence of SP (figure 1-2), the **R''R** resting complex is the major species while the ADP release from this complex is the rate limiting step. SP catalyzes the release of ADP and promotes the formation of the symmetric GroEL-GroES<sub>2</sub> “football” complex that populates. GroEL is cycling in the symmetric cycle while ATP hydrolysis becomes the rate limiting step<sup>43</sup>.

**Figure 1-2 The Asymmetric and Symmetric Chaperonin.** ATP binding promotes GroEL from **T**



state to **R** state and following binding of GroES allows the **R** to **R'** state transition. Hydrolysis of ATP makes the **R'** to **R''** transition while discharge of GroES is followed by the **R''** to **R** transition. Eventually release of ADP yields the **R** to **T** transition. In the absence of SP, the resting complex populates (green box) while the ADP release is the rate limiting step (purple arrow). In the presence of SP, the “football” complex populates (red box) while the ATP hydrolysis is the rate limiting step (purple arrow).

These transitions are accompanied by large conformational changes. Initially in the **T** to **R** transition, the helices F and M in the I domain tilt downward ~15° and several residues on these helices interact with the nucleotide-binding site in the E domain, thus creating a tight (closed) nucleotide binding pocket<sup>22</sup>. Within the A domain of the *cis* ring, which twists ~25° anticlockwise, the helices K and L tilt ~30°

while helices H and I elevate  $\sim 10^\circ$ . E386 on the tip of the M helix forms inter-subunit salt-bridges with R284, R285, and R197, which are disrupted in the transition to **R** state and are accompanied by a new salt-bridge between E386 and K80. The **T** to **R** transition relies mainly on the formation and breakdown of salt bridges, even though some remain intact during this transition (E409-R501, E408-K498, and E409-K498), which are thought to be important for enhancing intra-ring cooperativity and for stability of the structure<sup>44</sup>. The movement of the A domain exposes the SP binding site and binding interface for GroES. Upon binding of GroES, the A domain further tilts about  $50^\circ$  and  $115^\circ$  clockwise twist, doubling the volume of the central cavity. Other residues, notably 357-361 which are completely exposed on the exterior surface in the **T** state, move to the interior surface in the **R** state<sup>24</sup>.

Upon GroES binding and ATP hydrolysis, GroEL moves from the **R** state to **R'**, and then **R''** state. Helices F and M tilt by an additional  $10^\circ$  followed by helices K and L tilting another  $40^\circ$ . This movement places the K and L helices entirely inside the cavity of the **R''** state<sup>24</sup>. This results in number of polar and charged residues lining in the inner wall of the central cavity<sup>22</sup>. This is also accompanied by the formation of an inter-domain K80-D359 salt-bridge which further orients the position of the wing of domain A. To relieve the strain introduced by this transition, the A domain is forced to undergo a  $90^\circ$  clockwise rotation and  $40^\circ$  upward movement. Helices H and I, the SP binding site, are then oriented in the upward direction which reveals the binding site of the mobile loop from GroES. It is believed that hydrophobic interactions between the SP binding sites and GroES drive the **R** to **R''** transition.<sup>45,46</sup> The salt bridge formed between E409 and R501, which closes the



nucleotide binding site is maintained during all allosteric transitions, effectively preventing the free exchange of bounded ADP with ADP in solution<sup>47</sup>.

Salt bridges play important roles in the allosteric cycling switch from one state to another either by forming new pairs favoring the next state, or by reverting back to the original conformation. The nature of the electrostatic interactions associated with salt bridges has caused some to regard function as being a static phenomenon. Actually, the active role of salt bridges in balancing between different forces during allosteric transitions is investigated in this thesis.

#### **1.4 The Nested Allostery and Allosteric Ligands**

The two types of allostery often seen among bio-molecules are either the concerted, MWC (Monod-Wyman-Changeux) model<sup>48</sup>, or the sequential, KNF (Koshland-Nemethy-Filmer) model<sup>49</sup>. Allostery exists in GroEL in a hierarchy way mirroring the GroEL structure. Positive cooperativity, in the MWC-interaction manner, between the subunits of a rings (intra-ring). This first level of allostery describes each ring in an equilibrium of **T** and **R** states, and the conformational change of all the seven subunits in one ring is concerted. That is, all the rings are either in **t<sub>7</sub>** or **r<sub>7</sub>** state. As the ligand concentration increases, e.g. ATP, the equilibrium among all the rings is shifted to **R/r<sub>7</sub>** state. Negative cooperativity, in the KNF-interaction manner, exists between subunit of different rings in one GroEL molecule. This second level of allostery describes the transition of **TT** to **TR**, and then to **RR**. That is, as the ligand concentration increases, the transition of the first ring in a GroEL molecule from **T** to **R** disfavors the transition of the second ring to the **R** state. This is the so called nested model, in which MWC-type allostery is nested

inside KNF-type allostery, and not only mirrors the structure of GroEL, where one ring is nested in a stacked two ring structure, but also explains the two transitions of initial ATPase activity as a function of ATP<sup>39,50</sup>.



**Figure 1-3 Allosteric Ligands of GroEL.** Nucleotide binds, preferentially but non-exclusively, to the R state GroEL while SP binds, preferentially but non-exclusively, to the T state GroEL. GroES, however, binds exclusively to the R state GroEL.

Without positive intra-ring cooperativity in GroEL, steric interference would arise when one subunit undergoes **T** to **R** transition while its adjacent subunit stays in the **T** state<sup>24</sup>. Many elements, from biological co-chaperonin GroES to denatured polypeptide SP, to inorganic small molecules as ATP, ADP, and K<sup>+</sup>, affect the allosteric state and transition of GroEL in various ways<sup>51,52</sup>. Generally, nucleotide binding to GroEL drives GroEL from **T** state to **R** state due to the fact that although nucleotides bind to both **T** and **R** states, the **R** state has higher affinity towards the nucleotide binding. However, there are differences between ADP binding and ATP binding to GroEL: ADP binds to GroEL in a non-cooperative manner<sup>53</sup>, and only one GroES can bind to the ADP occupied GroEL tetradecamer; ATP binds to GroEL in cooperative manner, and two GroES could bind to one GroEL tetradecamer without necessarily hydrolyzing ATP. K<sup>+</sup> affects the allostery of GroEL by enhancing the affinity of nucleotide, e.g. the affinity of ATP to **R** state GroEL at 100 mM K<sup>+</sup> is about twenty folds as higher when the concentration of K<sup>+</sup> is only 1 mM<sup>51</sup>.

The binding of ATP promotes the association of GroES, which in turn promotes the **R** to **R'** transition of GroEL accompanied by a large conformational change at the apical domain<sup>22</sup>. GroES is not released after some hydrolysis of ATP on the *cis* ring and binding of seven other ATP molecules on the *trans* ring<sup>54</sup>. Thus GroES favors the **R** state (including the **R'** and **R''** state) of GroEL. The SP, on the other hand, favors the **T** state of GroEL since it has a higher affinity towards the SP<sup>52</sup>. Binding of SP to the **R** state GroEL dramatically pushes equilibrium to the **T** state, which leads to the release of ADP and exchange with ATP<sup>43</sup>.

## 1.5 Two Folding Theories

### 1.5.1 Active Unfolding Mechanism

After the SP binds with helix H and I, ATP binds to the equatorial domain of GroEL. This nucleotide binding induces a large, rigid body movement that leads to several Å moving apart of the peptide binding site in GroEL<sup>5</sup>. SP bound to these helices would become stretched as these subunits are moving apart from each other, and this is the so called active unfolding mechanism<sup>45,55,56</sup>. The experimental evidence of this active unfolding was revealed by monitoring the fluorescence of fluorescently labeled Rubisco as a SP<sup>57,58</sup>. The binding of ATP to the substrate bound ring of GroEL induces a rapid, forced unfolding of Rubisco indicated by a sharp increase of fluorescence<sup>59,60</sup>.

Crosslinking experiments in our lab have also indicated that the active unfolding of the SP is linked to the **T** to **R** transition of GroEL<sup>61</sup>. Based on the evidence that GroEL cross linked in the **T** state has a higher ATPase activity and SP stimulate the ATPase activity of GroEL, it has been proposed that SP mimics the

tether that holds GroEL in the **T** state. However, if the substrate is a short peptide not long enough to span the two adjacent subunits, GroEL undergoes the **T** to **R** transition freely as ATP binds. As the apical domain moves during the **T**→**R**→**R'** transition, SP is stretched and work is done on it<sup>45</sup>. The SP will be continuously stretched until the affinity of the SP decreases as more and more SP binding sites get buried during the motion. Eventually the now-unfolded SP is released into the central cavity as the apical domain is covered by GroES and cannot dissociate into solution. This active folding on the SP greatly increases its free energy and permits escape from local minima of the folding landscape<sup>4</sup>.

Computational work shows that the stretching force imparted by the twisting apical domain is about 20 pN, which is sufficient for partial unfolding of a single domain protein<sup>19</sup>. Atomic force microscopy measurements have also confirmed the force between GroEL and two representative SPs is 130 pN for  $\beta$ -lactamase and 20 pN for citrate synthase<sup>62</sup>.

### *1.5.2 Passive Folding Mechanism*

After being captured by GroEL and confined in its central cavity of GroEL, the SP is isolated from the molecularly crowded environment of cytosol. The volume of the central cavity is enlarged from 85,000 Å<sup>3</sup> to 175,000 Å<sup>3</sup> which is more than enough to accommodate a SP of MW 70 kDa<sup>22</sup>. Moreover, the enlarged central cavity changes from predominately hydrophobic to a more polar surface. This replacement not only releases SP from the wall of the central cavity, but also provides a hydrophilic lining conducive for the burial of the hydrophobic residues of the SP. This model is derived from experiment based on the single ring version of GroEL,

SR1, in which timer is artificially set to infinity. In the purely passive folding proposal, GroEL only blocks aggregation of the SP by capturing the SP and offering an infinite diluted environment where SP could have another chance to fold<sup>63,64</sup>. However, it does not answer the question of how SP overcomes the energy barrier that prevents it from reaching the productive folding intermediate.

### **1.6 The Physiological Significance of A Double Ring Structure**

Common wisdom takes the asymmetrical, GroEL-GroES<sub>1</sub> cycle as the functioning cycle in a cell, which describes the chaperonin folds protein once at a time with only one of the two chambers of the two-toroid structure<sup>65,66</sup>. In this scenario, the two rings of GroEL operate completely out of phase with each other. When one ring is occupied with ATP and GroES, the other ring is unable to bind the SP, nucleotide, or GroES.

However, previous research that shows that GroES binds with GroEL in an associative manner<sup>67,68</sup>, which means the second GroES binds to the same GroEL before the first GroES is released, indicating a transient formation of GroEL-GroES<sub>2</sub> complex (so called “football” complex due to the pointed ends of structural similarity related to American football). Emerging evidence has shown that both the “bullet” (the notation of asymmetrical GroEL-GroES<sub>1</sub> complex as shaped as a bullet) and the “football” exists in solution, and denatured SP facilitates the formation of the “football” complex<sup>42,69-75</sup>. Other researchers found that a version of the single ring of GroEL can function just as normally as the wild type double-ring GroEL after mutation of A92 into tyrosine<sup>76</sup>. Why did nature choose a double ring version of GroEL as the functioning molecule in the mitochondria if a single ring version is

good enough to induce proper folds in the SP? In other words, if one ring in a tetradecamer is only needed to fold the polypeptide, why bother to have two rings stacked together as a unit while the other ring is only idling?

Preliminary research shows that GroES can bind simultaneously on both rings of GroEL in the presence of ATP, but not in the presence of ADP<sup>72</sup>. The population of the “football” complexes in solution is proportional to the population of denatured SPs<sup>71</sup>. Here in my research, the real time formation of the “football” complex has been monitored by Förster resonance energy transfer (FRET), with a FRET donor on GroEL and a FRET acceptor on GroES. The relationship between “football” population and denatured SP is further resolved<sup>42</sup>.

## 1.7 Specific Aims

The goal of this research was to develop a better understanding of the role that intramolecular interactions, specifically salt bridges, play in allosteric transitions of GroEL. Their regulation and contribution to the chaperonin cycle and folding of SPs is illustrated in this study. Additionally, the formation, regulation and functioning properties of symmetric GroEL-GroES<sub>2</sub> complex is investigated.

- 1) As illustrated above, the salt bridge networks play a role in the allosteric transition of GroEL. After binding with nucleotide, the large, rigid body movement of apical domain of GroEL is accompanied with the serial breakages and formation of salt bridges. Some of these salt bridges are maintained while others are broken again during the conformational change induced by GroES binding and ATP hydrolysis<sup>41</sup>. After binding with nucleotides, GroEL populates in the **R** state.

GroEL should revert to the **T** state to start a new cycle with mis-folded SPs, since the **T** state is generally considered as the acceptor state of SPs. Horovitz *et. al.* found that even at saturating ATP concentration, only half of the GroEL (the single ring version of GroEL) remains in the **R** state<sup>77</sup>. They suggest that ADP release is used to tune the conformational cycling between **R** and **T** transition, which would offer a chance for SPs to bind it.

Binding with nucleotide promotes the transition from **T** state to **R** state. However, the **R** state of GroEL has higher affinity towards nucleotides, and releasing bound nucleotide is the rate-determining step in the asymmetric chaperonin cycle that operating without SPs<sup>43,52</sup>. The intrinsic mechanism that releases ADP from the nucleotide binding pocket still remains unknown. It is certain that in the **R** state, helices F and M clamp on top of the nucleotide binding site inhibiting the release of ADP<sup>22</sup>. Only when GroEL transitions to the **T** state will the nucleotide binding pocket open and ADP have a chance to diffuse out<sup>47</sup>. So the mechanism that ADP release is actually the same as the mechanism of GroEL visits **T** state from **R** state. Along with understanding the role salt bridges play in the allosteric transitions, studies performed on these salt bridges would offer insights into the mechanism of how GroEL visits the **T** state from the idling **R** state.

- 2) Emerging evidence shows that the symmetric, GroEL-GroES<sub>2</sub> complex is the active folding species in the chaperonin cycle<sup>42,69-74</sup>. However, the mechanism for the formation of the “football” complex and the relation between SPs and “football” complex remains unknown. Does the formation of “football”

complex require ATP or ADP binding to both rings? Do two GroES bind with one GroEL in a concerted or step-wise mechanism? What is the relation between the “football” complex and the denatured SPs? Multiple fluorescence and FRET experiments were conducted to reveal the mechanism of formation of “football” complex and their role in the refolding of SPs.



## Chapter 2 General methods and experimental procedures

### 2.1 Site Directed Mutagenesis of GroEL

Table 2-1 lists the primers used to generate the various mutations used in the study. These primers were purified on 20% acrylamide gel until a single band for each was obtained. The site directed mutagenesis was performed on, either the expression plasmid pkk223-3 (Pharmacia) with the cloned GroEL gene (pGEL1) or ptrcESL for the *in vivo* experiments, as instructed by the QuikChange Site-Directed Mutagenesis Kit except a few changes on the extension time and cycles (MJ Mini Personal Thermocycler, Bio-RAD). After the digestion with DpnI, the plasmids were then transformed into XL-1 Blue super-competent cells. Single colonies which grew overnight on amp containing LB-Agar plates were picked and incubated. Plasmids were extracted and concentrated as instructed by the bench protocol of QIAprep spin Miniprep Kit, Qiagen. All the small volume DNA concentration assays were performed on ND-1000 Spectrophotometer, NanoDrop. Plasmids from the single colonies were directly sent to sequencing at DNA Sequencing Facility with sequencing primers (table 2-1) in Center for Biosystems Research, UMBI.

Mutation	primers
D115A	5'-GGCATGAACCCGATGGCCCTGAAACGTGGTATC-3' 5'-GATACCACGTTTCAGGGCCATCGGGTTCATGCC-3'
D83A	5'-GCCTCTAAAGCAAACGCAGCTGCAGGCGACGGTACC-3' 5'-GGTACCGTCGCCTGCAGCTGCGTTTGCTTTAGAGGC-3'
R197A	5'-GGTATGCAGTTCGACGCTGGCTACCTGTCTCCTTAC-3' 5'-GTAAGGAGACAGGTAGCCAGCGTCGAACTGCATACC-3'
E315C	5'-GCTGGAAAAGCAACCCTGTGCGACCTAGGTCAGGCTAAACG-3' 5'-CGTTTAGCCTGACCTAGGTCGCACAGGGTTGCTTTTCCAGC-3'
D398A	5'-GGTCGCGTGGAGGGCAGCTTCAACG-3' 5'-CGTTGAAGCTGCCCTCCACGCGACC-3'
K105A	5'-CATCACTGAAGGTCTGGCAGCTGTTGCT-3' 5'-AGCAACAGCTGCCAGACCTTCAGTGATG-3'
Sequencing	Primers
EL5'	5'-PATGGCAGCTAAAGACGTAAAATTC-3'
SeqEL1261	5'-CGCGTAGCGTCTAAACTG-3'
SRSseq1123	5'-GGCGTTGCAGTTATCAAATG-3'

**Table 2-1 Mutation Primers and Sequencing Primers Used.** Mutation primers are listed with its reverse complementary and sequencing primers are complementary with the coding sequencing. Three sequencing results with these primers covers the whole GroEL sequence.

These verified plasmids were then transformed into BL21 cells as instructed by the user protocol of Novagen. Cells were plated on amp containing LB-Agar plate overnight. Single colonies were picked up and cultured till an OD value of 0.8 was reached. Then the cultures were mixed with 30% glycerol and stored at -80°C fridge.

## 2.2 Protein Purification

The purification of GroEL consists of the usual crude lysate preparation, an initial DEAE anion-exchange column, a crude ammonium sulfate preparation, a size exclusion column, a desalting step, and finally the acetone precipitation step as described previously<sup>51,61</sup>. There was no significant difference in purifying wild type GroEL and its variants, except GroEL variants eluted earlier on the DEAE anion-exchange column due to the missing charges on the surface.

The purification of GroEL<sup>WT</sup> and GroEL<sup>DM</sup> with an extra cysteine was essentially the same as described in the general methods except several operational steps: 1) Starting from the cell lysate, the purification solution contained fresh 10 mM

DTT (instead of 1 mM as of purifying GroEL<sup>WT</sup>) to prevent oxidation of the cysteine residues. 2) The GroEL carrying a cysteine at residue E315 generally eluted out earlier on the Q-Sepharose column than the GroEL<sup>WT</sup>. 3) When performing acetone precipitation to strip contaminating SP from GroEL, the E315C mutant seemed to have an increased affinity for SPs. The solution to this was to perform multiple acetone precipitations with the presence of 200  $\mu$ M ADP and fresh 10 mM DTT.

Purification of GroES and GroES<sup>98C</sup> followed the protocol as described<sup>61</sup>, except the column was run at pH 4.8 and GroES<sup>98C</sup> was eluted with 150 mL of 0 to 300 mM NaCl.

### **2.3 The Modification of GroEL and GroES**

To study the interaction between GroEL and GroES, two fluorescent dyes fluorescein-5-maleimide (F5M) and IAEDANS, both from Molecular Probes, were covalently linked to the modified protein. The change of an amino acid residue into cysteine on GroEL<sup>WT</sup>/GroEL<sup>DM</sup> was achieved by mutagenesis of the E315 into cysteine by a pair of mutagenesis primers (see table 2-1). The modification of GroES by the insertion of a cysteine into the 98<sup>th</sup> amino acid of the C-terminal of GroES was performed as previously described<sup>61</sup>.

The donor chromophore used in this FRET system was IAEDANS and the acceptor chromophore was F5M. Prior to labeling, all the proteins were freshly reduced at 10 mM DTT on ice for 30 min. The DTT was removed by running the protein through a PD-10 column pre-equilibrated with 10 mM Tris pH7.5 and 10 mM MgCl<sub>2</sub>.

GroEL (100  $\mu\text{M}$  subunits) with 315C mutation was labeled with 150  $\mu\text{M}$  IAEDANS in the dark for  $\sim 1$  hour at room temperature. The reaction was quenched by adding 10 mM DTT to the solution, and then concentrated with a 100 kDa cutoff concentrator (Amicon). The free IAEDANS dyes was removed by running the protein through a PD-10 column pre-equilibrated with the same 10:10 buffer containing 1 mM DTT. The labeled protein was then further concentrated and stocks were made. Due to the absorption interference with the chromophore, the protein concentration could not be measured spectrophotometrically. Instead, the unlabeled GroEL with a known concentration was run on a SDS-PAGE gel as a concentration ladder with the labeled GroEL of unknown concentration (figure 2-1). After stained with coomassie blue, the concentration of the unknown could be derived from the data obtained from densitometry. The extent of labeling was then calculated by measuring the labeled dye concentration of the protein on the spectrophotometer. IAEDANS was measured at 336 nm using extinction coefficient of  $5400 \text{ M}^{-1}\text{cm}^{-1}$ . In the previous research, it had been demonstrated that the number of dyes on GroEL ring did not affect the interaction between GroEL and GroES<sup>80</sup>. In this research, the general labeling efficiency was  $\sim 3$  IAEDANS labeled per GroEL ring.

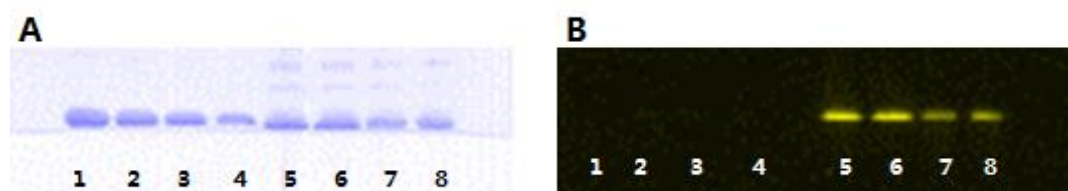


**Figure 2-1 Quantification of F5M labelled GroES with SDS-PAGE.** A) The concentration of GroES was measured by running labelled protein of unknown concentration with unlabeled protein with known concentration ladders. The gel was stained with coomassie blue and lane 1-4 are loaded with 20  $\mu\text{L}$  of 40, 80, 120, and 160  $\mu\text{M}$  GroES, lane 5-8 are unknown concentration samples. B) The same gel was visualized with the densitometer at fluorescence mode at red readings.

Labeling GroES<sup>98C</sup> was performed using essentially the same technique except the dye used here was F5M. All other procedures were the same as the labeling of GroEL. The quantification of GroES with dye bound was the same as discussed above. In this research, the F5M on GroES was measured at 491 nm using an extinction coefficient of 74500 M<sup>-1</sup>cm<sup>-1</sup>. The usual labeling extent of F5M on GroES<sup>98C</sup> yielded ~3.4 dye molecule per GroES ring.

#### 2.4 Characterization of the FRET Pair

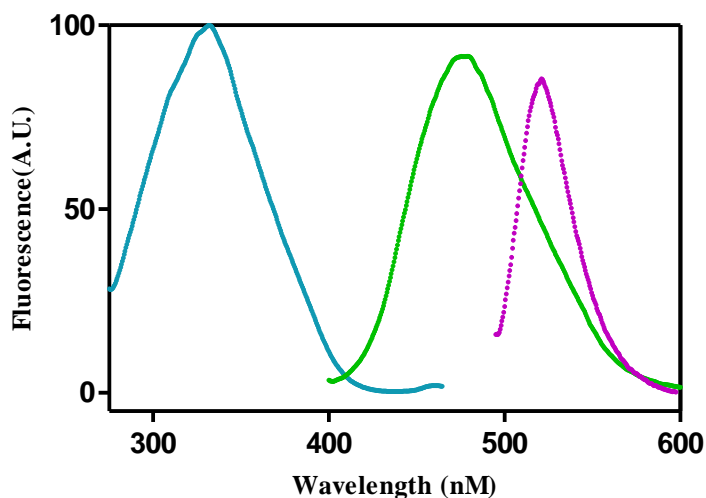


**Figure 2-2 FRET spectrum of IAEDANS and F5M.** IAEDANS has a maximum excitation wavelength at 336 nm (blue) and emission wavelength peak at 490 nm (green) while F5M gets excited maximally at 494 nm and emitting at 521 nm (purple). This dye pair has a Förster radius of 40 Å, and the distance between  $\alpha$ -carbon of GroEL 315C and GroES 98C is 36 Å. Thus it is possible for GroEL and GroES to bring these dyes together to form a FRET pair.

As the FRET donor, IAEDANS has its maximum excitation wavelength at 336 nm and emits at 490 nm. F5M, on the other hand, is excited at 494 nm and emits at 598 nm (figure 2-2). The overlap between the emission of IAEDANS and the excitation of F5M makes the energy transfer from IAEDANS to F5M possible. However, another critical value that affects the efficiency of FRET is the Förster

distance. The IAEDANS-F5M pair has a Förster distance of 40 Å, any distance between two chromophores beyond twice this distance does not result in significant FRET. The distance between  $\alpha$ -carbon of 315C on GroEL and 98C on GroES is 36 Å with a maximum FRET efficiency of 65.3%, thus it is within the Förster distance and capable of FRET (figure 2-2). The distance between the  $\alpha$ -carbon of 315C on GroEL and  $\alpha$ -carbon on the adjacent subunit of GroES is 83.3 Å which is larger than twice of the Förster distance and the FRET efficiency is 1.21%. This indicates the IAEDANS-F5M FRET occurs only between subunit of GroES binding right on top of the subunit of GroEL. This FRET specificity reduces the complexity when analyzing the FRET efficiency between GroEL and GroES, which will be discussed in later chapters.

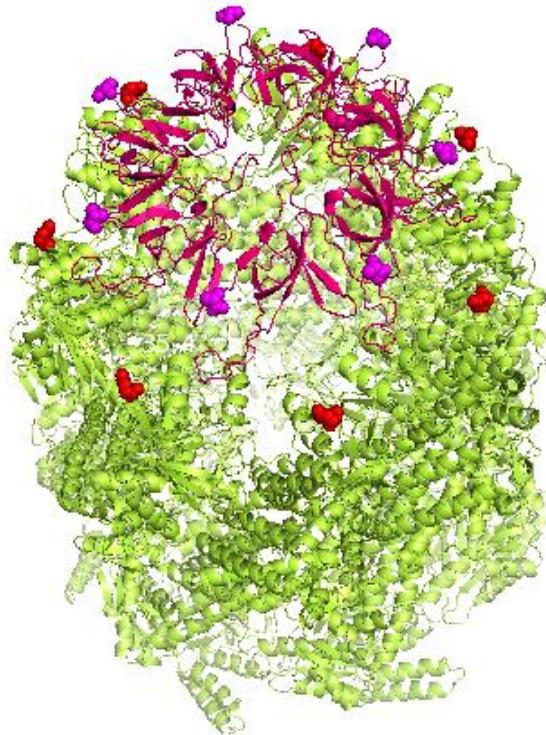


**Figure 2-3 The Architecture of GroEL-GroES<sub>1</sub> Complex and Its Labelling Positions.** In the asymmetrical GroEL-GroES<sub>1</sub> complex, GroEL is in green, GroES is in pink, the 98<sup>th</sup> residue on GroES labelled with F5M is shown in purple and the 315<sup>th</sup> residue on GroEL labelled with IAEDANS is shown in red.

However, there are still three natural cysteine residues in one GroEL subunit besides the one engineered at 315C. If non-specific labeling happened on other cysteine residues besides 315C, FRET would not occur due to the large space distance. Notice that the FRET only occurs when GroES binds with GroEL; no transfer of energy could occur if one of the dyes was missing or they were not close enough. To test the specificity of this FRET dye pair, the steady state FRET formation and stop flow FRET formation were both tested.

At steady state, the fluorescence emission at 520 nM was monitored using a variety of combinations: 1) the unlabeled GroEL and unlabeled GroES 2) the IAEDANS labeled GroEL and unlabeled GroES 3) the unlabeled GroEL and the F5M labeled GroES 4) the IAEDANS labeled GroEL and F5M labeled GroES. The excitation wavelength was set at 336 nM and both the excitation and emission slit width were set at 20 nM.

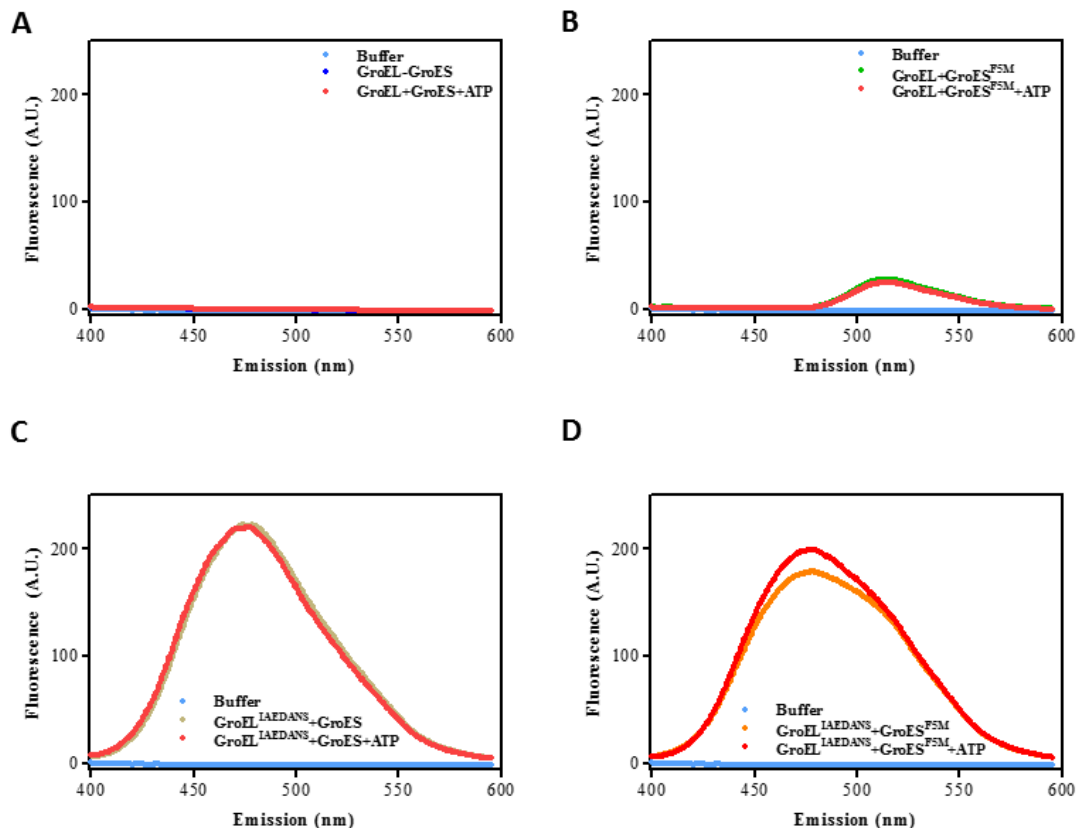


**Figure 2-4 Fluorescence Spectrum between GroEL and GroES.** The fluorescence emission at 520 nM was monitored using a variety of combinations: **A)** The unlabeled GroEL and unlabeled GroES **B)** The IAEDANS labeled GroEL and unlabeled GroES **C)** The unlabeled GroEL and the F5M labeled GroES **D)** The IAEDANS labeled GroEL and F5M labeled GroES. The excitation wavelength was set at 336 nM and both the excitation and emission slit width were set at 20 nM and the proteins are in buffer containing 20 mM Tris pH 7.5, 100 mM K<sup>+</sup>, and 10 mM Mg<sup>2+</sup> at 37°C.

As show in figure 2-3, there was only one condition that lead to increase of fluorescence at 520 nM when GroEL<sup>IAEDANS</sup> was mixed with GroES<sup>F5M</sup> and ATP. However, the experiment performed here is to observe the breakage of FRET pairs rather than the formation. After being challenged with ATP, GroES on the *cis* ring will be discharged and the pre-formed GroEL<sup>IAEDANS</sup>-GroES<sup>F5M</sup> FRET pair will break apart (figure 2-5, cartoon). Excessive unlabeled GroES will be mixed at the same time and the major complex formed would be GroEL<sup>IAEDANS</sup>-GroES<sup>unlabeled</sup>. By replacement of labeled GroES with unlabeled ones, the FRET pair becomes diluted



and the change in the fluorescence signal reflects the kinetics of GroES<sup>F5M</sup> discharged from GroEL<sup>IAEDANS</sup>. To test this idea, the asymmetric GroEL<sup>IAEDANS</sup>-GroES<sup>F5M</sup> complex was made by incubating 20  $\mu\text{M}$  GroEL<sup>IAEDANS</sup>, 30  $\mu\text{M}$  GroES<sup>F5M</sup> and 200  $\mu\text{M}$  ATP for 30 min in our standard buffer containing 20 mM Tris pH 7.5, 200 mM K<sup>+</sup> and 10 mM Mg<sup>2+</sup>. The complex was passed through a PD-10 column, pre-equilibrated with the same buffer to remove the free and *trans* bound ADP. The experiment was initiated by mixing 500  $\mu\text{M}$  and 10 fold of unlabeled GroES to this acceptor state complex. In a SX18MV-R stopped flow apparatus (Applied Photophysics), the excitation wavelength was set at 336 nm and a cutoff filter of 520 nm was installed on the detector which was set on the fluorescence mode. The syringes and cuvette were all incubated with a circulating water bath set at 37°C. For each reaction, a total of 100 seconds of data was collected where the data was split into two sections: the first 100 ms. and the later 199.9 seconds to resolve the early event. The complex was loaded into syringe A while syringe B was loaded with either the labeled or the unlabeled GroES with ATP.

As shown in figure 2-4, it was only when the FRET GroEL<sup>IAEDANS</sup>-GroES<sup>F5M</sup><sub>1</sub> complex was challenged with the unlabeled GroES, was there a significant FRET decrease in the course of time which could be used to monitor the interaction between GroEL and GroES.

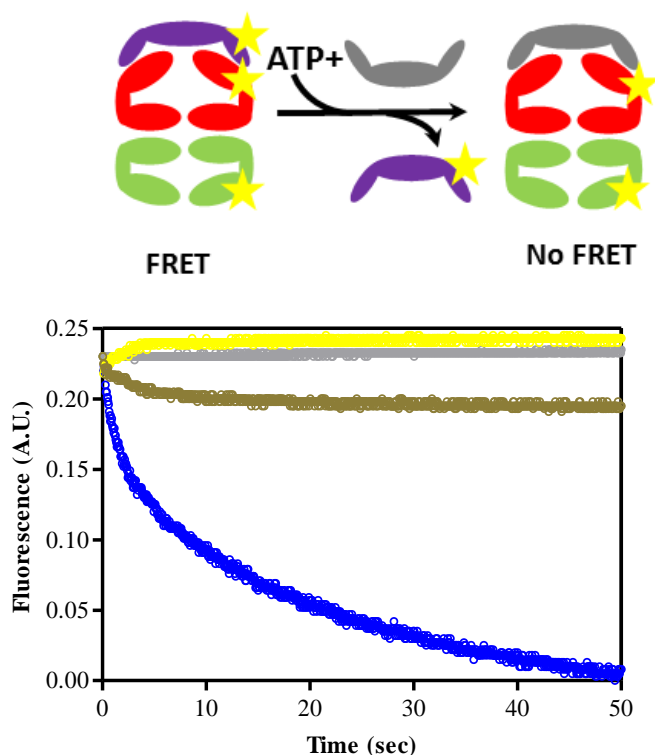


**Figure 2-5 Fluorescence Change upon Mixing with Different GroEL and GroES.** The fluorescence emission change at 520 nm was monitored using a variety of combinations: Grey, The unlabeled GroES challenged with and unlabeled GroES formed complex. Yellow, The F5M labeled GroES challenged with F5M labeled GroES formed complex. Brown, the IAEDANS labeled GroEL and the F5M labeled GroES formed complex challenged with IAEDANS labeled GroEL. Blue, the IAEDANS labeled GroEL and F5M labeled GroES formed complex challenged with unlabeled GroES.

## 2.5 FRET Efficiency Study of GroELS Stoichiometry

To translate the GroEL-GroES complex formation into a measurable biochemical signal, the FRET technique could be applied to quantitatively analyze the GroELS complex population as a function of other allosteric ligands. However, the extent of dye labelling on GroEL and GroES did affect the FRET efficiency in this system. If there was only one dye on GroEL, the chance for FRET was half of that if there were two dyes on one GroEL ring. Thus it was important to use the same labeled GroEL and GroES, at least in the same set of experiments, to justify the results regarding FRET efficiency.

The titration of GroES against GroEL while measuring the FRET efficiency was done using our standard buffer unless otherwise specified. On a fluorescence spectrophotometer (Perkin Elmer), both the excitation and emission slit width was set at 10 nm, the scan speed was set at 400 nm/min, and the cuvette chamber was circulated with a water bath set at 37°C. For GroEL<sup>IAEDANS</sup> and GroES<sup>F5M</sup> FRET, the excitation wavelength was set at 336 nm and emission at 470 nm was observed. In a 1 mL PK 1.000 quartz cuvette, GroES<sup>F5M</sup> was titrated into 200 µL buffer containing 2 µM GroEL<sup>IAEDANS</sup>, 500 µM ATP or ADP, 10 mM BeCl<sub>2</sub>, and 0.1M NaF. For each titration, 3 scans were taken and the average value of emission at 470 nm was taken.

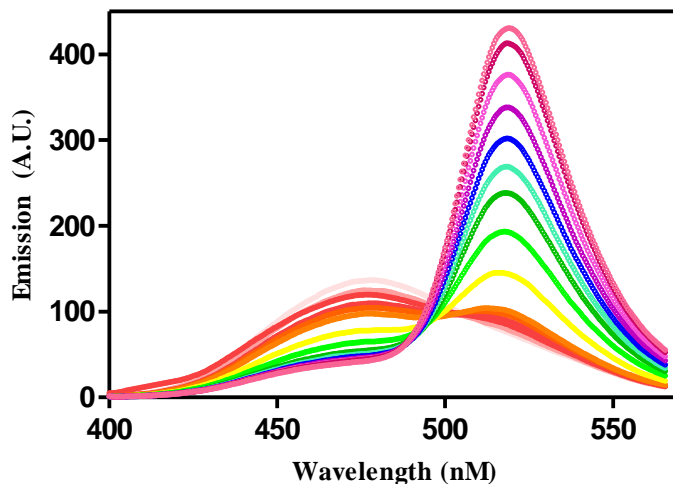


**Figure 2-6 FRET titration of GroES<sup>F5M</sup> to GroEL<sup>IAEDANS</sup>.** As more and more GroES<sup>F5M</sup> was titrated into the solution containing 2 µM GroEL<sup>IAEDANS</sup> + ADP + BeF<sub>x</sub>, the emission at 490 nm was decreasing while the emission at 521 nm was increasing. This indicated the occurrence of FRET where energy emitted from the fluorescent donor IAEDANS was transferred to the fluorescent acceptor F5M.

During FRET, the donor was excited at its maximum excitation wavelength and it emitted at the wavelength that excited the acceptor (figure 2-6). In the absence of the acceptor, all the energy from the donor was emitted as photons. In the presence of the acceptor, part of the energy was transferred to the acceptor and the emission

from the donor was weakened while the emission from the acceptor was enhanced. The phenomena that the weakening of the donor was called quenching. The unlabeled GroES, where there was no acceptor on the protein, was titrated exactly the same for calculation of FRET efficiency as following equation:

$$\text{FRET efficiency} = 1 - F_{IF}/F_I$$

Where  $F_{IF}$  was the fluorescence intensity of IAEDANS labeled GroEL (GroEL<sup>IAEDANS</sup> or GroEL<sup>DM-IAEDANS</sup>) at the presence of GroES<sup>F5M</sup>, and  $F_I$  was the fluorescence intensity of IAEDANS labeled GroEL (GroEL<sup>IAEDANS</sup> or GroEL<sup>DM-IAEDANS</sup>) in the presence of unlabeled GroES<sup>71</sup>. Each titration was repeated three times and kept using the same preparation of labeled proteins.

If titrating with SPs, 4  $\mu\text{M}$  GroES<sup>F5M</sup> was present in the same buffer without any BeCl<sub>2</sub> or NaF. The solution with different concentration of SPs was incubated for 2 min and a final concentration of 500  $\mu\text{M}$  ATP was mixed. Three scans were taken within 2 min after ATP was mixed. In each set of experiment, FRET efficiency at the presence of ATP, BeCl<sub>2</sub>, and NaF was set as the FRET efficiency of “football” complex, and FRET efficiency at the presence of ADP, BeCl<sub>2</sub>, and NaF is set as the FRET efficiency of “bullet” complex. GroEL-GroES complexes made at these conditions were examined by electron microscope and images were analyzed, which indicated almost 100% of “football” and “bullet” particles as discussed in Chapter 4. For titrations with SPs: the denatured malate dehydrogenase (MDH) and  $\alpha$ -lactalbumin ( $\alpha$ -LA) were utilized in this study. Due to the fast refolding nature of MDH, the enzyme was denatured with 0.01 N HCl on ice for 30 min in high concentration and then diluted into 50 mM Tris (pH 7.5) right before use.  $\alpha$ -LA was

denatured the same way and then buffer exchanged into a buffer containing 10 mM Tris (pH 7.5), 10 mM MgCl<sub>2</sub> and 1 mM DTT. Due to the presence of DTT,  $\alpha$ -LA remained unfolded all the time.

## 2.6 Stop Flow FRET Kinetics

The stop flow instrument was configured with a 20  $\mu$ L flow cell with a path length of 2 mm. The stop flow detector was set at fluorescence mode, and both the monochromator excitation and emission slit width were set at 46.5 nm. A 530 nm cutoff filter was installed for IAEDANS-F5M FRET.

A calibration suitable for use with the stopped-flow device during pre-steady state and steady state studies was routinely performed by mixing apo-GroEL<sup>IAEDANS</sup> and GroES<sup>F5M</sup> with either ADP·BeF<sub>x</sub> or with ATP·BeF<sub>x</sub>. The amplitude of the FRET signal in the presence of ATP·BeF<sub>x</sub> was exactly twice the amplitude of the FRET signal in the presence of ADP·BeF<sub>x</sub>, permitting us to quantify the population of symmetric GroEL-GroES<sub>2</sub> and asymmetric GroEL-GroES<sub>1</sub> complexes in real time. One thing that needs to be noticed is the PMT (voltage) directly affected the magnitude of the fluorescence signal. Usually for an increasing signal, the PMT is set at 80% as illustrated by the manual of the Photophysics Inc. Since the magnitude in an experiment is used to quantitatively measure the number of GroES associated with one GroEL molecule, the PMV is kept constant in the same experiment.

For GroES and SP dissociation experiment, there was no such a convenient way to calibrate. The identical condition of mixing on the stop flow instrument was applied to the Perkin Elmer fluorescence photometer to derive the stoichiometry of ligands to GroEL and then the kinetics derived from the stop-flow instrument was

normalized accordingly. Details upon different research purposes were described in detail in later chapters.

## 2.7 Steady-State FRET Kinetics

To monitor the “football” complex decay during the course of SP refolding, this experiment was conducted on the Perkin Elmer fluorescence spectrophotometer. In a quartz cuvette, a final concentration of 2  $\mu\text{M}$  GroEL<sup>IAEDANS</sup>, 5  $\mu\text{M}$  GroES<sup>F5M</sup>, 1 mM DTT, 5 mM PEP, 20 unit/mL of PK and 1g/L BSA was added. Rubisco or MDH was denatured as described above and added into the solution for a brief incubation. The excitation wavelength was set at 336 nm with slit width of 15 nm; the emission wavelength was set at 520 nm with slit width of 20 nm. Upon addition of 500  $\mu\text{M}$  ATP into the mixture, the emission signal was collected for 30 minutes.

Two control experiments were performed under the same conditions. In one of the control experiments, 10 mM BeCl<sub>2</sub> and 100 mM NaF were added in the presence of ATP; in the other, the ATP was replaced with ADP. As discussed in Chapter 4, this ATP/ADP·BeF<sub>x</sub> condition facilitates the formation of stable “football” and “bullet” complexes and the left Y axis of figure 5-2 and 5-5 was calibrated accordingly. After addition of ATP, the FRET emission of the denatured Rubisco or denatured MDH facilitated “football” complex at 530 nm was almost the same as the “football” complex formed by BeF<sub>x</sub>.

## 2.8 ATPase assay

### 2.8.1 Steady state ATPase Assay

This assay allows ATPase activity to be measured by coupling the production of ADP to NADH oxidation. The latter metabolite absorbs strongly at 340 nm and its disappearance can be followed spectroscopically. The detailed method is slightly modified from our previous lab protocols<sup>61</sup>, such as the temperature in this study is set at 37°C.

### 2.8.2 Pre-steady State ATPase Assay

The phosphate binding protein (PBP) has two domains connected together to form a cleft where the Pi is bound. The 197<sup>th</sup> residue, which is on the edge of the Pi binding site, is changed into cysteine covalently linking MDCC at its maleimide moiety<sup>78</sup>. Studies have shown that this mutation and its linkage with MDCC do not affect the affinity of Pi for PBP<sup>79</sup>. In the absence of Pi, the cleft is open and the fluorophore-coumarin is surrounded by hydrophilic residues from both the N and C terminal. Binding of Pi causes a conformational change that closes the cleft and the surrounding environment of coumarin becomes hydrophobic. This environmental change causes a change in the fluorescence emission<sup>78,80</sup>. Under saturating conditions of Pi, the fluorescence at 465 nm of PBP<sup>MDCC</sup> is increased ~7 fold higher (figure 2-7, A).

To test the binding of capture of Pi, the dissociation constant of Pi with PBP<sup>MDCC</sup> was determined. Pi standard purchased from Molecular Probe (Invitrogen) was diluted and titrated into a buffer containing 0.1  $\mu$ M PBP<sup>MDCC</sup>, 10 mM Tris (pH

7.5), and 10 mM MgCl<sub>2</sub>. Special attention needs to be paid to all the buffers used in this assay. There should not be any buffer containing inorganic phosphate, and the buffer could be treated with a phosphate MOP (PNPase and 7-methyl guanosine) if necessary. As Pi was added to the solution and excitation wavelength set at 425 nM, the increase of fluorescence at 465nM was recorded and normalized (figure 2-7, B).

The data were analyzed using Graphpad PRISM where data were fit according to a one site binding equation (figure 2-7, C). The fits yielded a dissociation constant of  $0.58 \pm 0.05 \mu\text{M}$  with  $R^2=0.9963$ . This  $K_d$  value was essentially the same as reported<sup>79</sup>. To determine the bimolecular association rate between Pi and PBP<sup>MDCC</sup>, the association rates and fluorescence signals as a function of Pi concentration were measured by a modified version of a previously described method<sup>61</sup>. Here 10  $\mu\text{M}$  labeled PBP<sup>MDCC</sup> was used throughout, and all of the measurements were conducted at 37°C. Whenever different concentrations of K<sup>+</sup> were used, Na<sup>+</sup> was used to balance the ionic strength such that  $([\text{K}^+] + [\text{Na}^+]) = 0.1 \text{ M}$ . The raw data without the first 4 pushes was collected, and more than five kinetic traces were collected and averaged.

In the experiment, different concentration Pi diluted from a standard stock was loaded into syringe A and in syringe B 20  $\mu\text{M}$  PBP<sup>MDCC</sup> was loaded. At time 0, the syringes were pushed together and the fluorescence was recorded (figure 2-8, A). To maintain the same experimental condition as was used to measure the Pi release from GroEL, the temperature of this measurement was taken at 37°C and the standard buffer was used.



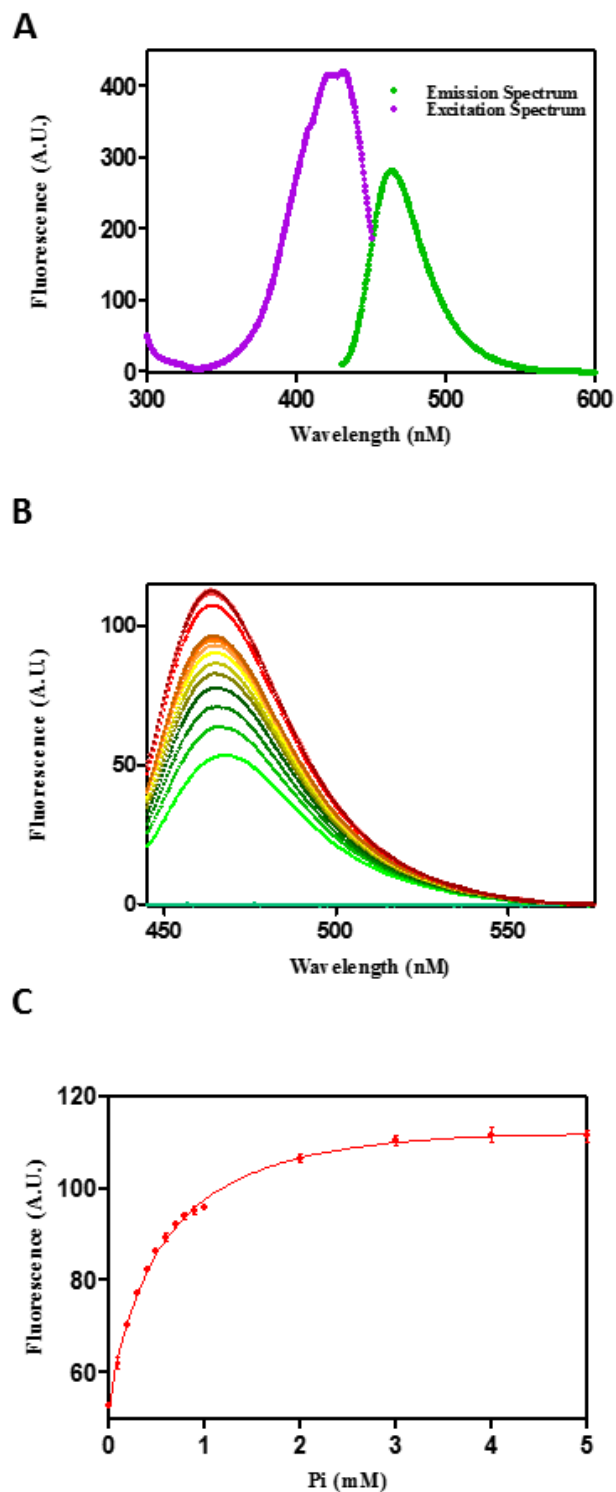


**Figure 2-7 Characterization of the Dynamics of PBP<sup>MDCC</sup>.** **A)** Excitation (purple) and emission (green) spectrum of PBP<sup>MDCC</sup>. **B)** Titration of Pi into PBP<sup>MDCC</sup> solution yielding an increase of fluorescence at 465 nm. **C)** The fluorescence signal at 465 nm is plotted against the Pi concentration used in the titration. The measurement was performed at 20 mM Tris pH 7.5, 100 mM K<sup>+</sup>, and 10 mM Mg<sup>2+</sup> at 37°C.

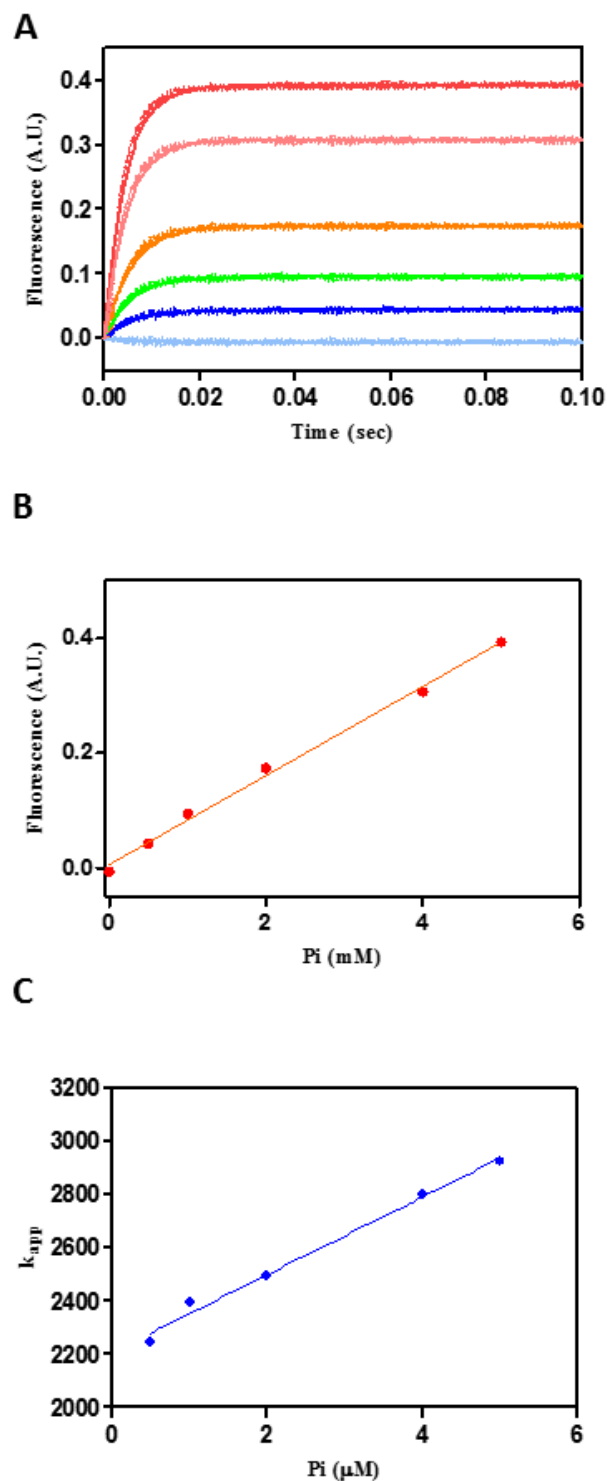


**Figure 2-8 Characterization of the Kinetics of PBP<sup>MDCC</sup>.** **A)** Upon mixing with Pi, PBP<sup>MDCC</sup> was giving off fluorescence signal with a cut-off filter of 455 nm. Cyan, blue, green, orange, pink, red were using 0, 0.5, 1, 2, 4, 5  $\mu\text{M}$  of Pi respectively. **B)** The fluorescence signals were plotted against the Pi concentration. **C)** The bimolecular association rates were derived by plotting the apparent rates against the Pi concentration. The measurement was performed at 20 mM Tris pH 7.5, 100 mM K<sup>+</sup>, and 10 mM Mg<sup>2+</sup> at 37°C.

The PBP<sup>MDCC</sup> emitted a fluorescence signal upon binding with Pi. The magnitude were plotted against the Pi concentration (figure 2-8, B). The magnitude of fluorescence taken on this instrument yielded a linear relation with the Pi concentration (with an R<sup>2</sup> value of 0.9957), suggesting a good indicator to quantify the Pi in the chaperonin system. The apparent rate of Pi binding at each Pi concentration was derived and the rates were plotted with its corresponding Pi concentration (figure 2-8, C). This yielded a bi-molecular association rate of  $1.46 \pm 0.09 \times 10^8 \text{ M}^{-1} \text{ Sec}^{-1}$  (with R<sup>2</sup> value of 0.9895). This large association constant indicated the association of Pi to PBP<sup>MDCC</sup> is diffusion limited and rapid enough to reflect the Pi release in our chaperonin system.

## **2.9 Pre-steady State ADP Release Assay**

In the steady state ATPase activity assay, coupling enzymes pyruvate kinase (PK from rabbit muscle, EC 2.7.1.40, Roche) and lactic dehydrogenase (LDH from rabbit muscle, EC 1.1.1.27, Roche) were utilized to monitor the hydrolysis of ATP, specifically the release of ADP from GroEL. Initiation of the reaction resulted in oxidation of NADH which could be seen by detecting a decrease in the absorption. The absorption data was transformed as the release of ADP. In the ADP release calibration experiment, different concentrations of ADP was mixed with the coupling enzyme system. The magnitude of the signals obtained from the detector and their corresponding ADP concentrations were plotted.

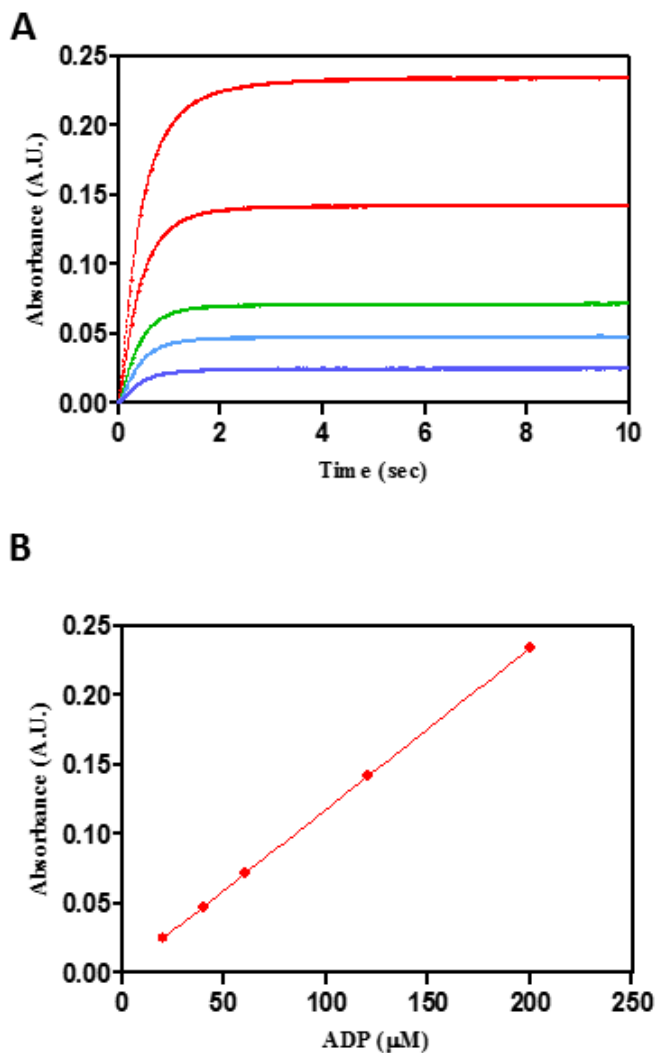


**Figure 2-9 Characterization of the Coupling Enzyme System.** **A)** Upon mixing with ADP, NADH was oxidized and the absorption at 430 nm decreased. The original absorption data was formatted that as an increasing signal indicating the release of ADP. Blue, cyan, green, red, and orange are the signal as mixing the coupling enzyme system with 20, 40, 60, 120, 200  $\mu\text{M}$  ADP. **B)** The magnitude of absorbance signal were plotted against ADP concentration. The measurement was performed at 20 mM Tris pH 7.5, 200 mM  $\text{K}^+$ , and 10 mM  $\text{Mg}^{2+}$  at 37°C.

The kinetics of ADP release was measured by monitoring the NADH catalyzed by coupling enzyme and was shown to be finished in ~2 seconds (figure 2-9, A). With the ADP concentration used (from 20-200  $\mu\text{M}$ ), the absorption at 340 nm collected on the detector yielded a perfect linear correlation with the ADP concentration with  $R^2$  value=0.9999 (figure 2-9, B). Thus our modified methods

offered a more accurate means to monitor the release of ADP from the chaperonin system.

To reveal the *in vivo*, physiological situation of ADP release from GroELS complex, the GroEL-GroES<sub>1</sub> acceptor state complex was made by mixing 420  $\mu\text{M}$  ATP into a solution containing 168  $\mu\text{M}$  GroEL<sup>WT</sup> or GroEL<sup>DM</sup> and 252  $\mu\text{M}$  GroES. The reaction was incubated for 30 min, and then flow through a PD-10 column to remove the free and *trans* bound ADP. LDH and PK were spin down from their ammonium sulfate suspension, and resuspended in a buffer containing 10 mM Tris pH7.5 and 10 mM MgCl<sub>2</sub>, before desalted through PD-10 column (GE). A final concentration of 1000 U/mL of both the coupling enzyme, 200  $\mu\text{M}$  ATP, 0.15 mM NADH (Sigma), 0.4 mM PEP (Sigma), and 2 mM DTT in a standard buffer was loaded in syringe A. In syringe B, 40  $\mu\text{M}$  GroEL-GroES<sub>1</sub> acceptor state complex (as monomers) was loaded. The stop flow detector was set in the absorption mode and the wavelength was set at 340 nm. The first 4 pushes were discarded before more than 5 traces of raw data were collected.

## 2.10 Electron Microscopy

Electron microscopic observation on large bio-molecules requires only a concentration of  $\sim 100$  ng/ml proteins, less than a minute negative stain and about half an hour operation on the electron microscope to reach the most direct conclusion about the structural information.

A carbon grid (square mesh copper, Electron Microscopy Sciences) was cleaned to remove the dust and grease in the electron beam in a vacuum chamber at 1000 Volts for 1 min. For apo-proteins, usually 4  $\mu\text{L}$  of GroEL<sup>DM</sup> and GroEL<sup>WT</sup>

solution of 1.75  $\mu\text{M}$  was loaded on the carbon film, and allowed to sit for 45 seconds. Drops of 0.2% uranium acetate solution was applied to the grid and allowed to sit for another 45 sec for staining. The excessive solution on the grid was removed by absorbing with the edge of a filter paper. The grid was left air dry for couple of minutes and then loaded into the electron microscope to find a field where the particles were evenly distributed with a clear background.

To exam the complex formed by GroES and GroEL, both proteins in a standard buffer containing  $\text{BeF}_x$  were prepared and diluted to a concentration of 10  $\mu\text{M}$ . 200  $\mu\text{M}$  ATP or ADP was then mixed into the solution and the reaction was allowed to take place for 5 min. The mixture was diluted 50 fold till a final concentration of 0.2  $\mu\text{M}$  was reached. 4  $\mu\text{L}$  of the protein solution was loaded onto one carbon film grid and allowed to sit for 45 sec. The specimen was stained and examined the same as described above.

### **2.11 MDH Activity and Encapsulation Measurement**

To measure the enzymatic activity of MDH during its refolding by GroEL, this methods was developed based on previous report with slight modification<sup>81</sup>. All buffer in this experiment contained 50 mM Tris-HCL pH 7.5, 200 mM KCl, 10 mM  $\text{MgCl}_2$  and 10 mM DTT. A concentration of 235  $\mu\text{M}$  MDH was denatured 10 fold into in 5 M urea in the above buffer for 1 hour at 30 °C. Then, 4.86 $\mu\text{L}$  of this denatured MDH solution was added in a final volume of 400  $\mu\text{L}$ , the same buffer containing 2  $\mu\text{M}$  GroEL, 4 $\mu\text{M}$  GroES, 1g/L BSA 5mM PEP and 20 units PK. The refolding was initiated by adding 2 mM ATP into the solution. At different time points, aliquots of the solution were taken to measure the enzymatic activity of MDH

as follows. The assay buffer is the same as above, but with 1.65 mM NADH and 16.5 mM oxaloacetic acid. Upon addition of refolded MDH, the oxidation of NADH was followed by measuring the absorption at 340 nM. The native MDH without urea denaturation was treated the same and measured at the same time point to calculate the percent recovery.

To measure how much denatured MDH was encapsulated in the “Anfinsen” cage along its folding trajectory, we specifically designed this experiment. Basically the idea was that at different time points in the turning over GroELS system,  $\text{BeF}_x$  was added into the reaction. The artificial, stable “football” containing MDH being refolded at a particular time point would then be captured and could be analyzed. The refolding was conducted the same as described above, except the GroES was replaced with the his-tag version.

The experimental detail is as follows: 18.75 $\mu\text{L}$  of 310 $\mu\text{M}$  MDH was mixed with 31.3 $\mu\text{L}$  of 8M urea and denatured at 30 °C for an hour. 14.5  $\mu\text{L}$  of denatured MDH was mixed with a buffer containing 4.27 $\mu\text{M}$  GroEL, 8.54 $\mu\text{M}$  GroES<sup>his</sup>, 500 mM PEP, 20 U/mL PK, 10 mM DTT and 500 $\mu\text{M}$  ATP. The final concentration was adjusted to such with the standard buffer to 550 $\mu\text{L}$ . The final ratio of denatured MDH to GroEL rings are 5:1. The reaction was initiated by adding ATP into the solution and incubated at 30 °C. At 0, 2, 4, 8 and 20 minutes, 100 $\mu\text{L}$  of the refolding solution was taken out and added to a  $\text{BeCl}_2+\text{NaF}$  solution to quench the GroELS dynamic system as the artificial “football” complex.

In a Qiagen small spin column, the filter was replaced by 2 layers of regular filter paper made by the size of a standard puncture hole. The Ni-NTA agarose resin

was mixed vigorously and 400 $\mu$ L of this mixture was loaded on the column. Four columns are made the same way to avoid cross-contamination between each other. After the elution of the storage solution, a net volume of 200 $\mu$ L of resin was left packed in the column. The column was equilibrated with 1 mL of the standard buffer (with 10 mM BeCl<sub>2</sub> and 100 mM NaF) and the quenched mixture was then loaded. The unbound protein, which was the un-encapsulated MDH, was washed away by rinsing the column with 600 $\mu$ L of the standard buffer. Another 600 $\mu$ L of 250 mM imidazole was loaded on the column 3 times to elute the bound, artificial “football” complex.

To quantify how much MDH was encapsulated in the artificial “football” complex, the elution was heat-denatured and loaded to SDS-PAGE. Three known concentrations of GroEL and MDH were loaded on the same gel as markers to quantify the unknowns (figure 2-10, A). For GroEL, 20  $\mu$ L 1.5 $\mu$ M, 1 $\mu$ M, and 0.5 $\mu$ M of protein were loaded with 4 $\mu$ L loading dye. For MDH, 20  $\mu$ L 0.5 $\mu$ M, 0.2 $\mu$ M, and 0.05 $\mu$ M of protein was loaded with the same dye. The amount of MDH encapsulated in the GroEL tetradecamer was small compared with the MW of GroEL, e.g. assuming two MDH subunit bound to each ring of GroEL the quantity ratio would be 70:798. This made it difficult to visualize both proteins with one staining methods. The same gel was stained with coomassie blue first to quantify GroEL and then destained before staining with silver to quantify MDH. The band density correlates well with the concentration loaded on the gel. For GroEL bands the R<sup>2</sup> value is 1.00 and for MDH bands the R<sup>2</sup> value is 0.97 (figure 2-10, B). This method allows us to



monitor the amount of MDH bound to GroEL in real time during its course of refolding.

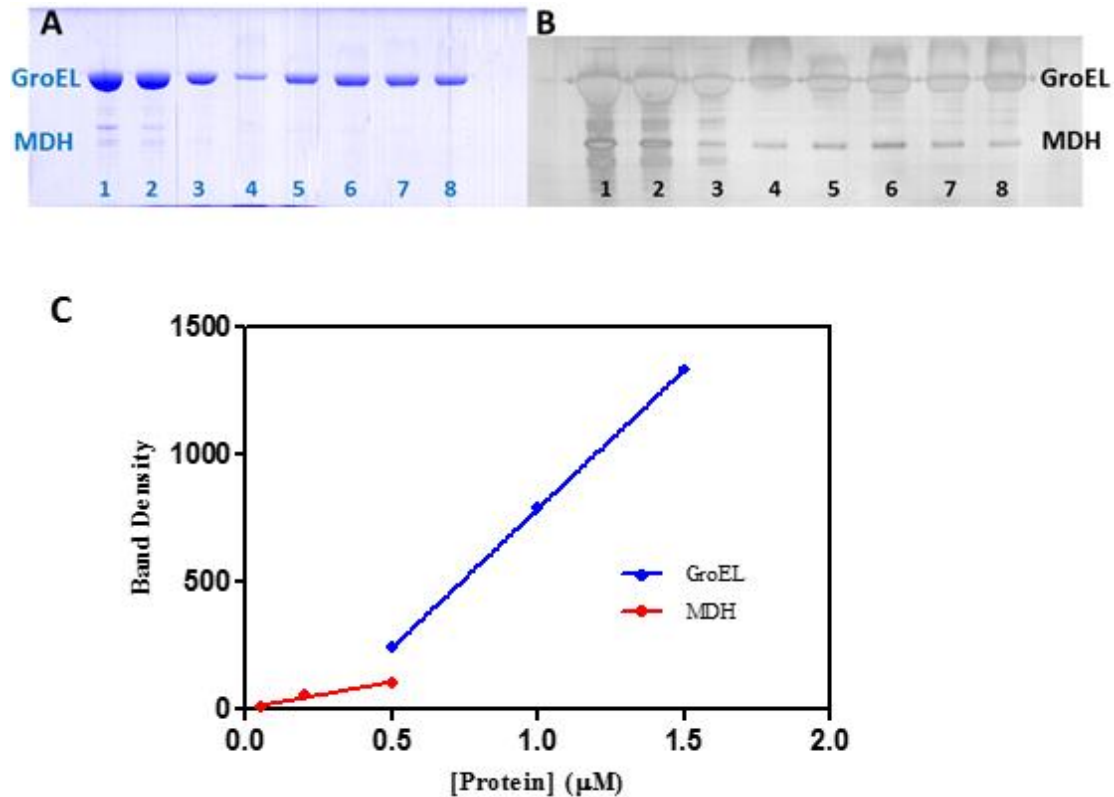


**Figure 2-10 Measurement of MDH Encapsulation during Its Refolding by GroEL.** A) The SDS-PAGE measurement of amounts of MDH bound by GroEL at different time points. The gel was stained with coomassie blue to view the GroEL bands B) and the same gel was destained before staining with silver to visualize the MDH bands. C) The band density obtained with the densitometer was plotted against their corresponding concentration and there was a linear relation between bands from standards and concentration: blue for GroEL and red for MDH.

## 2.12 Isothermal Titration Calorimetry Study of ADP Binding to GroEL

To investigate the binding affinity of ADP to GroEL<sup>WT</sup> and GroEL<sup>DM</sup>, the isothermal titration calorimetry (ITC) was performed. Dialysis buffer for this experiment was 50 mM Na<sup>+</sup> cacodylate, 200 mM K<sup>+</sup> and 10 mM Mg<sup>2+</sup>. The pH of the buffer was adjusted to 7.04 at 20 °C. The protein stock solution was dialyzed exhaustively (200 µL in 200 mL buffer for 3 times), and an ADP solution was made

with the final dialysis buffer to maintain the identical buffer composition. The ADP solution was also treated with glucose and hexokinase to remove any trace amount of ATP. For the titration, a final concentration of 28.8  $\mu\text{M}$  GroEL<sup>WT</sup> or 9.2 $\mu\text{M}$  of GroEL<sup>DM</sup> was made with the dialysis buffer, filtered with 2  $\mu\text{M}$  filter, degassed, and loaded into the syringe. A final concentration of 740.4 $\mu\text{M}$  ADP for GroEL<sup>WT</sup>, or 80.3  $\mu\text{M}$  ADP for GroEL<sup>DM</sup> was made the same way as described for the preparation of proteins.

The ITC sample cell was rinsed with 1 L of PBS followed by 3 L of milliQ water. The dialysis buffer was degassed for 10 min before use. The sample cell was rinsed twice with milliQ water and three times with degassed buffer. The protein sample was loaded to the chamber carefully to avoid bubbles, and ADP was loaded to the syringe. The instrument was set at 20 °C and the jacket was equilibrated before a 1000 sec delay. 25 injections of 10  $\mu\text{L}$  were delivered with each injection duration being 24 sec and 360 sec intervals in between injections. The normal 2  $\mu\text{L}$  injection before the 10  $\mu\text{L}$  injections was not used due to the tight binding of GroEL<sup>DM</sup> (figure 6-8).

### **2.13 *In vivo* Study of GroEL and Its Variants in Supplementing Cell Growth**

Site-directed mutagenesis was performed on this ptrcESL plasmid to generate three mutations on the groEL gene: D83A/R197A, D398A, and K105A mutations (see section 2.1). The MGM100 cell was purchased from Coli Genetic Stock Center (CGSC, Yale) and treated with Z-competent *E. coli* transformation buffer set (ZYMO Research) :1) the overnight culture was incubated on ice for 10 min and then pelleted at 1600-2500 g for 10 min at 4 °C 2) the supernatant was removed and cell gently

suspended in wash buffer, and then spun down 3) the supernatant was removed and cells gently suspended in the competent buffer 4) cell was aliquoted and stored in -80 °C fridge. Different plasmids were transformed into MGM100 cells and grown overnight on LB plates with 0.2% arabinose. Colonies were picked and different infected cells were cultured and cell stocks were made.

Strains transformed with the plasmids grown overnight in LB + 0.2% arabinose and pelleted. Cells were washed 3 times with LB media and  $OD_{600}$  was adjusted to 1.0. A series of 10 fold dilutions were made so the first concentration used is of  $OD_{600}$  equal to 1. With each cell concentration, 8  $\mu$ L of the dilution sample was spotted onto LA + 0.2% arabinose or glucose at the presence of amp. The plates were incubated overnight at 37 °C or 42°C.

## Chapter 3 Characterization of GroEL<sup>DM</sup> mutant

### 3.1 Introduction

#### 3.1.1 Allosteric Transitions during the Complete Chaperonin Cycle

Much like its man-made counterpart as a motor, GroEL does work by utilizing energy in a cyclic way. GroEL undergoes an allosteric transition from **T** to **R** upon binding ATP, **R** to **R'** by subsequent binding of GroES to the ATP bound ring, **R'** to **R''** driven by hydrolysis of ATP and eventually **R''** to **T** by the discharge of GroES and ADP (figure 1-2). Generally speaking, all machines share at least three common features: 1) The motion of the machine needs consumption of energy, 2) The motion of the machine runs in a cyclical way, 3) At least one step in the cycle is irreversible.

Many organisms use the hydrolysis of ATP as a primary energy source and expectedly, so does GroEL. For example, the binding energy of ATP is utilized to drive the large, rigid body movement of the apical domain. GroEL hydrolyzes ATP, at a much slower rate compared to other characterized ATPase enzymes and this process is likely irreversible. The release of the hydrolysis product, ADP, tunes the conformational cycling in the chaperonin cycle while the other product, inorganic phosphate release is rapid<sup>52</sup>. Thus the hydrolysis of ATP further makes this cycle irreversible, e.g. GroES could not be dissociated from the *cis* ring unless some ATP is hydrolyzed into ADP.

As stated previously, there is a logical comparison to the process of the GroEL cycle and the combustion cycle utilized in today's motors. In each, a force is used to drive the process forward and eventually allowing it to return to its starting point. In a motor, the difference of gas pressure between the outside and inside of the

combustion chamber, after the burning of fossil oil, drives the stroke back to its original position and the whole heat engine set back to the beginning of the induction step. The natural nano-machine GroEL, after hydrolyzing ATP, is mostly idling at its resting state where there is ADP bound to the *trans* ring in the absence of SPs (figure 1-2). The **T** state is considered as the acceptor state for SPs, and thus the obvious question is how does GroEL reset itself, e.g. undergo the transition from **R''** to **T** state?

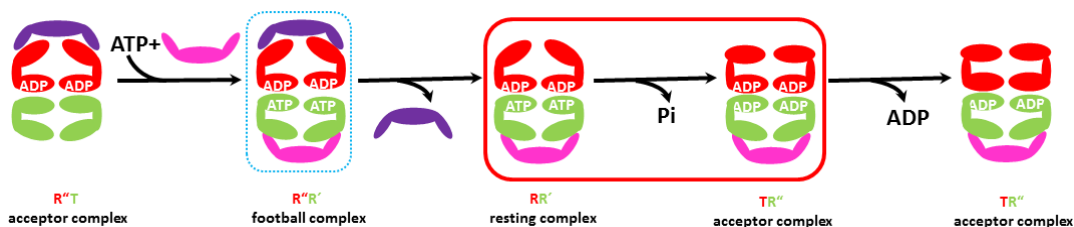


**Figure 3-1 Pre-steady State Assay with the Acceptor State Complex.** ATP binding to the vacant *trans* ring was followed by association of a second GroES indicated by the associative mechanism. This “football” complex in the absence of SPs was a transient intermediate (boxed with blue, dashed line). The discharge of GroES happened within ~5 msec. which was accompanied by the hydrolysis of ATP and immediate release of Pi. The new *trans* ring was sampling in between **R** and **T** state where the nucleotide binding pocket was open in the latter (boxed with red, solid line). Release of ADP was the rate limiting step and a SP-acceptor state, out of phase with the previous one, was formed.

Previous research indicates that even at saturating concentrations of ATP and in the absence of GroES, only half of the GroEL molecules are in the **R** state while the other half are sampling in the **T** state<sup>77</sup>. Crystal structure clearly shows that helices F and M move over the top of the nucleotide binding pocket at **R''** state of GroEL and close the gate for ADP release, which is open in **T** state of GroEL. The conformational cycling between the **R''** and **T** state thus becomes the chance for ADP to diffuse into solution<sup>22</sup> (figure 3-1, red box). Again, it is unclear what the intrinsic mechanism for how GroEL visits **T** state in the presence of ADP. That is, what is the

driving force that promotes this nucleotide bound state transit to a lower energy state-  
**T** state?

### *3.1.2 Allosteric Effectors during the Complete Chaperonin Cycle*

Today's combustion engines no longer utilize a single combustion chamber, but rather incorporate chambers working together in a single, concerted motion. It is the same in regards to the natural nano-machine GroEL, and it is described by the positive MWC cooperativity model. This model describes seven subunits in one ring of the double ring structure working in a concerted mode. It has been demonstrated via the computational work of molecular dynamic simulations<sup>34,35</sup> and by direct observation on the structure of GroEL: if one subunit in one ring is moving, the adjacent subunit has to move in accordance with it, otherwise there would be steric hindering for the first subunit.

Biochemical evidence, developed in this laboratory<sup>61,82</sup>, has demonstrated that by chemically cross linking one subunit of GroEL in the **T** state, the rest of the six subunits in the same ring are kept in the **T** state. By carefully setting the experimental conditions, they can control the extent of crosslinking by oxidation of the subunit between 0% and 100%. The result shows only one disulfide bond or cross-link is necessary to tether the entire ring in the **T** state and prevent GroES binding which indicates the **T** to **R''** transition is prohibited. The Hill coefficient measured by ATP binding to a tethered GroEL is approximately 1, further demonstrating that the whole ring is locked in the **T** state.

Salt bridges are typical, weak interactions between anionic carboxylate ( $\text{RCOO}^-$  of either aspartic acid or glutamic acid) and the cationic ammonium ( $\text{RNH}^{3+}$

from lysine or guanidinium from arginine) groups. Other ionizable side chains could also contribute to formation of salt bridges depending on their environmental pH that alters their pKa. A pair of salt bridges is essentially a combination of two non-covalent interactions: hydrogen bonding and electrostatic interaction. The nature of these interactions largely depends on the distance between atoms and requires the side chains of salt bridges to be within 4Å.

Besides contributing to the stability of the protein, salt bridges play important roles in the allosteric regulation of multi-subunit proteins. The transition from one allosteric state to another often results in the disruption and/or formation of salt bridges. There is a network of salt bridges forming and breaking during the allosteric transitions of GroEL. The nucleotide binding to GroEL promotes the transition from **T** state to **R** state. During this transition, the  $C_{\alpha}$  to  $C_{\alpha}$  distance among salt bridges D83-K327, R284-E386, R285-E386, R197-E386 and E257-R268 increases while that among salt bridges K80-E386, E257-K321 and E257-R322 decreases. The binding of GroES and hydrolysis of ATP promotes the transition from **R** to **R''** state. During this transition, the  $C_{\alpha}$  to  $C_{\alpha}$  distances among salt bridges D83-K327 and E257-R268 further increase. The salt bridge E257-K246 begins to break while E257-K321 and E257-R322, formed in the **T** to **R** transition, also break apart. The  $C_{\alpha}$  to  $C_{\alpha}$  distance for P33-N153 continues to get closer while two new salt bridges K80-D359 and I305-A260 begin to form during this transition<sup>41</sup>.

To understand the role that salt bridges play in the allosteric regulation of GroEL, mutations that eliminate salt bridges would shed light on the contribution of these salt bridges to the chaperonin system. D83 in the equatorial domain of one

subunit forms salt bridge with K327 in the apical domain within the same subunit, and R197 in the apical domain of one subunit forms salt bridge with E386 in the intermediate domain within the adjacent subunit (see figure 3-2). These two subunits break apart during the **T** to **R'** state transition. Site-directed mutagenesis, which mutates D83 and R197 into alanine, will eliminate the charges on these residues and remove the hydrogen bonding in between (GroEL<sup>DM</sup>). The result is a double mutant where the salt bridges that stabilize the **T** state are removed and the protein presumably favors the **R** state.

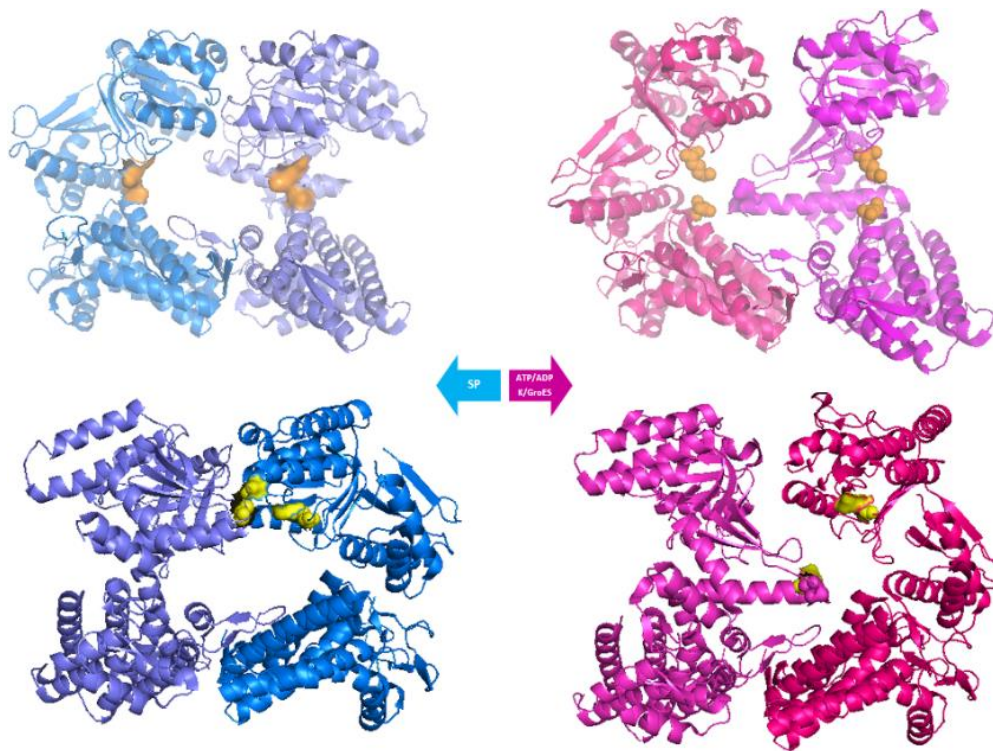


**Figure 3-2 Salt bridges D83-K327 and R197-E386 Involved in the T to R transition of GroEL.** During the transition of GroEL from **T** state (blue) to **R** state (purple), there is a pair of intra-subunit, inter-domain salt bridge D83-K327 (orange) and inter-subunit, inter-domain salt bridge R197-E386 (gold) break simultaneously. SP favors the **T** state of GroEL while ATP/ADP/K<sup>+</sup>/GroES favors the **R** state of GroEL, together they govern the chaperonin allosteric equilibrium.



The breakage and form of salt bridges D83-K327 and R197-E386 may play important roles in the cooperative allostery of GroEL. Mutations of D83A and R197A would eliminate two charges, thus two salt bridges for one subunit. A total of 14 salt bridges per ring are eliminated by this double mutation. If eliminating all the salt bridges eventually disassembles the highly oligomeric structure, elimination of 28 salt bridges would be a considerable loss of intra-molecular interactions. Thus, studying the effects of these mutations would be informative in understanding the role salt bridges play in the allostery of GroEL.

### **3.2 Structural Characterization of GroEL<sup>DM</sup> Mutant**

Mutations, especially those involved in the inter-subunit interactions, could possibly change the oligomeric state of a multi-subunit protein assembly. For example, mutation of four amino acids Arg452, Glu461, Ser463, and Val464 in the equatorial domain of double ring GroEL into alanine interrupts the inter-ring interaction. This makes GroEL a heptamer, composed of only one GroEL ring, so called single ring version (SR1) of the chaperonin<sup>27</sup>. Here in this research, we eliminated 1) a positive charge on Arg197 in one subunit that interacts with a negative charge on Glu386 in the adjacent subunit 2) a negative charge on Asp83 interacts with Lys327 within the same subunit. In all, a total of 14 positive charges and 14 negative charges that could be responsible for inter-subunit interactions were eliminated in this mutant. The oligomeric state of this double mutant protein was determined by a variety of methods to see whether it was still in the classical double ring structure.

### 3.2.1 Native-PAGE Analysis of GroEL Oligomeric State

The most common laboratory practice for assessing molecule weight is to perform a poly-acrylimide gel electrophoresis (PAGE), with denaturing SDS-PAGE for evaluating the isolated, subunit MW and native-PAGE for the oligomeric assembly. We used the later one to assess the MW of GroEL<sup>DM</sup>. Typically, an 8% of poly-acrylimide gel is made with only the continuous separating part was loaded with native protein marker and GroEL<sup>WT</sup>, GroEL<sup>DM</sup>. The gel was run at 100 volts for about an hour and stained with commassie blue. After being de-stained, a single band of both GroEL<sup>WT</sup> and GroEL<sup>DM</sup> was found located in between the marker of 1048 and 720 kDa (figure 3-3). As a control, the single ring version GroEL (SR1) was also loaded on the same gel and located in between markers of 460 and 242 kDa.

Furthermore, we plotted the distance each band travelled against the log of their MW. The five standard proteins each had a MW of 1236, 1048, 720, 460, and 242 kDa, and the plot with all of them would give the standard curve as to extrapolate the unknowns. The R<sup>2</sup> value of the standard curve yielded 0.9862 and the calculated MW from the distance the GroEL<sup>WT</sup>, GroEL<sup>DM</sup>, and SR1 travelled were: 684.9-721.6 kDa for both GroEL<sup>WT</sup> and GroEL<sup>DM</sup> and 475.1-501.3 kDa for SR1.

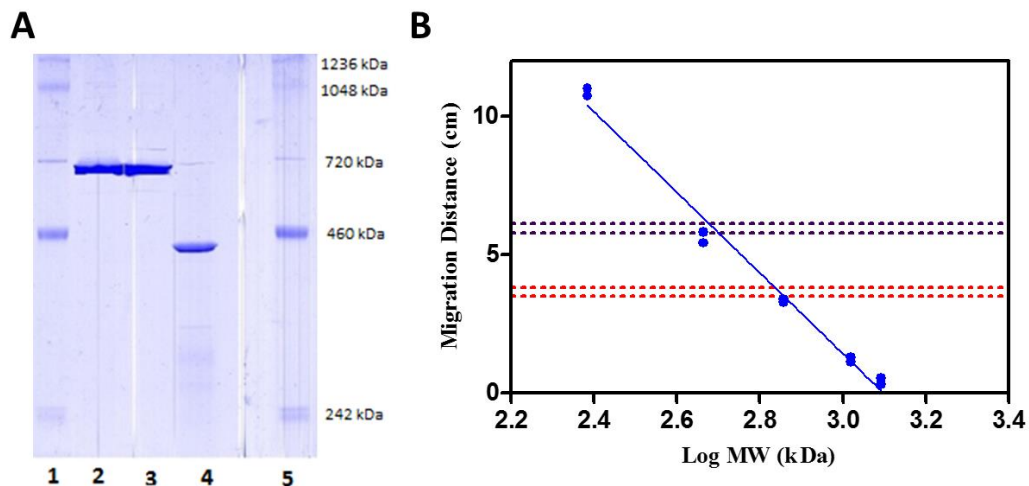


**Figure 3-3 Native PAGE Evaluation of GroEL.** A) The native PAGE of GroEL<sup>WT</sup>, GroEL<sup>DM</sup> and SR1 stained with coomassie blue. Lane 1 and 5 are native molecular makers, lane 2 is GroEL<sup>WT</sup>, lane 3 is GroEL<sup>DM</sup>, and Lane 4 is SR1. B) The plot of distance each band migrated as function of the log of their MW. Red dotted line is the region where GroEL<sup>WT</sup> and GroEL<sup>DM</sup> migrated and black is for SR1.

### 3.2.2 Electron Microscopy Study

To view the GroEL structure directly, both apo-GroEL<sup>WT</sup> and GroEL<sup>DM</sup> were examined with transmission electron microscopy (TEM) as described in Chapter 2.

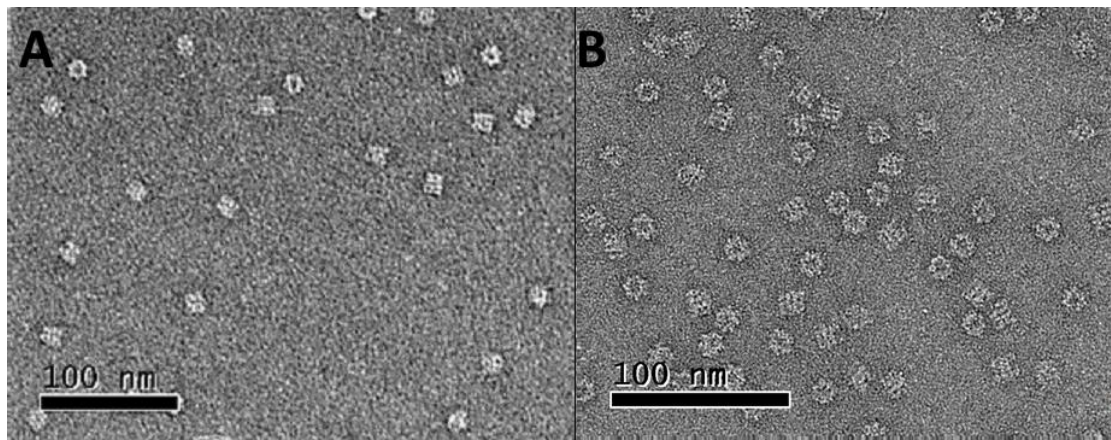


**Figure 3-4 Negative Stain Electron Microscopic of GroEL.** A) The microscopic image of GroEL<sup>WT</sup>. B) The microscopic image of GroEL<sup>DM</sup>. Both samples were stained with 0.2% uranyl acetate and examined under the microscope. The scale bar shows 100 nM.

As shown in figure 3-4, both the GroEL<sup>WT</sup> and GroEL<sup>DM</sup> particles exhibited a clear, double ring structure. Some of the top views of the GroEL particles even allowed one to see the seven fold symmetry of subunits on the ring.

### 3.2.3 Analytical Ultracentrifugation

#### 3.2.3.1 Sedimentation Equilibrium

GroEL<sup>WT</sup> and GroEL<sup>DM</sup> proteins were dialyzed exhaustively against a buffer containing 20 mM Tris, 200 mM K<sup>+</sup>, and 0.1 mM EDTA (pH 7.5 at 20°C). The proteins were prepared at a concentration that yielded an absorption of 0.5 at 276 nm in a double sector cell with charcoal-filled Epon centerpieces and a path length of 1.2 cm. The samples were centrifuged at 7000 and 9000 rpm, 20°C for 20 hours before the equilibrium was reached for the first scan and a second scan was taken 2 hours after in an Optima XL-1 analytical ultracentrifuge (Beckman Coulter). The absorption as a function of the radial position was fit using the following equation:

$$C_r = C_{r_0} e^{\sigma(r^2 - r_0^2)}$$

using WinNonLin software<sup>83</sup>. The MW was calculated using the following equation:

$$\sigma = \frac{M(1 - \bar{V}\rho)\omega^2}{2RT}$$

where M is the molecular weight,  $\bar{V}$  is the partial specific volume of the protein calculated from Sednterp (<http://www.rasmb.bbri.org>),  $\omega$  is the angular velocity of the rotor, R is the gas constant, T is the absolute temperature, and the density of the buffer  $\rho=1.018$  g/mL was measured pycnometrically.

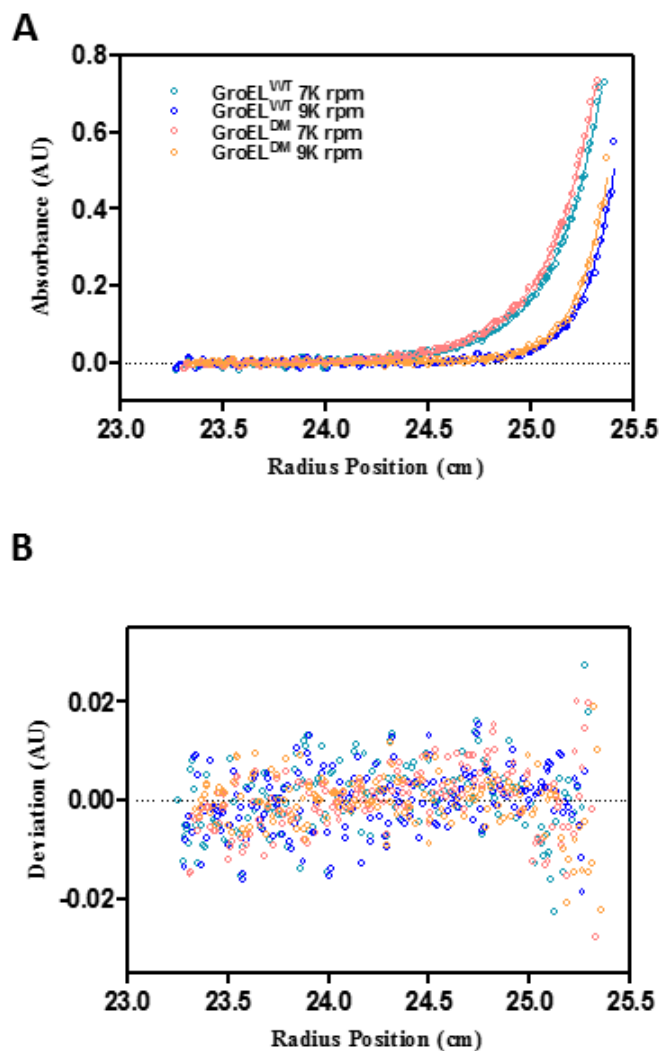


**Figure 3-5 Sedimentation Equilibrium Analysis of GroEL.** **A)** The absorption of proteins was monitored against the radial position as spinning at 7000 (green and red) and 9000 rpm (blue and orange) at 20°C for GroEL<sup>WT</sup> (green and blue) and GroEL<sup>DM</sup> (red and orange). **B)** The data was fitted by WinNonLin with randomly distributed residuals yielding MW as shown in Table 3-1.

Protein species	$\sigma$	$\sigma$ range	Partial specific volume	Derived MW
GroEL <sup>WT</sup>	4.256	4.022-4.351	0.7420	800 <sub>±</sub> 33 kDa
GroEL <sup>DM</sup>	4.296	4.087-4.513	0.7424	800 <sub>±</sub> 39 kDa

**Table 3-1 Parameters in Sedimentation Equilibrium Analysis.** The  $\sigma$  value and its range obtained by fitting the absorption against the radial position using WinNonLin were combined with the partial specific volume to calculate MW of each protein.

As shown in figure 3-5, the concentration distribution of both GroEL<sup>WT</sup> and GroEL<sup>DM</sup> were overlapping with each other at 7000 and 9000 rpm and the fitting results showed randomly distributed residues, suggesting the data fitted well with the single-species model of purely one protein specie. The MWs derived were almost identical from the theoretical value calculated from amino acid composition (table 3-1).

### 3.2.3.2 Sedimentation Velocity

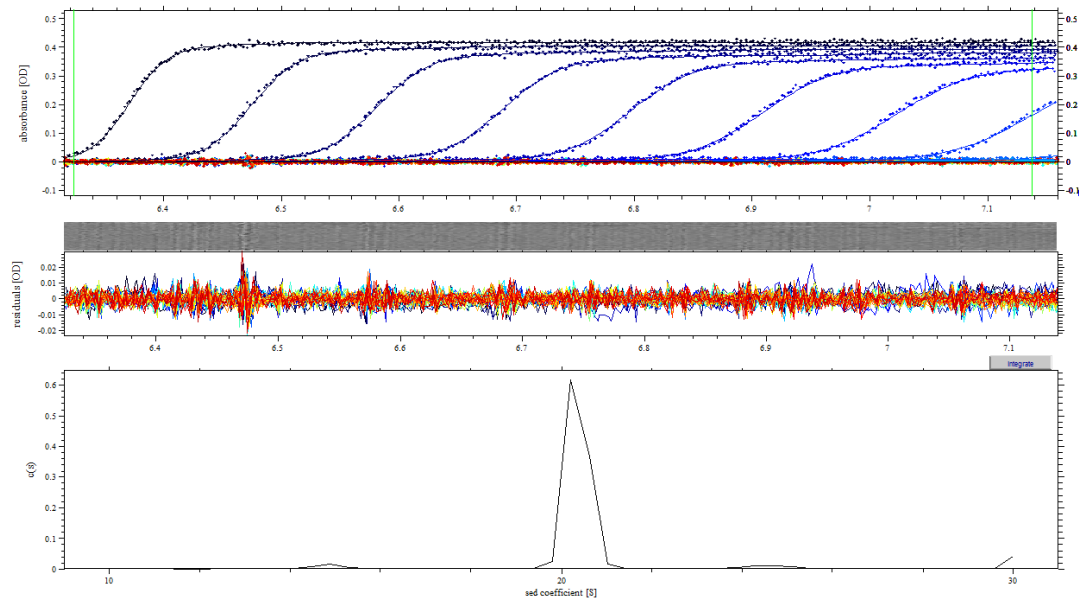


**Figure 3-6 Sedimentation Velocity Analysis of GroEL<sup>WT</sup>.** A) The absorption of proteins was monitored against the radial position as spinning at 40,000 rpm at time intervals, 20°C. B) The residuals of the data fitting with SEDFIT and C) the distribution of the sedimentation coefficient yielded a MW of 800<sub>±</sub>20 kDa.

Using the same buffer as in the sedimentation equilibrium, the protein was loaded into a double sector cell with charcoal-filled Epon centerpieces. Scans across the centrifuge cell were taken at 278 nm versus radial position within the cell. The sedimentation was equilibrated at 20.3°C for at least an hour and run at 40,000 rpm. The sharp vertical spike at 6.0998 cm was taken as the position of the air-solution

meniscus and a total of 10 scans were taken in the experiment (figure 3-6). The sedimentation coefficient  $S$  derived for GroEL<sup>WT</sup> was  $20.405 \pm 0.007$  and a MW of  $800 \pm 20$  kDa was derived with SEDFIT<sup>84</sup>. The single peak distribution of sedimentation coefficient suggested the GroEL<sup>WT</sup> in this solution is uniformly in one species.

### 3.2.4 Mass Spectrometry

To address the question if the GroEL<sup>WT</sup> sample was intact in its amino acid sequence, matrix assisted laser desorption ionization (MALDI) mass spectrometry was employed to measure the MW of a single subunit of GroEL<sup>WT</sup>. The protein was dialyzed exhaustively against 10 mM NH<sub>4</sub>CH<sub>3</sub>COOH, where both ammonium and acetate ion would evaporate in the matrix upon laser illumination. Three molecular markers insulin, apo-myoglobin and albumin were mixed with GroEL sample as inserted maker. At pH 7.0, the GroEL<sup>WT</sup> monomer carried around 18.8 charges and at this condition showed a clear spectrum of mass/charge ratios (figure 3-7, A). The convolution of the mass spectrum yielded a single peak of 57198 Da, which was close to the 57329 Da calculated from the amino acid sequence (figure 3-7, B).

The native PAGE, electron microscopy and sedimentation equilibrium experiments offered unequivocal evidence that GroEL<sup>DM</sup>, which lacks 14 charges within its molecule, still maintained the tetradecameric structure and enabled us to further investigation on it.

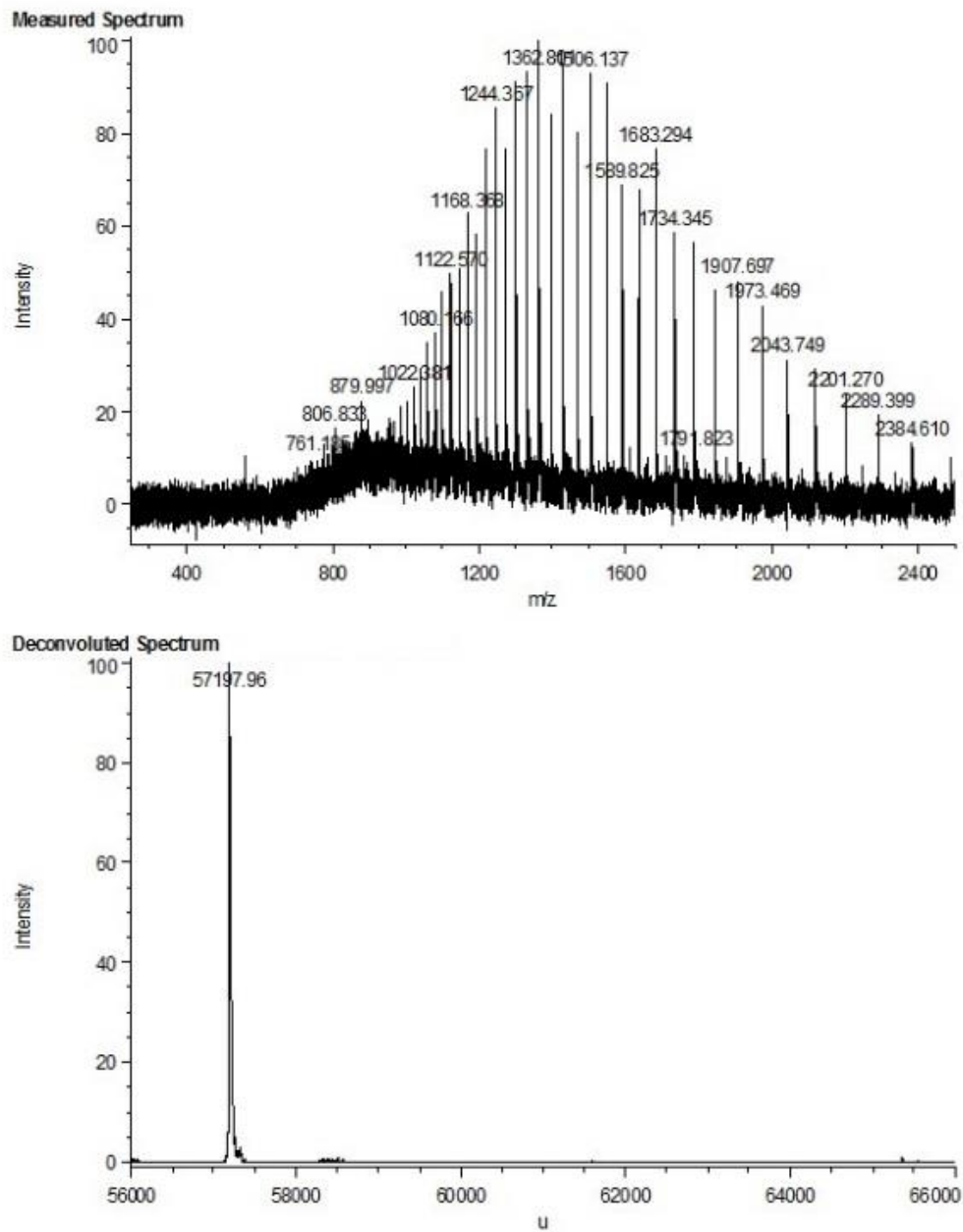


**Figure 3-7 Mass Spectrometry Analysis of GroEL<sup>WT</sup>.** **A)** The distribution of ionized mass over charge of peptides from GroEL<sup>WT</sup>. **B)** The convoluted spectrum shows a peak of 57197Da, consistent with the MW calculated from amino acid sequence.



### 3.3 Steady State ATPase Assay

The rate of GroEL hydrolyzes ATP at steady state is the result of an equilibrium between many allosteric effectors. The ATPase profile as a function of an allosteric ligand concentration reveals the intrinsic modulating mechanism of this ligand. As discussed in the introduction, there are many allosteric ligands of GroEL: GroES, ATP, ADP, K<sup>+</sup>, and SPs. Their role in the chaperonin cycle can be investigated by measuring the ATPase profile as a function of their concentration.

#### *3.3.1 Steady State ATPase Assay as of [ATP] under Standard Condition*

The estimated GroEL<sub>14</sub> concentration in a living cell is 2.6 μM<sup>85</sup> and the physiological K<sup>+</sup> and Mg<sup>2+</sup> concentration is 100-200 mM and 10 mM respectively<sup>86</sup>. In a standard ATPase assay, the GroEL subunit concentration was at 2 μM, K<sup>+</sup> concentration was 100 or 200 mM, and Mg<sup>2+</sup> was 10 mM as detailed in each assay. The standard ATPase assay performed using both GroEL<sup>WT</sup> and GroEL<sup>DM</sup> in the presence and absence of SP as described in Chapter 2.

For the GroEL<sup>WT</sup> ATPase profile, there were two distinctive transitions. As the [ATP] increased from 0 to ~7 μM, the ATPase activity increased from 0 to 6.2±0.1 turnovers/min. As [ATP] increased more from 7 μM to 1000 μM, the ATPase activity decreased from 6.2±0.1 to 2.02±0.08 turnovers/min (see figure 3-8, blue empty dots). These two successive activity transitions were typical revelations of the allosteric transitions within the two rings of GroEL. The first transition came with the binding of ATP to the vacant rings, and this ring was going from **T** state to **R** state. This was generally noted the transition from **TT** to **TR** for the two ring GroEL. Since **T** state had a higher ATPase activity<sup>82</sup>, the first transition came out as an increase of

ATPase activity. Subsequent binding of ATP to the other ring of GroEL promoted the second ring to transit from the **T** state to the **R** state, and this was generally noted as **TR** to **RR** transition. The behavior of GroEL<sup>WT</sup> steady state ATPase activity at 37°C was more or less the same as it was at 30°C<sup>52</sup>.

SP binds to the **T** state of GroEL and displaced the equilibrium to the **T** side, even in the presence of nucleotide. For GroEL<sup>WT</sup>, the ATPase profile in the presence of saturating SP showed only one transition (see figure 3-8, blue filled dots). From 0 to 25 μM, the rate of ATP hydrolysis increased from 0 turnovers/min to 10.4±0.4 turnovers/min. From 25 μM to 1000 μM, the ATPase rate remained constant at 10.4±0.4 turnovers/min. Compare this result with the ATPase profile in the absence of SP, the second **TR** to **RR** transition disappeared. This is due to the fact that SP binds to the *trans* ring of GroEL, promoted its transition from the **R** state to the **T** state. SP binding to GroEL was favored that at saturating concentration of ATP both rings of GroEL could not fully be converted to their **R** state and this was different as to GroEL<sup>DM</sup> as discussed later.

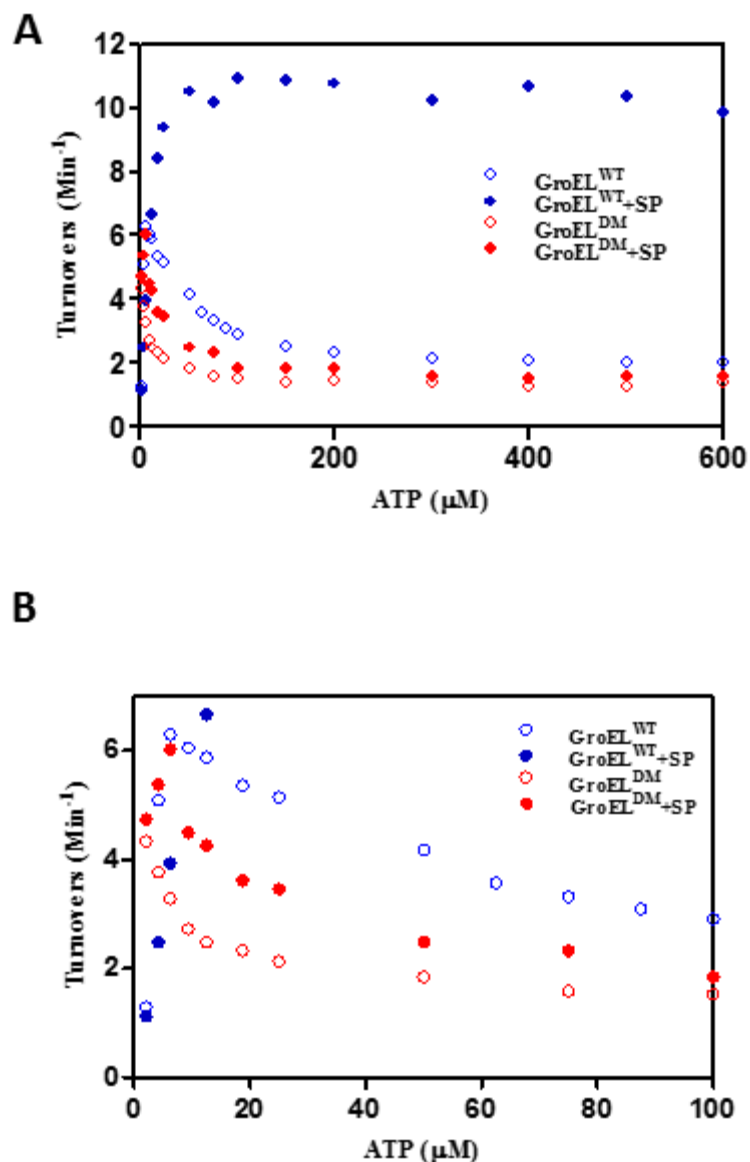


**Figure 3-8 Steady State ATPase of GroEL<sup>WT</sup> and GroEL<sup>DM</sup>.** Empty blue dot is for GroEL<sup>WT</sup> in the absence of SP and filled blue dot was for GroEL<sup>WT</sup> in the presence of SP. Empty red dot was for GroEL<sup>DM</sup> in the absence of SP and filled red dot is for GroEL<sup>DM</sup> in the presence of SP. The measurement was performed at 20 mM Tris pH 7.5, 100 mM K<sup>+</sup>, and 10 mM Mg<sup>2+</sup> at 37°C. **B** is an expansion of the lower ATP concentration region in **A**.

For GroEL<sup>DM</sup>, the ATPase profile as a function of [ATP] was distinctive (figure 3-8, empty red dots). From 2 μM to 1000 μM, the ATPase activity decreased from 4.30±0.04 turnovers/min to 1.35±0.06 turnovers/min. This single declining transition resembled the second transition with GroEL<sup>WT</sup>, the **TR** to **RR** transition.

This exhibited an unusual property of GroEL<sup>DM</sup> at the point where ATP concentration equaled to the concentration of subunits, i.e. 2  $\mu$ M, all the GroEL were already in the **R** state.

### 3.3.2 Steady State ATPase Assay as of [ATP] at Altered Condition

As discussed above, the absence of the **TT** to **TR** transition of GroEL<sup>DM</sup> was attributed to the fact that all the GroEL<sup>DM</sup> was bound with ATP at concentrations where it was equal to the subunit concentration. To test this idea, ATPase activity was measured at lower GroEL<sup>DM</sup> concentrations. The reason for this was: 1) once the subunit concentration was lowered, ATPase activity at lower ATP concentrations could be measured without going into the sub-stoichiometric region, 2) we proposed that these mutations destabilize **T** state and thus favor the **R** state of GroEL which had a higher affinity towards nucleotides. Only when we lowered the subunit concentration could one observe the ATP concentration region where the first transition took place.

The result was as predicted (figure 3-9). Once the concentration of GroEL<sup>DM</sup> was lowered to 1, or 0.5  $\mu$ M, the first transition where ATPase activity increased as ATP concentration increased was seen. Still, for assays performed at 1 and 0.5  $\mu$ M GroEL<sup>DM</sup>, the lowest ATP concentration used to measure the ATPase activity was 1 and 0.5  $\mu$ M respectively. The second transition started at  $\sim$ 2  $\mu$ M ATP for both of these GroEL<sup>DM</sup> concentrations. Like the standard assay, ATPase activity measured at 4  $\mu$ M showed a single **TR** to **RR** transition. I concluded that the loss of the first **TT** to **TR** transition was due to GroEL<sup>DM</sup> being fully saturated at the starting ATP concentration with subunits concentration higher than 2  $\mu$ M.

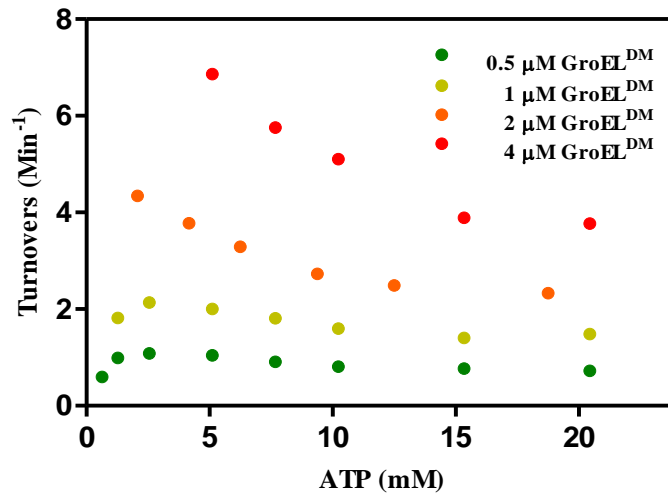


**Figure 3-9 Steady State ATPase of GroEL<sup>DM</sup> at Lower Subunit Concentration.** Red, orange, yellow, and green were at 4μM, 2μM, 1μM, and 0.5μM of subunit respectively. The measurement was performed at 20 mM Tris pH 7.5, 100 mM K<sup>+</sup>, and 10 mM Mg<sup>2+</sup> at 37°C.

Another way to reveal the first transition was to measure the ATPase activity as a function of [ATP] at a lower K<sup>+</sup> concentration. K<sup>+</sup> affected the allosteric equilibrium of GroEL by increasing the affinity of nucleotide binding. The crystal structure also revealed there was a K<sup>+</sup> binding site at the nucleotide binding site<sup>37,87</sup>. When the K<sup>+</sup> concentration was lowered to 1 mM, the ATPase activity of GroEL<sup>DM</sup> showed two successive transitions, just like GroEL<sup>WT</sup> (figure 3-10, blue circle). The **TT** to **TR** transition occurred at ATP concentration from 0 to ~12 μM, and the **TR** to **RR** transition occurred from ~12 μM and higher concentrations. The ATPase rate increased from 0 to 2.0±0.1 turnovers/min, and then decreased to 1.25±0.04 turnovers/min. The highest ATPase activity at 1 mM K<sup>+</sup> concentration was the same as the initial ATPase activity at 100 mM K<sup>+</sup>. This further supports the conclusion that the single, declining transition at 100 mM K<sup>+</sup> was the **TR** to **RR** transition.

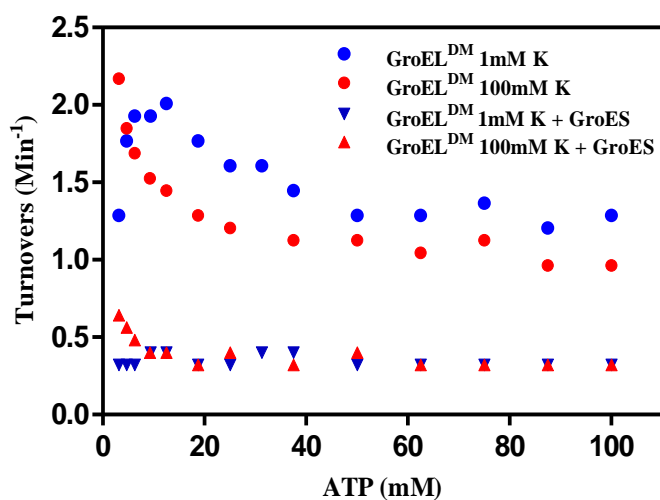


**Figure 3-10 Steady State ATPase of GroEL<sup>DM</sup> at Lower K<sup>+</sup> Concentration.** Red traces were for GroEL<sup>DM</sup> measured at 100 mM K<sup>+</sup> and blue traces were at 1 mM K<sup>+</sup>. Circles were for GroEL<sup>DM</sup> measured at the absence of GroES and triangles were for measurement at the presence of GroES. 2 $\mu$ M GroEL<sup>DM</sup> subunit and 2.5 $\mu$ M of GroES subunit were used in this measurement. The measurement was performed at 20 mM Tris pH 7.5, 100 mM K<sup>+</sup>, and 10 mM Mg<sup>2+</sup> at 37°C.

The ATPase activity measured at both 1 and 100 mM K<sup>+</sup> in the presence of GroES yielded 0.320 $\pm$ 0.001 turnover/min. This slow ATP hydrolysis was comparable to that of SR1 in the presence of GroES. Due to the lack of the *trans* ring which sent the signal to dissociate GroES, SR1 did not hydrolyze ATP once bound with GroES. Here, the low ATPase activity of GroEL<sup>DM</sup> in the presence of GroES probably suggested that GroEL<sup>DM</sup> and SR1 terminated ATP hydrolysis after binding GroES. The slow residual turnover could be attributed to the occasional dissociation of GroES. Further discussion on GroEL<sup>DM</sup> interaction with GroES will be found later in the chapter.

More interestingly, the ATPase activity of GroEL<sup>DM</sup> in the presence of saturating SP was largely different from that of GroEL<sup>WT</sup>. The overall ATPase activity of GroEL<sup>DM</sup> in the presence of SP showed a single, declining transition

parallel to the ATPase activity in the absence of SP (figure 3-8 A, filled red dots). From 2  $\mu\text{M}$  to 100  $\mu\text{M}$ , SP stimulated the ATPase activity by merely  $\sim 2$  fold, and it did not stimulate the hydrolysis of ATP at ATP concentrations higher than 100  $\mu\text{M}$ . SP stimulated ATPase activity of GroEL by displacing the equilibrium to the **T** side. At low ATP concentrations range (0-100  $\mu\text{M}$ ), although the GroEL<sup>DM</sup> was converted to the **R** state, SP could still displace the equilibrium to the **T** state slightly. However, at ATP concentrations higher than 100  $\mu\text{M}$ , SP barely affected the equilibrium of GroEL<sup>DM</sup>. Thus one could conclude at physiological conditions, ATP dominated the allosteric state of GroEL<sup>DM</sup> and SP did not have any effect on it.

### 3.3.3 Steady State ATPase Assay as of [SP]

The ATPase activity measured at 500  $\mu\text{M}$  ATP and 100 mM  $\text{K}^+$  as a function of [SP] yielded two distinctive behaviors between GroEL<sup>WT</sup> and GroEL<sup>DM</sup> (figure 3-11). For GroEL<sup>WT</sup>, as the SP concentration increased, the ATPase activity increased. At saturating SP concentrations, the ATPase activity was stimulated  $\sim 5$  fold. The ATPase activity as a function of SP concentration fitted well with the one site binding equation, and a binding affinity of  $\alpha$ -LA of  $0.29 \pm 0.4$   $\mu\text{M}$  was derived. This dissociation constant is similar to the measurement as reported by ITC analysis previously<sup>88</sup>.

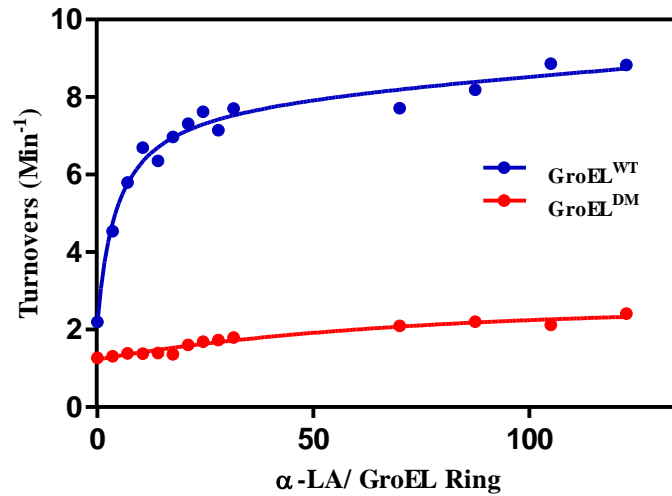


**Figure 3-11 Steady State ATPase of GroEL<sup>DM</sup> and GroEL<sup>WT</sup> as function of [SP].** Red traces were for GroEL<sup>DM</sup> measurement and blue traces were for GroEL<sup>WT</sup>. Each trace was fit into one site binding model yielding a binding affinity of  $0.29 \pm 0.4 \mu\text{M}$ . The measurement was performed at 20 mM Tris pH 7.5, 100 mM K<sup>+</sup>, 1 mM DTT, and 10 mM Mg<sup>2+</sup> at 37°C.

However, the same measurements on GroEL<sup>DM</sup> yielded totally different results (figure 3-11, red dots). SP did not stimulate the ATPase activity of GroEL<sup>DM</sup>, even at saturating concentrations of denatured α-LA, the ATPase activity was merely ~1.6 fold as in the absence of SP. This was consistent with the previous result in section 3.3.1.1 that at concentrations higher than 100 μM ATP, SP did not stimulate the ATPase activity.

ATP promoted the transition of GroEL from the **T** state to the **R** state and, thus displaced the equilibrium to the **R** side in the GroEL allostery. SP, on the other hand, binds preferentially to the **T** state of GroEL and thus favored the **T** state side. At 100 mM K<sup>+</sup>, ATP displaced the equilibrium of GroEL to the **R** side while SP shifted it to the **T** side. For GroEL<sup>WT</sup>, SP dominated the equilibrium to the **T** side and the effect of ATP in the presence of SP was negligible. This was shown by the fact that at saturating ATP concentration, SP still stimulated ATPase activity of GroEL<sup>WT</sup>



by the same magnitude as it did at lower ATPase concentrations. However, removal of these salt bridges destabilized the **T** state and thus, GroEL<sup>DM</sup> favored **R** state. At low ATP concentration (0-100  $\mu$ M) although the majority of GroEL<sup>DM</sup> was in the **TR** state, SP still stimulated the ATPase activity slightly, suggesting it displaced the equilibrium to the **T** state by certain extent. At high ATP concentration (>100  $\mu$ M), even using saturating amounts of SP did not stimulate the hydrolysis of ATP, indicating an inability of SP to shift GroEL<sup>DM</sup> back to **T** state. The result was consistent with the idea that the mutations disrupted these salt bridges, destabilizing the **T** state GroEL and thus favoring its **R** state.

### 3.4 Pre-steady state ATPase Analysis

It was observed that the steady-state rate of hydrolysis of ATP by GroEL<sup>DM</sup> was generally lower than that of GroEL<sup>WT</sup>; the highest rate of GroEL<sup>WT</sup> at the transition from **TR** to **RR** was  $6.2 \pm 0.1$  turnovers/min while GroEL<sup>DM</sup> had a highest ATPase activity of  $4.30 \pm 0.04$  turnovers/min. It was even more clear in the presence of GroES, GroEL<sup>WT</sup> ATP hydrolysis occurred at a rate of  $0.50 \pm 0.02$  per minute while GroEL<sup>DM</sup> only at  $0.320 \pm 0.001$  per minute. The decrease in ATPase activity raised the question of whether these mutations actually compromised the intrinsic ATPase activity of GroEL.

To address the possibility that the intrinsic chemistry of ATP hydrolysis was affected in the nucleotide binding pocket of GroEL by these mutations, the pre-steady state ATP hydrolysis analysis was performed with multiple strategies. Among them, PBP<sup>MDCC</sup> was employed to monitor the release of the ATP hydrolysis product, phosphate, in real time as described in Chapter 2.

### 3.4.1 Measurement of Pi release from GroEL-GroES<sub>1</sub> complex

Other research in our lab indicated that the hydrolysis of ATP by the asymmetric GroEL-GroES<sub>1</sub> complex, as revealed by the release of Pi, could be described by a complex kinetics mechanism<sup>43</sup>. After the initiation of the reaction with the acceptor state GroEL-GroES<sub>1</sub> complex, where there is no ADP bound to the *trans* ring, the Pi release could be described as a burst kinetics with a linear phase (figure 3-12). The burst phase corresponded to the hydrolysis of ATP at the vacant *trans* ring of GroEL and the linear phase was indicated by the entering of steady state hydrolysis.

A more detailed examination of the effectors and their impact on each phase of the Pi release is not the focus of this study but others in our lab<sup>43</sup>. The main purpose here is to exam whether the intrinsic ATPase activity is affected by these mutations. Among these phases, the burst phase actually represents the chemistry of ATP hydrolysis in the active site as reasoned above (figure 3-1). The burst kinetics described by this curve fits well as a pseudo first order reaction and the rate of this phase for GroEL<sup>WT</sup> and GroEL<sup>DM</sup> are  $0.49 \pm 0.03 \text{ s}^{-1}$  and  $0.45 \pm 0.02 \text{ s}^{-1}$  respectively. This indicates the intrinsic ATPase activity, where the breakage of the  $\gamma$ -phosphate from ATP catalyzed in the active site of GroEL, is not altered by these mutations.

For GroEL<sup>WT</sup> in the presence of 5 and 10 fold of SP, the slope of the linear phases increased (figure 3-12). This indicated the steady state ATPase activity was stimulated by SP, and it was in an agreement with the rate measured in the SP titration with GroEL<sup>WT</sup> ATPase assay. For GroEL<sup>DM</sup>, the slope of the linear phase was not affected by the SP added to the reaction. This was also in an agreement with

the steady state ATPase assay that SP did not stimulate the ATPase activity of GroEL<sup>DM</sup>.

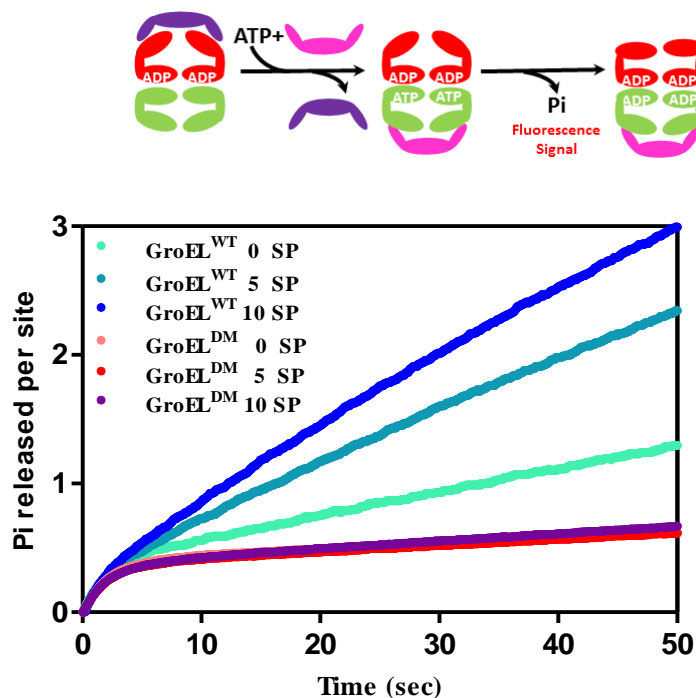


**Figure 3-12 Pre-steady State ATPase activity of GroEL<sup>WT</sup> and GroEL<sup>DM</sup>.** The release of Pi from the GroEL<sup>WT</sup> or GroEL<sup>DM</sup> acceptor complex were monitored with the PBP<sup>MDCC</sup> in a stop flow instrument installed with a cut-off filter of 455 nm. Green, cyan, blue traces were of GroEL<sup>WT</sup> with 0, 5, and 10 fold of denatured  $\alpha$ -LA. Pink, orange, and purple were of GroEL<sup>DM</sup> with 0, 5, and 10 fold of denatured  $\alpha$ -LA. Both GroEL<sup>WT</sup> and GroEL<sup>DM</sup> released one Pi per *trans* ring site and the burst phase yielded a rate of  $0.49 \pm 0.03 \text{ s}^{-1}$  and  $0.45 \pm 0.02 \text{ s}^{-1}$  respectively. The measurement was performed at 20 mM Tris pH 7.5, 100 mM K<sup>+</sup>, and 10 mM Mg<sup>2+</sup> at 37°C.

### 3.4.2 Measurement of ADP Release from GroEL-GroES<sub>1</sub> Complex

Previous research in our lab indicated that the release of ADP from the *trans* ring of GroEL complex was the rate limiting step in the chaperonin cycle in the absence of SP<sup>43</sup>. In the previous section we showed that the hydrolysis of ATP was not compromised by GroEL<sup>DM</sup> and explained that the reason this variant hydrolyzes ATP slower could be a result of the fact the releasing ADP by GroEL<sup>DM</sup> was hampered.

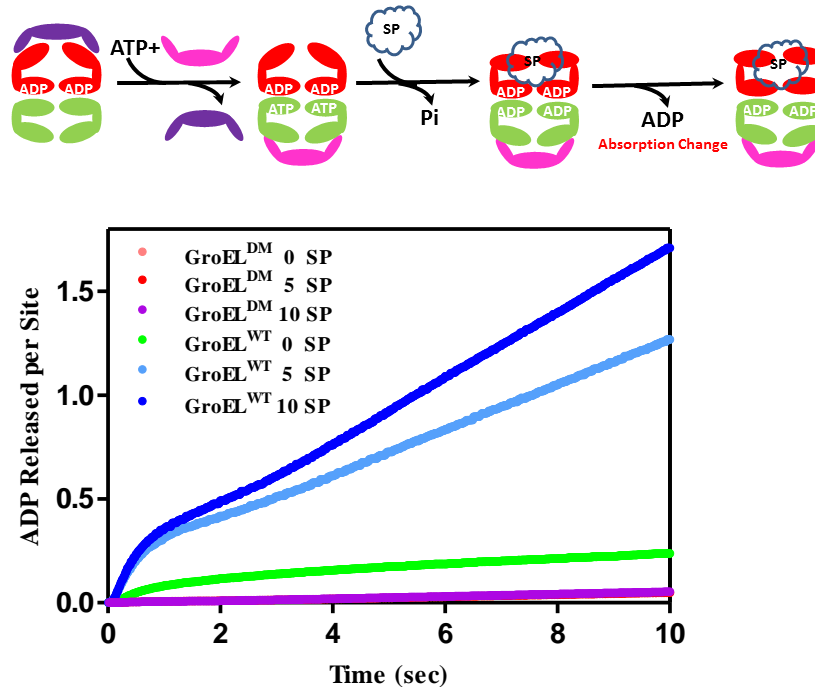


**Figure 3-13 Pre-steady State ADP Release from GroEL<sup>WT</sup> and GroEL<sup>DM</sup>.** The release of ADP from the GroEL<sup>WT</sup> or GroEL<sup>DM</sup> acceptor complex were monitored with the coupling enzyme system in a stop flow instrument set in absorption mode. Green, cyan, blue traces were of GroEL<sup>WT</sup> with 0, 5, and 10 fold of denatured  $\alpha$ -LA. Pink, orange, and purple are of GroEL<sup>DM</sup> with 0, 5, and 10 fold of denatured  $\alpha$ -LA. The measurement was performed at 20 mM Tris pH 7.5, 100 mM K<sup>+</sup>, and 10 mM Mg<sup>2+</sup> at 37°C.

The release of ADP from GroEL<sup>WT</sup>-GroES<sub>1</sub> acceptor state complex was different in the absence and presence of SP (figure 3-13). In the absence of SP, the GroEL<sup>WT</sup>-GroES<sub>1</sub> acceptor state complex released ADP at a very slow rate, and there was an initial burst of ADP release with a small amplitude about 0.2 ADP released per GroEL subunit as reported<sup>43</sup>. However, in the presence of SP, the release of ADP was greatly accelerated. The initial burst of ADP release corresponded to ~0.5 ADP per subunit and then it was followed by a brief lag phase<sup>43</sup>. The system then entered the steady-state ADP release where the rate was linear with time. This steady state ADP release rate was positively proportional to the SP concentration. It was observed that more SP present in the solution, the rate ADP released was greatly accelerated.

For GroEL<sup>DM</sup>, no matter in the presence or absence of SP, the ADP release was significantly slower than GroEL<sup>WT</sup> with no apparent burst phase (figure 3-12).

This multi-phase ADP release mirrors the multiple events that occurred with the release of Pi in this GroEL-GroES system (figure 3-11). First, ATP bound to the vacant *trans* ring of the acceptor state complex. This binding triggered the dissociation of the GroES on the *cis* ring and it took about 100 ms as described previously<sup>52</sup>. The nucleotide binding pocket remained closed until GroES was discharged, so there was no ADP release on this time scale. The previous vacant *trans* ring became bound with ATP and GroES, namely the new *cis* ring while the previous *cis* ring discharged GroES and became the new *trans* ring.

After that came along the release of ADP from the new *trans* ring, which was largely dependent on SP. In the absence of SP, the amplitude of the burst was ~0.2 ADP per subunit. As rationalized before, only one ring was releasing ADP at a time, so it was about 2.8 ADP released in the burst phase from the new *trans* ring. Contrastingly, in the presence of SP the amplitude of the burst was ~0.5 per site corresponding to ~7 ADP released per *trans* ring. This means almost all the ADP on the *trans* ring was released upon binding of ATP on the other side of GroEL<sup>WT</sup> in the presence of SP.

The dissociation of GroES from the previous *trans* ring allowed the nucleotide binding pocket to be open by visiting the **T** state (figure 3-11, red box). This made the release of ADP from this ring possible<sup>47</sup>. The following release of ADP and loss of synchronicity indicated the beginning of the steady state ADP release phase. Still, the rate of steady state ADP release was dominated by the concentration of SP for

GroEL<sup>WT</sup>. The more SP present, the faster the release of ADP in the steady state. For GroEL<sup>DM</sup>, the steady state ADP release was independent of SP present at the ATP concentration used in this experiment.

Other groups have measured the ATPase activity by following the oxidation of NADH on the stop flow instrument with this coupling enzyme system<sup>89</sup>. They reached the opposite conclusion and found that ADP release from GroELS complex was not the rate limiting step. Their experiment was compromised when: 1) the K<sup>+</sup> concentration in the experiment they carried out was at 5 mM. As mentioned above, the physiological K<sup>+</sup> concentration is actually 100-200 mM. Previous data showed that at 5 mM K<sup>+</sup>, where this group performed their research, GroEL actually lies in the **TR** state where it had the highest ATPase activity and ADP release at that K<sup>+</sup> concentration was not the limiting step<sup>51</sup>. 2) The coupling enzyme in the assay this group used was only 5 U/mL and to our knowledge this coupling enzyme concentration could not consume the released ADP from GroEL in a timely manner and ADP release was no longer the rate limiting step. Since their data was not the real time representation of the release of ADP, the conclusion based on that should not reach a solid conclusion about the limiting step in the chaperonin cycle.

### **3.5 GroES dissociation kinetics from GroEL<sup>WT</sup> and GroEL<sup>DM</sup>**

Binding of ATP to the *trans* ring sends an allosteric signal to the *cis* ring that discharges bound GroES (figure 3-11). In the previous section, we examined the inherently low ATPase activity of GroEL<sup>DM</sup> and attributed this to the slow release of ADP from the *trans* ring of GroEL<sup>DM</sup>. However, the release of ADP from the new *trans* ring was preceded by two successive events were happening ahead of time: 1)

the GroES on the *cis* ring was discharged first; 2) the previous *cis* ring, now a *trans* ring, had to visit **T** state in order to open its seven nucleotide binding pocket (figure 3-1, red box). It was worth questioning if the slow release of ADP was due to the impeded discharge of GroES from the *cis* ring as a result of the designed mutations.

To address this concern, the acceptor GroEL-GroES<sub>1</sub> FRET complex was made as described in Chapter 2. Note that there was no ADP bound on the *trans* ring and the discharge of GroES on the *cis* ring was mainly dependent on the binding of ATP on the *trans* ring and the allosteric signal sent on *trans* ring.

For the GroEL<sup>WT</sup>-GroES complex, the dissociation of GroES<sup>F5M</sup> from the acceptor complex yielded a half-life of  $4.6 \pm 0.2$  ms and the GroEL<sup>DM</sup>-GroES acceptor state complex yielded  $4.8 \pm 0.2$  ms (figure 3-14). This indicates after binding of ATP to the *trans* ring, the discharge of GroES from the *cis* ring of GroEL<sup>WT</sup> and GroEL<sup>DM</sup> took the same amount of time. The mutations D83A/R197A did not compromise the ability of GroEL to undergo the conformational change that discharges GroES.

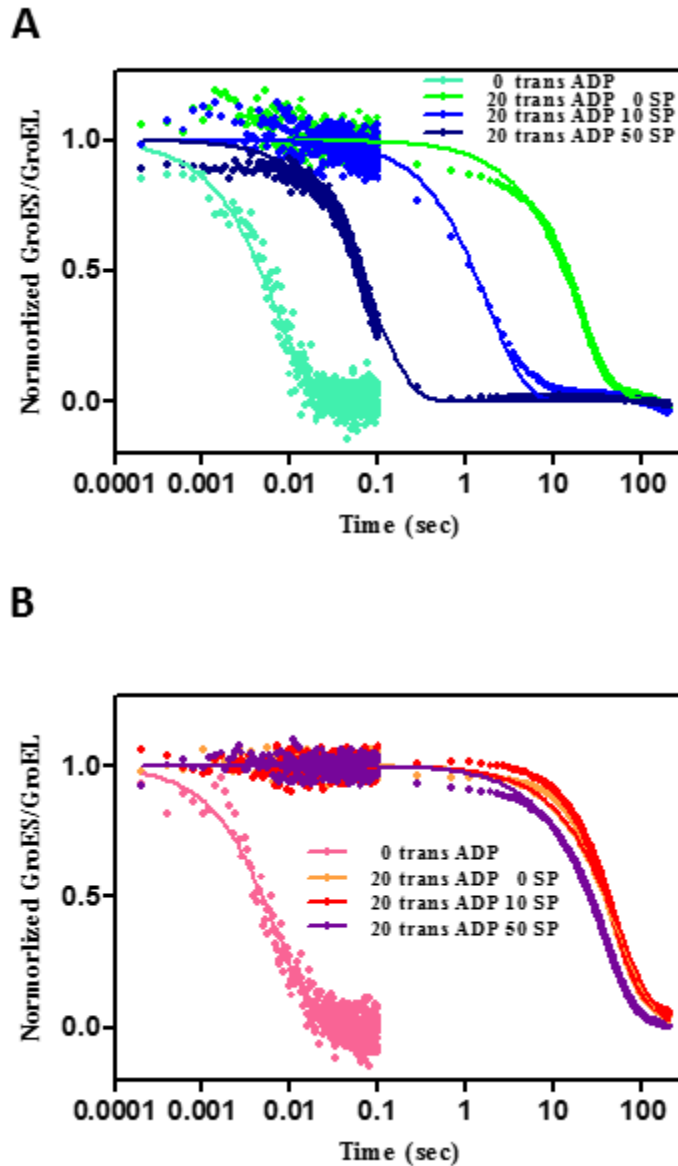
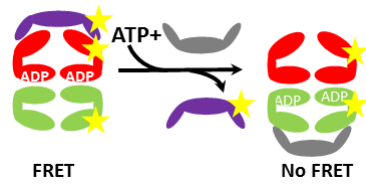


**Figure 3-14 Dissociation of GroES from the GroELS Complex.** In a stop flow instrument, the fluorescence emission change at 520 nm was monitored as GroES dissociate from GroELS complex. **A)** GroES dissociation from GroEL<sup>WT</sup>-GroES complex: cyan was from the acceptor complex, green was from the resting complex with no SP, blue was from the resting complex with 10 fold SP, and dark blue was from the resting complex with 50 fold SP. **B)** GroES dissociation from GroEL<sup>DM</sup>-GroES complex: pink was from the acceptor complex, orange was from the resting complex with no SP, red was from the resting complex with 10 fold SP, and purple was from the resting complex with 50 fold SP.



ADP	0 $\mu$ M		20 $\mu$ M		
	SP	0 fold	0 fold	10 fold	50 fold
GroEL <sup>WT</sup>	4.6 $\pm$ 0.2 ms	12.9 $\pm$ 0.3 sec	1.2 $\pm$ 0.1 sec	60 $\pm$ 1.0 m.sec	
GroEL <sup>DM</sup>	4.8 $\pm$ 0.2 ms	37.4 $\pm$ 0.7 sec	38.8 $\pm$ 0.9 sec	24.6 $\pm$ 0.4 sec	

**Table 3-2 Half-Life of GroES Dissociation from the “Bullet” Complex.** The FRET signal obtained of GroES dissociation from the GroEL-GroES<sub>1</sub> “bullet” complex under each condition by fitting the fluorescence signal with one phase decay. The experiments were conducted in buffer containing 20 mM Tris pH 7.5, 200 mM K<sup>+</sup>, and 10 mM Mg<sup>2+</sup> at 37°C.

The experimental procedure for making the acceptor complex was the same as above except 40  $\mu$ M ADP was supplemented into the complex to make it the resting complex. After initiation of the release, the half-life of GroES dissociation was greatly elongated compared that with the acceptor complex. GroEL<sup>WT</sup>-GroES resting complex yielded a half-life of 12.9 $\pm$ 0.3 sec and GroEL<sup>DM</sup>-GroES resting complex yielded 37.4 $\pm$ 0.7 sec. The half-life of GroES release from GroEL<sup>DM</sup> resting complex was almost tripled compared with that of GroEL<sup>WT</sup>. Previous experiment in our lab obtained a half-life of ~50 sec for GroEL<sup>WT</sup>. In that experiment, the condition was such that it was performed at 30°C which is 7°C lower than this set up<sup>52</sup>. Since GroES dissociation from the acceptor state complex suggested that the conformational change that discharges GroES was not hampered by these mutations, the only reason could be that the *trans* bound ADP on GroEL<sup>DM</sup> exchanged slower than that of GroEL<sup>WT</sup>.

Previous research suggests SPs binds to the **T** state of GroEL and promotes the release of ADP from *trans* ring. To test this suggestion, SP were added to the initiation step of the experiment. When 10 fold and 50 fold SP were added to syringe B, the half-life of GroES dissociation from GroEL<sup>WT</sup>-GroES complex was shortened to 1.2 $\pm$ 0.1 sec, and 60 $\pm$ 1.0 ms respectively. However, the same SP did not affect the

kinetics of GroES dissociation from GroEL<sup>DM</sup>-GroES resting complex. The half-life of GroES dissociation yielded  $38.8 \pm 0.9$  sec and  $24.6 \pm 0.4$  sec at 10 and 50 fold of SP. This again, confirmed that SP did not affect the release of ADP from the *trans* ring and thus ATP/ADP exchange was not affected even at the presence of SP. In turn it explains why SP are unable to alter the residence time of GroES.

In this chapter, we examined the structural and enzymatic characteristics of GroEL<sup>DM</sup>. Mutations destabilized **T** state did favor the **R** state of GroEL, as shown in the steady state ATPase assay, but did not hinder the intrinsic ATPase activity or the conformational change from **R** to **T**. SPs could not displace this mutant to its **T** side, and ADP release was greatly slowed. The interaction between GroEL<sup>DM</sup>, SPs and ADP is discussed in the following chapters.

## Chapter 4 Characterization of “Football” Complex-its Formation and Allosteric Regulation

### 4.1 Introduction

The current dogma of the chaperonin cycle involves the asymmetric, GroEL-GroES<sub>1</sub> complex, as the folding active complex. In this model, ATP binds to one of the GroEL ring followed by binding of SP which takes ~0.2 sec. GroES association to the *cis* ring accomplishes the closure of the “Anfinsen” cage where the SP folding inside the GroEL cavity is isolated from the cytosol<sup>65</sup>. This hydrophilic environment of the “Anfinsen” cage mimics an infinite dilute solution that SP is passively folded. The only assistance offered by GroEL is merely a cage where isolation prevents aggregation<sup>63</sup>. There is an intrinsic timer laid inside the chaperonin and it is controlled by the hydrolysis of ATP (~10 sec). Following this, it takes less than 10 ms to trigger the release of GroES from the *cis* ring after the binding of ATP to the *trans* ring. The hydrolysis product ADP on the *trans* ring, however, takes a fixed amount of time (~0.8 sec) to dissociate and this dissociation of ADP is independent from other allosteric interactions, e.g. SP, on GroEL.

This view of chaperonin cycle was established on several experiments carried out with assumptions and procedure flaws that will be discussed later. However, emerging evidence shows that in the presence of SPs, the major population of GroELs complex is the symmetric, GroEL-GroES<sub>2</sub> “football” complex. There are two major findings that support this view: 1) The dynamics of the “football” population in the folding process are correlated with the amount of denatured SPs and 2) The kinetic properties of this symmetric complex. Currently, Sameshima *et al*

titrated the GroELS complex in the presence of ATP with SPs<sup>71</sup>. By calculating the FRET efficiency generated by Cy3 labeled on GroEL and Cy5 labeled on GroES, they concluded that the population of “football” complex increases as the SP concentration increases in a dynamically turning over system. However, there is little detail on how the “football” complex is formed and what role it plays in the chaperonin folding cycle.

Initially there was speculation that the GroEL-GroES<sub>2</sub> symmetrical complex was the major species in the chaperonin folding cycle since it has been proved that GroES binds to GroEL via an associative mechanism<sup>68</sup>. That is, the second GroES binds to the GroEL molecule when there is still the first GroES on board. The dissociative mechanism, on the other hand, points that the second GroES associates with GroEL after the first GroES molecule is fully discharged. The finding of such associative mechanism provides the mechanistic basis for the formation of “football” complex starting at the asymmetric “bullet” complex. However, the mechanism to form a GroEL-GroES<sub>2</sub> symmetric complex starting with the apo-GroEL remains unknown.

To further investigate the kinetics of “football” formation and its role in chaperonin-assisted protein folding, the FRET GroELS system developed in our lab was utilized. The IAEDANS was labeled on the K315C and F5M was labeled on the 98C on GroES. Various dynamic and kinetic experiments could be performed using this FRET system. There was one major limitation in the previous research that they defined the FRET efficiency of Cy3-Cy5 dye pair system in the presence of ATP·BeF<sub>x</sub> as 100% “football” population without actually supplying experimental

evidence. This could lead to serious theoretical over-interpretation of the data as it pertains to the negative cooperativity of GroEL study. In this research, the details of the population of “football” and “bullet” complex were examined in the molecular level. That was, the population of symmetrical GroEL-GroES<sub>2</sub> particles and asymmetrical GroEL-GroES<sub>1</sub> particle was examined by visualizing them under the electron microscope. Later research on the population of “football” and “bullet” complex were all based on this quantification which unequivocally established the experimental conditions for the complete formation of each complexes.

#### **4.2 Calibration of FRET Based System to Determine GroELS Stoichiometry**

GroELS nano-machine is one of the largest biological assemblies identified in nature. The asymmetric “bullet” complex has a diameter of ~140Å and height of 184 Å that can be clearly observed by transmission electronic microscope. Taguchi *et al* found that beryllium fluoride (BeF<sub>x</sub>) stops the hydrolysis of ATP by GroEL and upon addition the GroELS complex is sequestered at the double chamber “football” complex<sup>90</sup> while ADP·BeF<sub>x</sub> is formed and bound stably at the nucleotide binding site of the “bullet” complex. This ADP·BeF<sub>x</sub> formula is mimicking the  $\gamma$ -Pi of ATP via the Pi of ADP·Pi. Once the BeF<sub>x</sub> is present, the ADP· BeF<sub>x</sub> is recognized as non-hydrolysable ATP analogue and the complex formed in the presence of BeF<sub>x</sub> is stable.

Based on this, the complex formed by GroES and GroEL in condition containing ATP·BeF<sub>x</sub> and ADP·BeF<sub>x</sub> were examined under the electronic microscope as described in Chapter 2. Pictures were taken where the particles were distinguishable and clearly distributed. The particles in the image were purely of GroEL particles as indicated by mainly two types of observations: the top view and

the side view particles (figure 4-1, A). The side view took the majority and the two-fold symmetry could be observed that the GroEL structure was composed of two rings. There were a few top views among these where the seven-fold symmetry could be seen through the central cavity. For each of the nucleotide conditions (either ATP·BeF<sub>x</sub> or ADP·BeF<sub>x</sub>), the particles were categorized into three classes: the top view, the side view as “football” complex, and the side view as “bullet” complex. The number of each type of particles was analyzed by manually counting each type in the picture (figure 4-1, B). More than 1000 particles were analyzed and statistical analysis on the results was performed.

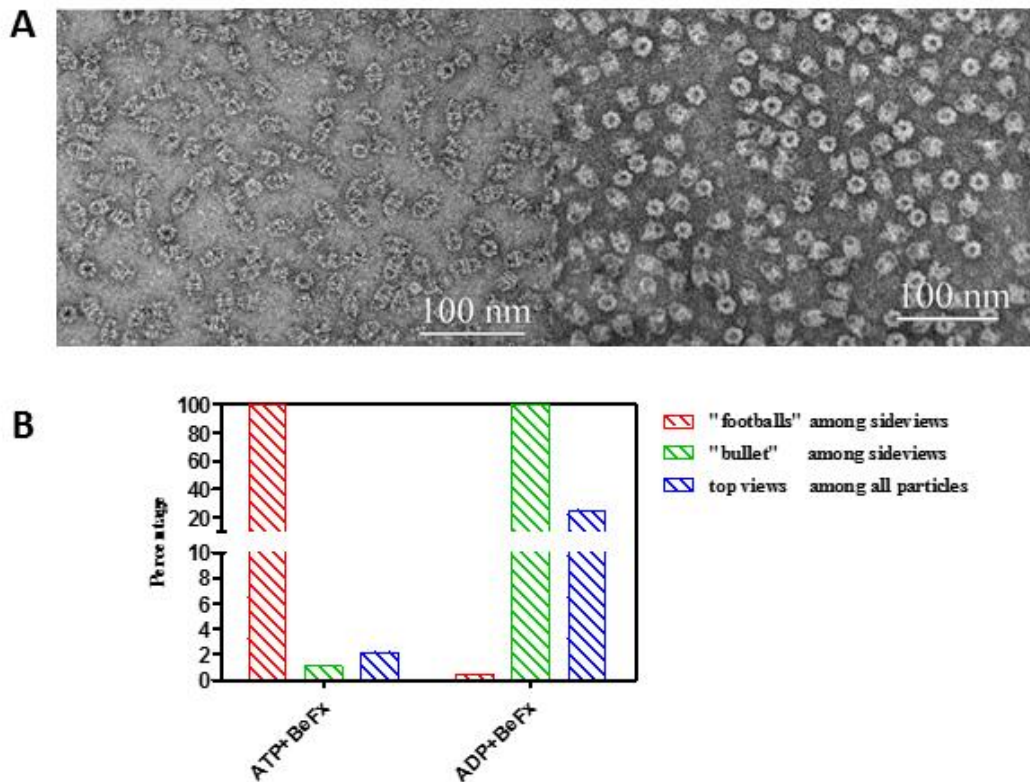


**Figure 4-1 Electron Microscopy of GroELs Complexes.** **A**, the electron microscope view of GroEL-GroES complex formed at the presence with ADP·BeF<sub>x</sub> (right) and ATP·BeF<sub>x</sub> (left). The scale bar was of 100 nm. **B**, statistics of the electron microscopy where the particles were categorized into two conditions each with two types: side views and top views. The red bar shows the “football” population among all side views and the green bar shows the “bullet” population among all side views. The blue bar shows the population of top views among all particles.

In general the particles yielded more top views in the ADP·BeF<sub>x</sub> condition than the ATP·BeF<sub>x</sub> condition (figure 4-1, B). 24.9% of particles were in the top view position (“standing” on the grid) when the complex was formed with ADP·BeF<sub>x</sub> and only 2.2% of them doing so when the complex was formed with ATP·BeF<sub>x</sub>. In the ADP·BeF<sub>x</sub> condition, 99.57% of the side views were of asymmetrical GroEL-GroES<sub>1</sub> “bullet” complex while only 0.43% of them were the symmetric GroEL-GroES<sub>2</sub> “football” complex. For the complex formed with ATP·BeF<sub>x</sub>, the numbers were inverted: there were 98.9% of “football” complex and 1.08% of “bullet” complex among all the side view particles.

The major conclusion drawn from the electronic microscope study was consistent with previous research<sup>90</sup>, that in the ADP·BeF<sub>x</sub> condition the GroELS complex was overwhelmingly GroEL-GroES<sub>1</sub> “bullet” complex while at the ATP·BeF<sub>x</sub> condition the GroELS complex was mostly the GroEL-GroES<sub>2</sub> “football” complex. A possible reason for the significantly higher amount of top view particles in the ADP·BeF<sub>x</sub> condition was that the “bullet” complex had a considerable flat surface area located on the *trans* ring apical domain of GroEL which could firmly stick with the carbon film of the copper grid via electronic static interactions. However, for the symmetric “football” complex where the entire molecule surface was curved, it was less likely for the complex to stably stick to the surface of the grid via the interaction between the tip of GroES and the carbon film. The electron microscopic observations reported here offered a solid path to obtain an almost complete “football” and “bullet” complex. Thus further research about the complex population could be established using this technique.

### 4.3 FRET Efficiency Study of GroELS Complex

#### 4.3.1 FRET Efficiency of GroELS Complex in the Presence of ATP/ADP·BeF<sub>x</sub>

To determine the FRET efficiency of “football” and “bullet” complex with the modified GroEL<sup>IAEDANS</sup> and GroES<sup>F5M</sup>, the latter was titrated into standard buffer containing GroEL<sup>IAEDANS</sup> in the presence of ATP·BeF<sub>x</sub> or ADP·BeF<sub>x</sub>. The unlabeled GroES was titrated exactly the same for calculation of FRET efficiency as described in chapter 2.

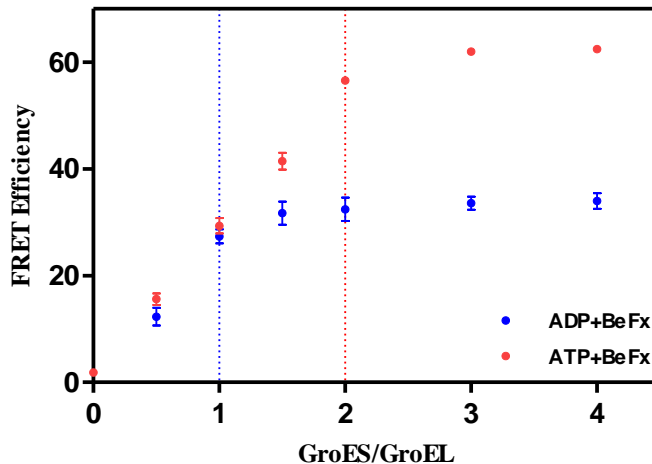


**Figure 4-2 Steady State FRET Titration of GroES<sup>F5M</sup> to GroEL<sup>WT-IAEDANS</sup>.** FRET efficiency was calculated as GroES<sup>F5M</sup> was titrated into a solution containing 2  $\mu$ M GroEL<sup>WT-IAEDANS</sup> in the presence of 0.5 mM ATP·BeF<sub>x</sub> or ADP·BeF<sub>x</sub>. FRET efficiency increased as more and more GroES<sup>F5M</sup> was titrated and the plateau corresponds the stoichiometry of GroES binding to GroEL. Blue circles were titration performed in the presence of ADP·BeF<sub>x</sub> and red circles were in the presence of ATP·BeF<sub>x</sub>

The stoichiometry of the titration of GroES to GroEL in ADP·BeF<sub>x</sub> condition showed saturation after the 1:1 ratio of GroES heptamer over GroEL tetradecamer, meaning the formation of GroEL-GroES<sub>1</sub> “bullet” complex was the major complex under these conditions (see figure 4-2). The stoichiometry, when ATP·BeF<sub>x</sub> was present, showed a 2:1 ratio of GroES heptamer over GroEL tetradecamer. Under



these conditions, the GroEL-GroES<sub>2</sub> “football” complex was the major species formed. What matters in this experiment is the FRET efficiency when these two complexes were formed. When the “bullet” complex was formed, the average FRET efficiency was 34±2% and it became 62.2±0.7% when the “football” complex was formed. The almost doubling of FRET efficiency indicated more energy from the donor on GroEL was transferred to the acceptor on GroES which was in accordance with the logic that more GroES binds to GroEL.

In general, the titration result was in accordance with the results obtained from electron microscopy, that with ATP·BeF<sub>x</sub> GroELS formed “football” complex while with ADP·BeF<sub>x</sub> it formed “bullet” complex and the FRET efficiency generated in this experiment offered an indicator to measure the population of each complex under different physiological conditions.

#### *4.3.2 Titration of GroELS Complex by SPs*

The same experiment was performed in the presence of SPs. In this study, the GroES concentration (both labelled and unlabeled as for calculation of FRET efficiency) was kept at 4 μM while the GroEL concentration was kept at 2 μM. In the absence of BeF<sub>x</sub>, the solution with a different concentration of SPs (MDH or α-LA) was incubated for 2 min and ATP was mixed to reach a final concentration of 500 μM. Three scans were taken within 2 min after ATP was mixed (figure 4-3).

The FRET efficiency at different SP concentrations was calculated as above. Based on the calculated FRET efficiency with the presence of ATP·BeF<sub>x</sub> and ADP·BeF<sub>x</sub>, the population of each GroELS complex was calculated. Generally, as the concentration of SPs increased, the population of GroEL-GroES<sub>2</sub> “football” complex

in the solution increased. For  $\alpha$ -LA the population of “football” increased from 6.7% to 75.7% until saturation. For MDH, the “football” population reached 69.0% after saturation and each titration yielded a single site binding curve with a binding affinity of  $1.3 \pm 0.5 \mu\text{M}$  for denatured  $\alpha$ -lactalbumin (which was consistent with the steady state ATPase titration data, and previously reported data<sup>88</sup>) and  $0.4 \pm 0.2 \mu\text{M}$  for denatured MDH.

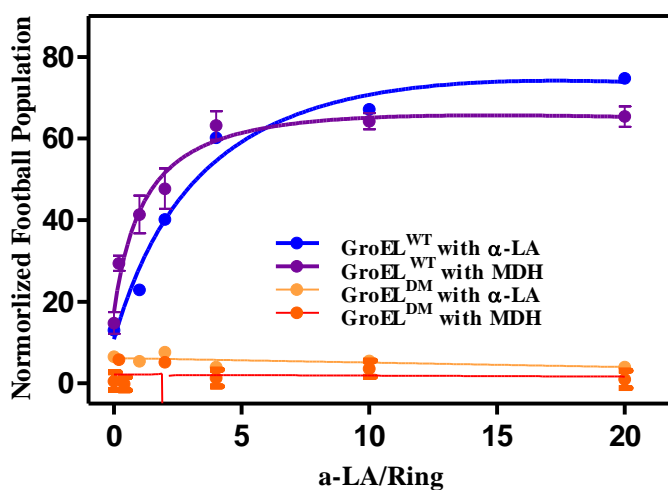


**Figure 4-3 Steady State FRET Titration of SP to GroELS complex.** FRET efficiency was calculated as SPs were titrated into a solution containing  $2 \mu\text{M}$  GroEL<sup>WT-IAEDANS</sup>/ GroEL<sup>DM-IAEDANS</sup> and  $4 \mu\text{M}$  GroES<sup>F5M</sup> in the presence of a  $0.5 \text{ mM}$  ATP regenerating system. FRET efficiency increased as more and more SP was titrated and the binding constant of each SP was derived using a single site binding model. Blue and purple traces were titrations of denatured  $\alpha$ -LA and MDH to GroEL<sup>WT</sup>-GroES complexes and yellow and orange traces were denatured  $\alpha$ -LA and MDH to GroEL<sup>DM</sup>-GroES complexes.

Attention should be drawn to the fact that this titration was performed under turning over conditions where ATP was constantly being hydrolyzed. In this situation, the GroELS complex was turning over via the symmetric cycle where was slight population of “bullet” complex<sup>42</sup>. It was necessary for part of GroELS complex to discharge GroES and then discharge folded or partially folded SPs. At any specific time point, this would yield some “football” complex mixed with “bullet” complex

and incomplete population of symmetrical particles. The overall population of “football” complex as a function of denatured SPs was unequivocally established on this experiment.

#### *4.3.3 Titration of GroELS Complex by Potassium Ions*

There are a handful of allosteric ligands that modulate the GroEL allostery, however, the regulatory mechanism of formation of the “football” complex has not been investigated yet. Among them, GroES is required to be present in at least two fold higher concentration than GroEL to be able to form GroEL-GroES<sub>2</sub> “football” complex. SPs promote the formation of “football” formation as illustrated above, and the only other allosteric factors are physiological ions. Therefore to determine what the roles of physiological ions play in the formation of “football” formation, titrations of GroELS complex with potassium and magnesium ions were performed here.

The role of potassium ions in the chaperonin cycle has been demonstrated to enhance the binding affinity of nucleotides to the nucleotide binding pocket of GroEL. Thus, at a constant concentration of ATP, increasing the [K<sup>+</sup>] promotes the allosteric transition of GroEL from **TT** to **TR**, and from **TR** to **RR**. Titration of K<sup>+</sup> into the turning over GroELS complex can also reveal the role of K<sup>+</sup> in the GroELS complex formation.

In this experiment, the GroES concentration (both labelled and unlabeled as for calculation of FRET efficiency) was kept at 2.5 μM while the GroEL concentration was kept at 2 μM. The ATP regenerating system was made in a standard solution in the absence of K<sup>+</sup>, and 2 U/mL pyruvate kinase and 5 mM PEP were added to maintain a stable concentration of 500 μM ATP. In either the presence

or the absence of 20 fold SP (denatured  $\alpha$ -LA), an aliquot of stock  $K^+$  solution was added to reach the desired final concentration. ATP was finally added to initiate the reaction and three scans were taken within 2 min after ATP was mixed.

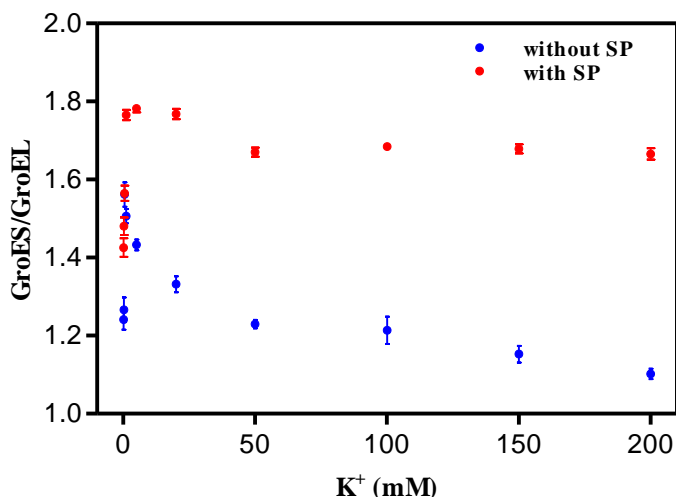


**Figure 4-4 Steady State FRET Titration of  $K^+$  to GroELS complex.** FRET efficiency was calculated as  $K^+$  were titrated into a solution containing 2  $\mu$ M GroEL<sup>WT-IAEDANS</sup> and 4  $\mu$ M GroES<sup>F5M</sup> in the presence of an ATP generating system. In the presence of SP (red), 20 fold denatured  $\alpha$ -LA was used with 1 mM DTT in the buffer while there was no thing in absence of SP (blue).

Again FRET efficiency with the presence of ATP·BeF<sub>x</sub> and ADP·BeF<sub>x</sub> were used to set the standards for “football” and “bullet” complexes, and the calculation of FRET efficiency at different [ $K^+$ ], both in the presence and absence of SP (figure 4-4) was performed. The titration of GroELS complex with [ $K^+$ ] started from 0.1 mM [ $K^+$ ] and gradually increased to 200 mM. In the absence of SP, the population of “football” increased initially as the [ $K^+$ ] increased from 0.1 mM to 0.5 mM. The population of “football” increased from 24.2% to 56.2% as the initial [ $K^+$ ] increased. As the [ $K^+$ ] increased further on from 0.5 mM to 200 mM, the population of “football” decreased to 10.2%. In the presence of SP, the initial “football” population was 42.6% at 0.1

mM  $K^+$  and the population of “football” increased until 78.2% at 5 mM  $[K^+]$  as saturation with  $[K^+]$  was reached.

The titration of “football” population with  $K^+$  was similar to the steady state ATPase activity profile of GroEL as a function of  $[K^+]^{51}$ . In the absence of SP, the transitions of increasing and then decreasing ATPase activity reflected the allosteric transition from **TT** to **TR** and then **TR** to **RR**. A similar transitions took place as the population of “football” increased first and decreased as  $[K^+]$  increases. In the presence of SP, the **TR** to **RR** transition was suppressed due to the largely favored **T** state by the binding of SP, and the increasing population of the “football” complex as increasing  $K^+$  just mirrors the relation with this allosteric transition.

In all, the potassium ion affected the population of “football” complex in a fashion that was much similar to that of ATP. The initial increase and then decrease of “football” population mirrored the relation between the  $K^+$  modulated nested allostery and the formation of symmetrical GroELS complex. As suggested before,  $K^+$  increased the affinity of nucleotide to GroEL. At a constant concentration of ATP, the increasing of  $[K^+]$  increased the affinity of ATP towards GroEL which promoted the binding of ATP to the second ring of GroEL. Thus the formation of “football” complex was favored over the initial increasing region of  $[K^+]$ . Since this was a turning over system, continuous increasing of  $[K^+]$  also raised the affinity of ADP on the *trans* ring of GroEL which prevented the ATP exchange with ADP. Since “football” complex was only formed in the ATP condition, this lead to a decrease in the overall “football” population. At physiological condition, the  $K^+$  concentration was ~0.2 M where the discharge of ADP from the *trans* ring was the rate determining

step in the chaperonin cycle. Few “football” complexes were formed due to the inability of ADP to enable the binding of GroES on both rings. However, when SP was present, which greatly accelerated the release of ADP from the *trans* ring, the association of GroES to the *trans* ring was prominent. In this scenario the “football” complex became the major species in the chaperonin cycle.

#### **4.4 The Mechanism of Formation of “Football” Complex**

Much remains unknown about the mechanism behind the formation of the “football” complex. There are two GroES rings on the GroEL molecule and many aspects remain unclear regarding this, such as the order GroES binds to GroEL, the requirement of ATP hydrolysis and the effect of each GroES molecule has on the other after one binds GroES.

##### *4.4.1 The Association of GroES to apo-GroEL*

*In vivo*, GroEL and GroES molecules are synthesized separately. The very first event of binding of GroES to GroEL must take place as GroES associates to the apo-GroEL molecule, although we have proven that the asymmetric GroEL-GroES<sub>1</sub>-ADP complex is the idling component in the absence of SP. To test how the very first GroES (or two) associates to GroEL, the fluorescent GroES<sup>F5M</sup> and GroEL<sup>IAEDANS</sup> pairs were utilized.

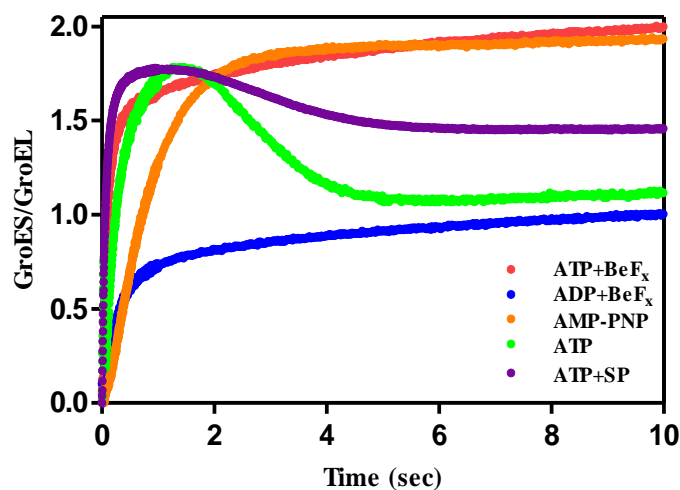


**Figure 4-5 Pre-Steady State FRET Formation of GroELs Complex.** In a stopped flow setup described previously, 2  $\mu\text{M}$  GroEL<sup>IAEDANS</sup> was loaded in syringe A and 2.5  $\mu\text{M}$  GroES<sup>F5M</sup> and 1.0 mM ATP and other ligands was loaded in syringe B. The collection mode was set as fluorescence and a cut-off filter of 530 nm was installed. The excitation wavelength was set at 336 nm. The syringes were equilibrated at 37 °C with a circulating water bath. FRET emission was recorded upon mixture of GroEL<sup>WT-IAEDANS</sup> and GroES<sup>F5M</sup> in the presence of different ligands. In the presence of ATP • BeF<sub>x</sub> (red) and ADP • BeF<sub>x</sub> (blue), the magnitude of the FRET emission were set as two GroES per GroEL and one GroES per GroEL. Green trace was obtained in the presence of ATP, purple trace was obtained in the presence of ATP+SP and orange trace was in the presence of AMP-PNP.

As shown in the figure 4-5, the magnitude of FRET signal obtained by ATP • BeF<sub>x</sub> (red) control was twice as much as that of the ADP • BeF<sub>x</sub> control (blue). This was consistent with the fact that in the presence of BeF<sub>x</sub>, ATP formed a symmetric GroEL-GroES<sub>2</sub> “football” complex whereas ADP formed an asymmetric GroEL-GroES<sub>1</sub> “bullet” complex. In the absence of BeF<sub>x</sub>, apo-GroEL first bind two GroES molecules at about 1.5 seconds and then the GroEL-GroES<sub>2</sub> complex subsequently decayed to a “bullet” complex (figure 4-5, green). Five seconds after mixing, only one GroES remained in the form of GroEL-GroES<sub>1</sub> “bullet” complex. In the presence of non-hydrolysable ATP analogue, AMP-PNP, there was a formation of stable GroEL-GroES<sub>2</sub> in the experimental time we observed (figure 4-5, orange), showing that the breakage of GroES symmetry required the hydrolysis of ATP. However,

when SP was present (10 fold excess of denatured  $\alpha$ -LA) was added in syringe B before mixing, not all of the GroEL-GroES<sub>2</sub> complex was decayed into GroEL-GroES<sub>1</sub> complex (figure 4-5, purple). There was still around 46% of the complex remained “football” formula while the rest were in the “bullet” complex.

#### 4.4.2 The Hydrolysis of ATP during the GroES Association to apo-GroEL<sup>WT</sup>

To follow ATP hydrolysis during these transitions, the release of Pi during the “football” formation process was measured by PBP<sup>MDCC</sup>.

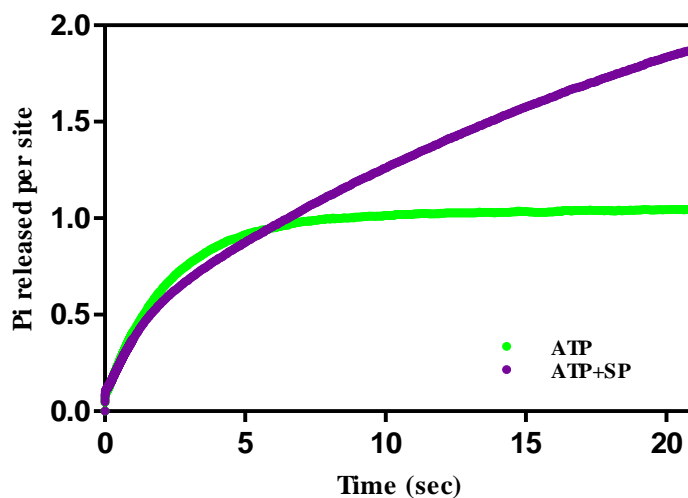


**Figure 4-6 Pre-Steady State ATP Hydrolysis during GroELS Complex Formation.** The detailed experimental set up was the same as described in chapter 2. In syringe A, 2 $\mu$ M GroEL<sup>WT</sup> was loaded and in syringe B 2.5 $\mu$ M GroES and 20 $\mu$ M PBP<sup>MDCC</sup> were loaded with the presence or absence of SP. Fluorescent emission was recorded upon mixture of GroEL, GroES, and PBP<sup>MDCC</sup> in the presence (purple) or absence (green) of SP. The Y axis was calibrated with inorganic phosphate standards and calibrated as Pi released by subunit.

In the absence of SP (figure 4-6, green), each subunit in the two rings of GroEL<sup>WT</sup> hydrolyzed ATP once. This process was complete within 5 seconds. Then the ATPase activity decreased to almost 0.36 turnover. However in the presence of SP (figure 4-6, purple), after one ATP was hydrolyzed in each subunit, but GroEL continued hydrolyzing ATP at a rate of about 5 turnover/min.



It was worth noting that in the experiment of GroES association with GroEL, two GroES completely associated with one GroEL in one second. In this experiment, less than half (40.7%) of the subunits had completed the hydrolysis of ATP. Considering the binding of ATP to GroEL was much faster than its hydrolysis, this indicated that the binding of two GroES to one GroEL molecule did not necessarily require the hydrolysis of ATP but only the binding of ATP to both rings. Within the first second, the hydrolysis of ATP on the two rings were different. The whole complex was then composed of two GroES on both rings with asymmetric nucleotide identity on each ring. The symmetrical “football” complex then underwent breakage of GroES symmetry; one or other GroES dissociated from the “football” complex.

After 5 sec, all the subunits in GroEL had hydrolyzed ATP once and all the “football” complex had decayed to the “bullet” complex. The composition of the “bullet” complex could be easily deduced as one GroES on the *cis* ring and 7 ADP on each ring. This is the resting state complex of GroEL. In the presence of SP, the hydrolysis of ATP continued and the GroEL-GroES complex kept turning over. The previous experiment showed that at the presence of SP, some of the GroELs complex maintained in the “football” formation. Since we already know that the resting complex was the major idling species in the absence of SP, the question becomes: 1) how does the “football” complex form from the resting complex? 2) How is the “football” complex turning over as a dynamic species?

#### *4.4.3 The Association of GroES to GroELs Resting State Complex*

To study the association of the second GroES to the resting state complex, the GroES<sup>F5M</sup>-GroEL<sup>IAEDANS</sup> FRET system was employed again.

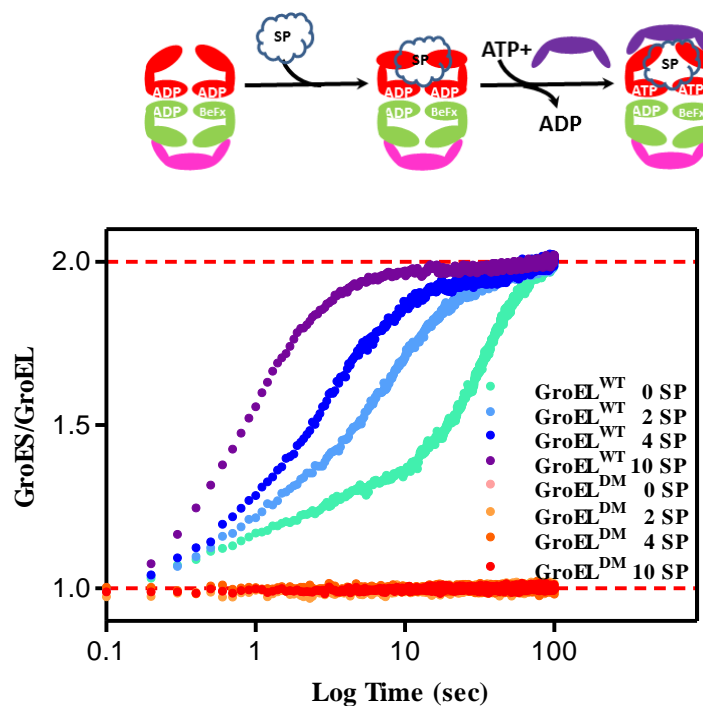


**Figure 4-7 GroELS Complex Formation of from the Resting State Complex.** As shown in the cartoon, the resting complex was made by mixing 4  $\mu\text{M}$  GroEL<sup>IAEDANS</sup> and 2  $\mu\text{M}$  GroES<sup>F5M</sup> with 50  $\mu\text{M}$  ADP. The mixture was incubated in the dark for 30 min and loaded into syringe A. In syringe B, 1.0 mM ATP, 2.5  $\mu\text{M}$  GroES<sup>F5M</sup> and different concentration of SP (denatured  $\alpha$ -LA) were loaded. To stabilize the resting complex and the “football” product, 10 mM BeCl<sub>2</sub> and 100 mM NaF was added in both syringes. At 37 °C, the increase of the FRET signal generated by the association of the second GroES to the resting state complex was collected. Fluorescent emission was recorded upon mixture of BeCl<sub>2</sub> stabilized GroEL<sup>IAEDANS</sup>-GroES<sub>1</sub> resting state complex with GroES<sup>F5M</sup> in the presence of ATP and different concentrations of SP. For GroEL<sup>WT</sup> the SP concentrations were: 0 fold (green), 2 fold (blue), 4 fold (dark blue) and 10 fold (purple) and for GroEL<sup>DM</sup> the SP concentrations were: 0 fold (pink), 2 fold (yellow), 4 fold (orange) and 10 fold (red).

BeF<sub>x</sub> was used here to calibrate the FRET signal as before (figure 4-7). Since the first GroES on board was stabilized on the resting state complex, the FRET magnitude of the association of the second GroES was just half of the formation of the artificial “football” complex. In the absence of SP, the half-time for the second GroES to associate with the resting complex was 25.0±0.5 sec. However, in the presence of 2, 4 and 10 fold of SP, the half time was shortened to 6.4±0.1, 3.0±0.1, and 0.88±0.02 sec respectively. The same experiment was performed on GroEL<sup>DM</sup> and discussed in Chapter 6.

In the previous research, the dissociation of ADP in the *trans* ring was the rate limiting step in the chaperonin cycle in the absence of SP. As illustrated elsewhere, the ADP on the *trans* ring did not support the binding of the second GroES to this ring. Thus ADP on the *trans* ring had to be exchanged with ATP to enable the formation of the “football” complex. Unequivocally, SP accelerated this exchange as our results showed here that the rate of the second GroES association to the *trans* ring was increasing as the SP concentration increased.

#### 4.4.4 The Association of GroES to GroELS Acceptor State Complex

After ADP is released from the *trans* ring, the binding of ATP to this vacant ring is followed by the association of GroES and the discharge of GroES on the opposite ring. To study the process that the second GroES associates after the rapid binding of the GroES, the GroES<sup>F5M</sup> association to the GroEL<sup>IAEDANS</sup>-GroES<sub>1</sub> acceptor state complex was measured.

Again, here the ATP·BeF<sub>x</sub> and ADP·BeF<sub>x</sub> control was used to quantify the number of GroES associated with one GroELS acceptor state complex (figure 4-8). The process of this association was complicated but can be divided into three steps: 1) the rapid binding of ATP on the vacant *trans* ring and discharge of the unlabeled GroES from the *cis* ring. This process was complete in the dead time. 2) The following, comparatively faster, association of the first GroES<sup>F5M</sup> to the ATP bound *trans* ring and 3) the ATP/ADP exchange on the former *cis* ring and association of the second GroES<sup>F5M</sup> to it. As the SP concentration after equilibrium increased from 0 to 2, 4, and 10 fold, the population of “football” formed increased from 14%±1% to 39.5%±0.5%, to 54%±1%, to 69%±1% respectively. These numbers were consistent

with the numbers derived from the “football” population titrated with denatured  $\alpha$ -LA since it was also used here as the SP.

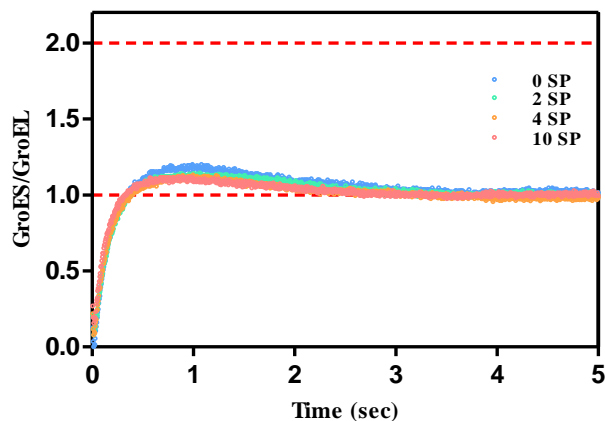
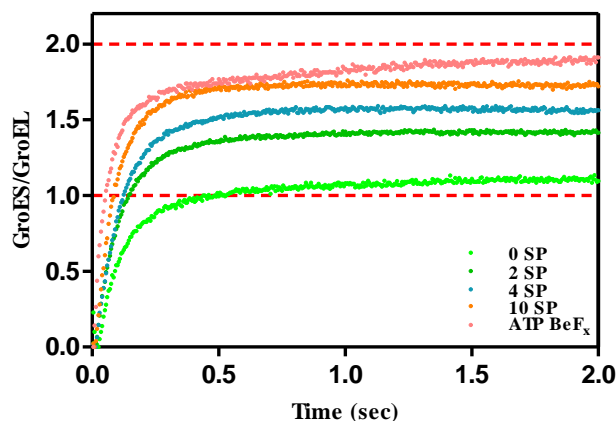


**Figure 4-8 GroELS Complex Formation of from the Acceptor State Complex.** As shown in the cartoon, the acceptor state complex was made by mixing 20 $\mu$ M GroES, 40 $\mu$ M GroEL<sup>IAEDANS</sup> and 400 $\mu$ M ATP reacting for 30 min. The mixture was then passed through a PD-10 column to remove the free and *trans* bound ADP. This acceptor state complex was loaded into syringe A with a final concentration of 2 $\mu$ M GroEL. In syringe B, 1.0 mM ATP and 2.5 $\mu$ M GroES<sup>F5M</sup> along with different concentration of SP (denatured  $\alpha$ -LA) was loaded. The experimental set up was the same as above. Fluorescent emission was recorded upon mixture of GroEL<sup>IAEDANS</sup>-GroES<sub>1</sub> acceptor state complex, where there was no ADP bound on the *trans* ring, with GroES<sup>F5M</sup> in the presence of ATP and different concentrations of SP. For GroEL<sup>WT</sup> (top panel): 0 fold (green), 2 fold (blue), 4 fold (dark blue) and 10 fold (red). For GroEL<sup>DM</sup> (bottom panel): 0 fold (blue), 2 fold (green), 4 fold (yellow) and 10 fold (red).

The increasing of number of GroES associated to the acceptor complex did not differ from the GroES on the newly formed *cis* ring but from the GroES on the newly formed *trans* ring. Different SP concentrations promoted various ATP/ADP exchange on the *trans* ring, thus allowing different numbers of GroES to bind to it. This experiment explicitly showed the availability of a vacant ring was critical for the association of GroES to it and SP promoted the release of the hydrolysis product ADP from this ring. The same experiment was performed on GroEL<sup>DM</sup> and discussed in Chapter 6.

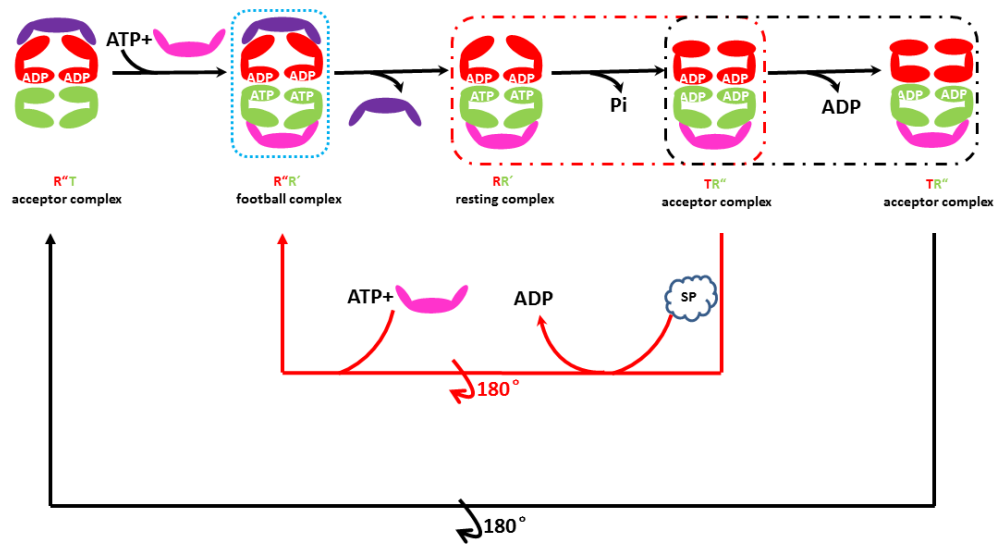


**Figure 4-9 SP Switches The Chaperonin from Asymmetric to Symmetric Cycling.** In the absence of SP, the *trans* ring in the resting complex is sampling between **T** and **R** state (red box). ADP is only released from the **T** state GroEL and release of ADP from the resting complex is the rate limiting step (black box). Although GroES binds GroEL via an associative mechanism, however, in the absence of SP the “football” complex is only an intermediate (blue box). GroE is cycling in the GroEL-GroES<sub>1</sub> asymmetric cycle (black pathway). In the presence of SP, binding of SP to the acceptor state is preferred and sampling of **T** state is favored. ADP release from the resting complex is accelerated and hydrolysis of ATP becomes the rate limiting step (red box). GroE is cycling in the GroEL-GroES<sub>2</sub> symmetric cycle (red pathway).

In all, the formation of “football” complex depends on the presence of ATP on both rings of GroEL. In the absence of SP, the release of the hydrolysis product-ADP is the rate determining step of the chaperonin cycle and the binding of ATP to the *trans* ring is hindered (figure 4-9). Thus there is no chance for ATP to bind at both rings of GroEL to form the symmetrical particle. However in the presence of SP, the release of ADP is greatly accelerated and ATP hydrolysis becomes the rate determining step of the chaperonin cycle. When ATP binds to the *trans* ring where the *cis* ATP is not completely consumed, the second GroES can still bind to the opposite ring and the symmetric “football” complex can be formed.

## Chapter 5 The “Football” Dynamics and Its Role in Chaperonin Assisted Protein Folding

The currently accepted model for how GroEL assists SP folding in the cell takes the asymmetric GroEL-GroES<sub>1</sub> complex as the major folding active complex and GroEL is described as folding the SP in a passive fashion<sup>65</sup>. In this model, ATP binds to one ring of GroEL and the negative cooperativity prevents binding of ATP to the other ring<sup>54</sup>. Since GroES binding is dependent on the ATP binding to GroEL, the only possible GroELs complex formed is the asymmetric GroEL-GroES<sub>1</sub> complex. Furthermore this model proposes that SP binds to the GroEL ring after ATP has bound to it. This is followed by the docking of GroES to the apical domain of the *cis* ring which forms a folding dorm that lasts ~10 seconds to allow the SP folding inside and there is little known about the timing mechanism of the folding chamber. Subsequent ATP hydrolysis, which is the rate determining step of the chaperonin folding cycle, weakens the assembly and allows the binding of ATP to the *trans* ring. This ATP binding to the *trans* ring sends the allosteric signal that disassembles the *cis* ligands as GroES, ADP, folded or unfolded SP. In all, GroEL utilizes one of its ring in the chaperonin cycle to fold and alternates back and forth regarding hydrolysis of seven ATP per cycle.

As mentioned to in the Introduction if nature only needs one ring to fold a variety of SP in the GroEL chamber, why a double toroid structure made? Much existing research provides evidence to question the current model described above<sup>42,69-74</sup>. We have shown that ATP can bind to both of the GroEL rings and a symmetrical GroEL-GroES<sub>2</sub> complex can be formed without necessarily hydrolyzing

ATP. We also showed that SP binds to the GroEL ring with ADP bound to it, promoting the ATP/ADP exchange and forms the “football” complex. However, the direct evidence for the relation between SP and the “football” complex has not been revealed yet. Here in this chapter, the detailed study on how the “football” complex functions as the major folding active complex is discussed.

Almost one third of the proteins in *E. coli* needs the assistance of GroEL for proper folding<sup>33</sup>. Except proteins in *E. coli*, many other proteins whose folding being assisted by chaperonin, have been studied intensively and three of them are utilized to investigate the mechanism between “football” complex and folding of SPs.

## **5.1 Substrate Case I-Rubisco**

Rubisco was the first *in vitro* tested, stringent SP that undergoes productive GroEL assisted re-folding<sup>8,9,91</sup>. As a model SP, Rubisco has been extensively used to investigate the chaperonin function.

### *5.1.1 The Interaction between Rubisco and GroEL*

There are 8 tryptophan residues in one Rubisco large subunit and most of them are buried in the core region when Rubisco is in the native state. After being denatured with acid, the tryptophan in Rubisco are exposed to the outside where the hydrophobic SP binding groove between helix H and I of the apical domain on GroEL is accessible.

As an aromatic amino acid, tryptophan has its intrinsic fluorescence. Tryptophan gets excited with a maximum excitation wavelength of ~280 nM and emits its emission peak is solvatochromic, which means the maximum emission



depends on the polarity of the local environment, ranging from 300 to 350 nM. In our buffer system, the denatured Rubisco emits maximally at the peak of 330 nM, which is quite close to the excitation wavelength of IAEDANS (336 nM). Thus by exciting tryptophan at 295 nM and when the tryptophans are close enough with IAEDANS on GroEL, IAEDANS labelled on GroEL would be excited and emits at 470 nM (figure 5-1). Since both GroEL and GroES are free of tryptophans, this experiment can be conducted to observe the interaction between tryptophan containing SP and GroEL<sup>IAEDANS</sup>.

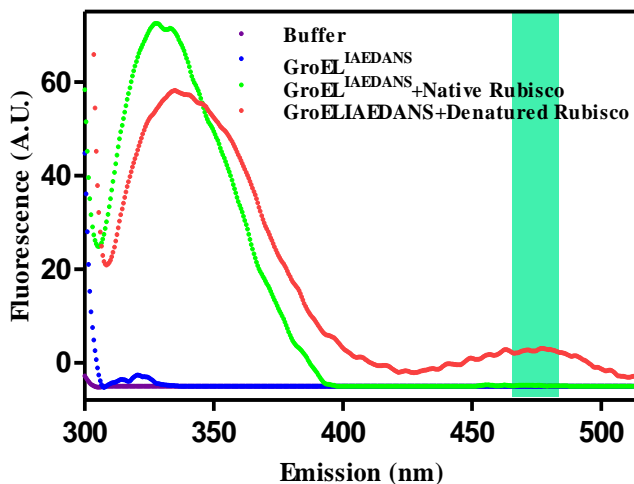


**Figure 5-1 FRET Spectrum between Trp on Rubisco and IAEDANS on GroEL.** The tryptophan on Rubisco was excited at 295 nM and emission spectrum from 300 to 550 nM was recorded. The purple trace was a control experiment where emission from the buffer solution was recorded. The blue trace was only GroEL<sup>IAEDANS</sup> was added in the solution and there was no emission at either 330 nM or 470 nM. The green trace was recorded in the presence of both native Rubisco and GroEL<sup>IAEDANS</sup> where there was only emission at 330 nM but not at 470 nM. The red trace was recorded with carefully measured, same amount of denatured Rubisco and GroEL<sup>IAEDANS</sup> where there was emission at both 330 and 475 nM. The green region showed the photons from 465-485 nM were collected as the slit width was set at 10 nM.

As shown in figure 5-1, the mixture in the cuvette was excited at 295 nM. In the absence of Rubisco, but only the presence of GroEL<sup>IAEDANS</sup>, there was no fluorescence at ~470 nM. This was because the excitation at 295 nM was too far to

directly excite IAEDANS on GroEL at the absence of the FRET donor. When native Rubisco and GroEL<sup>IAEDANS</sup> were present in the cuvette, there was a maximum emission at ~325 nM corresponding to the emission from tryptophans on native Rubisco. However, due to the nature that GroEL did not bind native SP, the energy was not transferred from tryptophan on Rubisco to IAEDANS on GroEL. Thus there was no apparent fluorescence at ~470 nM. Only when both the denatured Rubisco and GroEL<sup>IAEDANS</sup> present in the mixture was there a significant fluorescence emission at ~476 nM. This indicated that IAEDANS on GroEL was getting excited by tryptophan on Rubisco. In this experiment, the amount of native and denatured Rubisco were carefully controlled to be the same. However, when there was FRET between Rubisco<sup>trp</sup> and GroEL<sup>IAEDANS</sup>, the fluorescence at 325 nM was lower compared with that when there was no FRET. This is because when FRET took place, part of the energy from the donor-tryptophan was transferred to the acceptor thus less energy was emitted as photons. This quenching phenomenon further identified the existence of FRET between Rubisco<sup>trp</sup> and GroEL<sup>IAEDANS</sup>.

With this system we could monitor the interaction between Rubisco and GroEL during the course of its folding. The Perkin Elmer fluorescence spectrophotometer was set at time driven mode. The excitation wavelength was set at 295 nM and the slit width of 15 nM; the emission of 475 nM was monitored with an emission slit width of 20 nM. The water bath was set at 25 °C and monitoring of the reaction begins upon the addition of ATP. Two controls were made for this experiment: 1) no ATP was added in the solution (figure 5-2, purple) and 2) native Rubisco was used in this experiment instead of denatured Rubisco (brown).

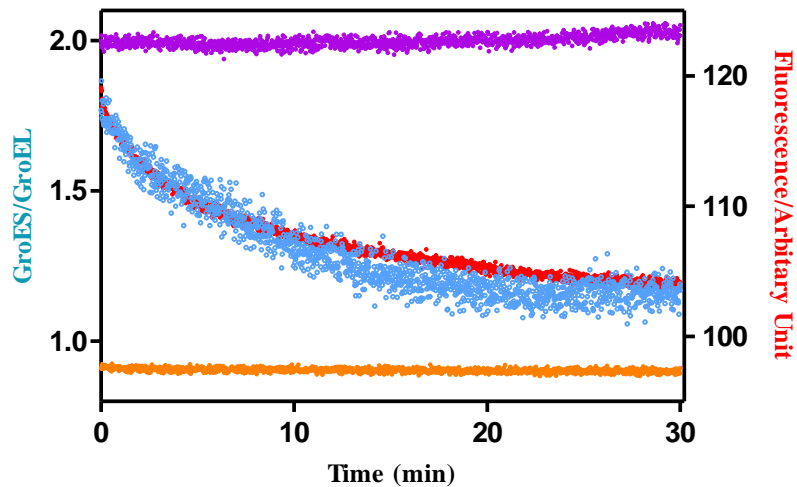


**Figure 5-2 FRET Indicating Interaction between Rubisco and GroEL<sup>IAEDANS</sup> during Its Refolding.** 230  $\mu\text{M}$  Rubisco was diluted 10 fold into 50 mM Glycine-HCl (pH 2.72) and denatured for 210 seconds on ice right before the experiment. In a squats cell, a final concentration of 2  $\mu\text{M}$  GroEL<sup>IAEDANS</sup>, 5  $\mu\text{M}$  unlabeled GroES, 1 mM DTT, 5 mM PEP, 20 U PK and 1g/L of BSA was mixed. Subsequently, 2.5  $\mu\text{L}$  of 23  $\mu\text{M}$  denatured Rubisco was added into the reaction and allow to incubate for 5 min before addition of a final concentration of 500  $\mu\text{M}$  ATP. The tryptophan on Rubisco was excited at 295 nM and emission at 475 nM was recorded. The refolding reaction was initiated by adding 0.5 mM ATP and the decay of FRET between Rubisco<sup>trp</sup> and GroEL<sup>IAEDANS</sup> was observed (red trace). The purple trace was recorded as the same except no ATP was added in the reaction, the brown trace was using native Rubisco instead of denatured one while other conditions were identical. The blue trace was monitoring the “football” complex formed by FRET GroEL-GroES during the course of Rubisco refolding and the left Y axis was calibrated with ATP·BeF<sub>x</sub> and ADP·BeF<sub>x</sub> methods.

Upon addition of ATP, GroEL, GroES and denatured Rubisco, a substantial population of tertiary complex began to form as the folding of Rubisco took place. As more and more denatured Rubisco was refolded, less were interacting with GroEL<sup>IAEDANS</sup>. Thus, the FRET between tryptophan on denatured-Rubisco and IAEDANS on GroEL decreased as Rubisco was refolded. However when there was no ATP, the reaction could not be initiated and the interaction between denatured Rubisco<sup>trp</sup> and GroEL<sup>IAEDANS</sup> dominated. In another case, if there was native Rubisco in the reaction where no GroEL assisted refolding was needed, there was no FRET signal from GroEL<sup>IAEDANS</sup>. The half-life of the FRET decayed, where denatured

Rubisco was refolded in the presence of the ATP regenerating system, is ~3.5 min and this was in accordance with the half-life reported before<sup>20</sup>.

### *5.1.2 The Interaction between Rubisco and “Football” Complex*

As discussed in the previous chapter, the population of the “football” complex can be directly measured by determining the FRET efficiency in between GroEL<sup>IAEDANS</sup> and GroES<sup>F5M</sup>. Here in this chapter, the population of the “football” complex in the course of refolding denatured Rubisco was measured as described in Chapter 2.

As the refolding system was turning over, the population of “football” refolding Rubisco decreased (figure 5-2, blue). Eventually the population of “football” decreased to the level of the population of “football” in the ADP·BeF<sub>x</sub> condition. The decay kinetics of denatured Rubisco facilitated “football” yielded a half-life of ~3.8 min. This was in an agreement with the half-time of refolding of acid denatured Rubisco as we measured in the previous section.

In this section, we studied the interaction between denatured Rubisco and the “football” population during the trajectory of Rubisco refolding. Acid denatured Rubisco interacts with GroEL as a necessary biological step to be captured by the SP binding helix H and I in the apical domain of GroEL. The subsequent encapsulation, refolding in the central cavity and ejection steps are not revealed by this study. However, as more denatured Rubisco becomes folded, less is available to interact with GroEL. The decreasing of interaction between Rubisco and GroEL verifies the structural re-folding of acid denatured Rubisco.

## 5.2 Substrate Case II-Malate Dehydrogenase

Malate dehydrogenase contains two similar subunits of 35,000 kDa, and is one of the tightest binding SP of GroEL<sup>10</sup>. Because it is convenient to assay the enzymatic activity of MDH and other well-known properties of this enzyme, it is used here to illustrate the role of “football” complex in chaperonin assisted protein folding.

### 5.2.1 *The Refolding of MDH by GroELS Complex*

The interaction between MDH and GroEL<sup>IAEDANS</sup>, by observing the tryptophan-IAEDANS FRET as performed with the denatured Rubisco, could not be performed because there was no intrinsic tryptophan in MDH (from pig heart, mitochondrial). However, the enzymatic activity of MDH could be easily evaluated by a coupled enzyme assay. By measuring the enzymatic activity of MDH and its binding to GroELS complex, the interaction between this SP and GroEL could be resolved. The experimental procedure was described in Chapter 2.

Upon addition of ATP to the refolding system, the enzymatic activity of refolded MDH reached 20% of native MDH. Eventually after 30 min it resumed 86.3% of its native enzymatic activity. The recovery of the enzymatic activity as a function of time could be modeled as one phase exponential increase with a half-time of ~5.4 min.

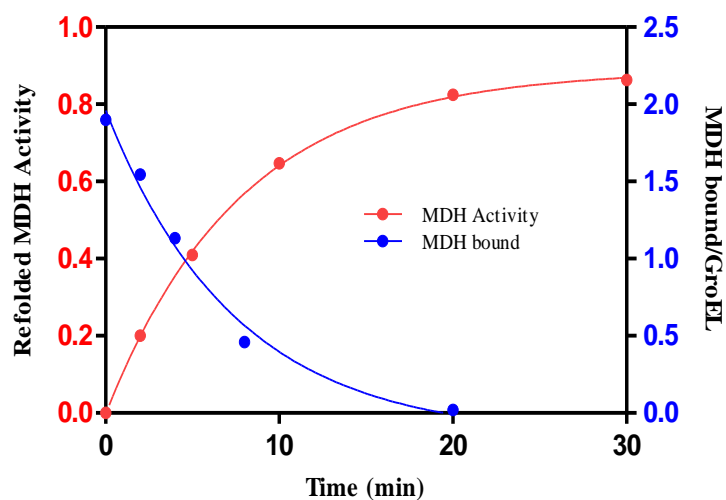


**Figure 5-3 MDH Activity and Encapsulation during Its Refolding by GroEL.** The enzymatic activity of MDH (red) to catalyze the oxidation of NADH was measured at different time point during its refolding by GroEL. Another aliquot of MDH without using urea denaturation was assayed as the fully active enzyme to calculate the percent recovery. The enzymatic activity as time was fitted with one phase exponential equation. The amount of MDH encapsulated within GroEL was measured with SDS-PAGE and the amount of protein bound was decreasing as being refolded (blue). This trace was fitted using a one phase decay equation.

### 5.2.2 The Encapsulation of MDH by GroELS Complex

The amount of MDH encapsulated during the course of its refolding was measured as described in Chapter 2. The amount of GroEL and MDH in each elution was calculated using the information from the marker controls. The data analysis yielded an initial 1.9 MDH per GroEL tetradecamer at time 0, which was before the addition of ATP (figure 5-3, blue). After addition of ATP the GroELS system began to fold the denatured MDH. As time passed more MDH was refolded and less MDH was encapsulated in the central cavity. By the end of 20 minute, there was only ~0.02 MDH encapsulated per tetradecamer of GroEL. The decreasing amount of MDH encapsulated in the central cavity of GroEL could be modeled as a single exponential decay with a half-life of ~5.2 min. This indicated as more MDH was refolded by GroELS complex it was no longer recognized by GroEL.

### 5.2.3 The Interaction between MDH and “Football” Complex

The observation of the population of “football” complex and the refolding of MDH was carried out the same as described in section 5.1.2, except the preparation of denatured MDH was different: 1) MDH can refold itself spontaneously so it had to be freshly denatured before each experiment 2) a concentrated aliquot of the protein was reduced with 10 mM DTT for 10 min and then diluted 5 fold into 10 mM HCl to denature for an hour.

In the same experimental set up as described before, denatured Rubisco was replaced by freshly denatured MDH. The control experiment was performed by replacing denatured MDH with denatured  $\alpha$ -LA. Due to the nature that  $\alpha$ -LA remains unfolded in the presence of DTT and in the absence of calcium ion, one can expect to observe the relationship between SP refolding and the population of “football” complex.

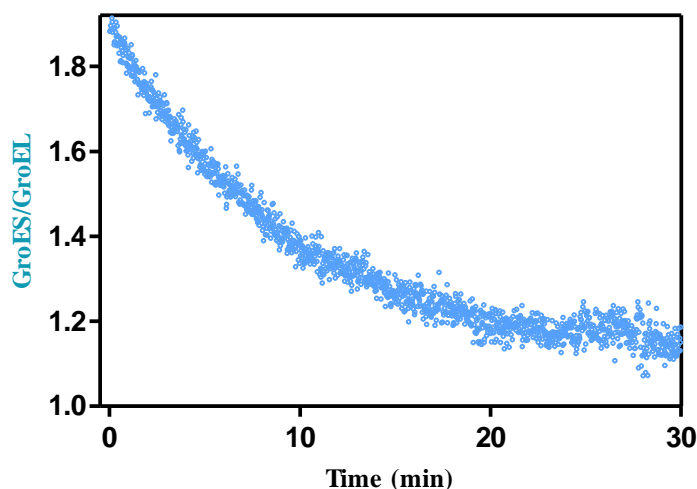


**Figure 5-4 MDH Stimulated “Football” Complex during Its Refolding by GroEL.** The FRET emission between GroEL<sup>IAEDANS</sup> and GroES<sup>F5M</sup> was recorded as denatured MDH being refolded. The reaction was initiated upon ATP addition and the emission at 530 nm was recorded. The data was fit with one phase exponential decay equation and Y axis was calibrated using the same amount of GroEL<sup>IAEDANS</sup> and GroES<sup>F5M</sup> and the ATP·BeF<sub>x</sub> and ADP·BeF<sub>x</sub> methods.

When the experiments were performed with denatured MDH, upon addition of ATP the population of the “football” complex reached approximately 95%. As the denatured MDH was refolded by GroELS in the ATP-regenerating system the population of “football” complex began to decrease. This decay could be modeled with a single exponential decay process with a half-life of ~5.7 min, and this was in agreement with previously reported value (figure 5-4). Meanwhile, for the refolding of denatured  $\alpha$ -LA, the “football” population stayed at a certain level and is stable (data not shown). This was because the presence of DTT and absence of  $\text{Ca}^{2+}$  impeded the refolding of denatured  $\alpha$ -LA.

We again saw the same phenomena where the population of denatured SP determined the population of the “football” complex in the dynamic chaperonin cycle. As both substrates, Rubisco and MDH, were refolded in the chaperonin cycle, the population of the “football” complex decreased. For MDH, as its enzymatic activity increased and less of MDH was being encapsulated in the trajectory of folding. If the SP did not or could not be refolded, e.g.  $\alpha$ -LA, the population of the “football” complex remained the same. These experiments demonstrated that the symmetric “football” complex was the folding active species in the chaperonin cycle.

The role of “football” complex in the course of SP refolding was clear: it was the symmetric GroEL-GroES<sub>2</sub> complex, rather than the asymmetric GroEL-GroES<sub>1</sub> “bullet” complex that was the folding active state in the chaperonin cycle. In the initial time period upon addition of ATP, the population of the “football” complex was almost close to 100%. As the SP population in the mixture became refolded in the ATP-regenerating system, the “football” complex decreased, which illustrated



that the “football” complex was the folding active species in the chaperonin cycle. By the end of the folding process, the FRET emission was close to the  $\text{BeF}_x$  stabilized “bullet” complex. This indicated that the “bullet” complex was merely a resting state of the chaperonin, rather than the main folding active complex.

### 5.3 Substrate Case III- $\alpha$ -LA

$\alpha$ -LA has been extensively studied regarding its interaction with GroEL and used many times in the previous research as the SP. In the absence of  $\text{Ca}^{2+}$ ,  $\alpha$ -LA reaches the molten globule state and does not get recognized by GroEL. However when all of the four disulphide bonds are reduced by DTT,  $\alpha$ -LA has less secondary structures and can be recognized by GroEL<sup>92,93</sup>. This makes it an advantageous SP since the spontaneous folding does not take place as long as there is a reducing agent in the buffer.

Many studies have been done on the interaction between  $\alpha$ -LA and GroEL as described in previous sections. Here we are offering a simple example on how this non-refold-able SP alters the chaperonin cycle. In the absence of SP, GroEL-GroES<sub>1</sub> turned over in the asymmetric cycle and excessive amount of SP was introduced into the system while the GroES associated with GroEL was monitored (figure 5-5).

The control experiment was performed by mixing the standard buffer with the dynamic turning over system rather than SP. The ATP/ADP· $\text{BeF}_x$  method was used to define the magnitude of two/one GroES FRET signal. Upon adding SP, the number of GroES on board increased from 1.17 to 1.74 (figure 5-5, red) within one second. In contrast, introducing the standard buffer into the dynamic system did not change the number of GroES on board (figure 5-5, blue).

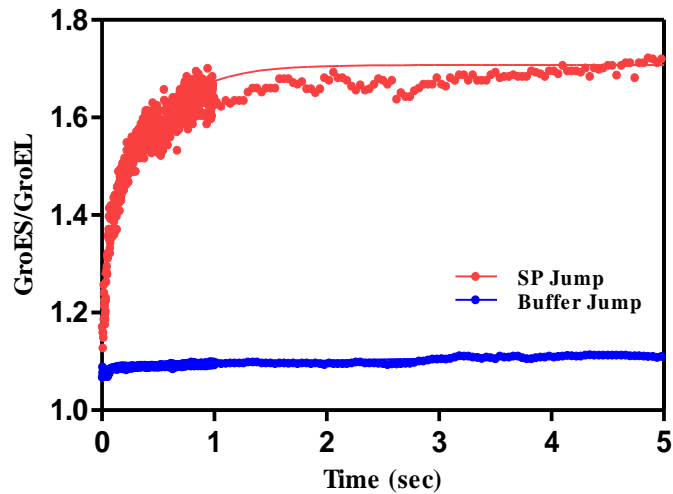


**Figure 5-5  $\alpha$ -LA Switched Asymmetric Cycle to Symmetric Cycle.** A standard buffer containing 10 mM DTT, 4 $\mu$ M GroEL<sup>IAEDANS</sup>, 10 $\mu$ M GroES<sup>F5M</sup> and 500  $\mu$ M ATP in the presence of the ATP regenerating system (2 mM PEP and 20 U/mL PK) was loaded in syringe A. This made a turning over, dynamic GroELS system where the asymmetric GroEL-GroES<sub>1</sub> “bullet” complex was the major species as indicated before. In syringe B, a concentration of 20 fold denatured  $\alpha$ -lactalbumin was loaded. Upon mixing SP would be introduced into the turning over system. In a stop flow instrument, the FRET emission between GroEL<sup>IAEDANS</sup> and GroES<sup>F5M</sup> was recorded as denatured  $\alpha$ -LA was introduced into a turning over GroELS system in the absence of SP. The reaction was initially cycling in the “bullet” cycle and rapidly switched into the “football” cycle upon introduction of denatured  $\alpha$ -LA (red), and the data was fit into one phase exponential increase. The control experiment was performed by using buffer instead of denatured  $\alpha$ -LA where there is no significant stimulation of FRET signal (blue).

This experiment vividly shows the switch between the asymmetric GroEL-GroES<sub>1</sub> chaperonin cycle in which asymmetric GroEL-GroES<sub>1</sub> “bullet” complex predominate, to the symmetric GroEL-GroES<sub>2</sub> complex chaperonin cycle in which GroEL-GroES<sub>2</sub> “football” predominate. SP is the key allosteric ligand that regulates the system cycling from one to the other. That is, in the absence of SP, the GroELS complex idles in the asymmetric cycle and switches to the symmetric cycle in the presence of unfolded SP<sup>43</sup>.

## 5.4 The Dynamics of “Football” Complex

There are two symmetric rings in one GroEL tetradecamer and each of them has an opening formed by seven apical domains adjacent to each other. After binding two GroES to each of the ring, the nucleotide binding pocket is closed by the helix F and M clamping onto the equatorial domain. Even the  $Mg^{2+}$  ions are not freely exchanging in this scenario<sup>94</sup>. The system is in a closed state to the outside allosteric ligands. Common wisdom<sup>95</sup>, without a solid idea of dynamics in the mind, would think this “football” complex is a dead end for the chaperonin cycle.

However, in such conditions where there are both regenerating ATP and SP present, the steady state assay shows that the system is vigorously releasing ADP. FRET titration data shows that in the presence of both ATP and SP, the “football” complex is the major species. Altogether, this indicates the “football” complex is actually a dynamic complex. In this section we investigated the dynamics of this “football” complex. For all the allosteric ligands, the Pi and ADP release have been measured in previous sections as small ligands. Here we focus on the dynamics of GroES and SP.

### 5.4.1 The “Football” GroES is Exchanging with Others

To monitor the motion of GroES on board of the “football” complex, a similar FRET experiment was performed as described previously. In a stop flow instrument, the FRET emission between GroEL<sup>IAEDANS</sup> and GroES<sup>F5M</sup> was recorded as unlabeled GroES was introduced into a turning over GroEL system in the presence of SP. The reaction was cycling in the “football” cycle and GroES<sup>F5M</sup> rapidly exchanges with unlabeled ones as the “football” complex was turning over. The decrease of FRET

signal indicated the rate of the GroES dissociation from a turning over “football” complex. The number of GroES on GroEL was determined by mixing components in the same conditions on the fluorescence spectrometer.

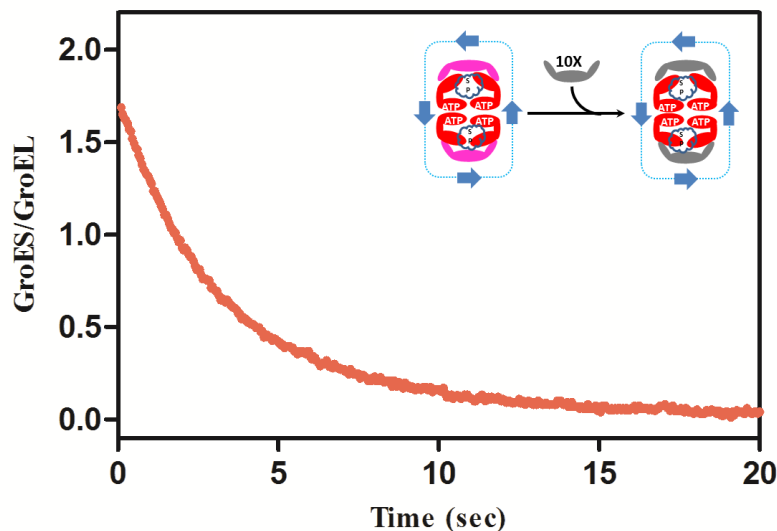


**Figure 5-6 Dynamics of GroES in The “Football” Cycle.** In a standard buffer, the GroELS system was mixed with the ATP regenerating system and SP:  $2\mu\text{M}$  GroEL<sup>IAEDANS</sup>,  $2.5\mu\text{M}$  GroES<sup>F5M</sup>, 10 mM DTT, 10 fold denatured  $\alpha$ -LA,  $500\mu\text{M}$  ATP, 5 mM PEP, and 20 U/mL PK was mixed. The solution was quickly loaded to the syringe A where it is equilibrated at  $37^\circ\text{C}$ . In syringe B,  $25\mu\text{M}$  unlabeled GroES and the same amount of denatured  $\alpha$ -LA was loaded. The reason denatured  $\alpha$ -LA is also loaded in syringe B is to prevent the dilution of SP after it is mixed in the reaction cell which will affect the population of the “football” complex. To prevent the consumption of PEP, the mixture was loaded as soon as it was mixed.

Upon mixing, the FRET signal generated by GroEL<sup>IAEDANS</sup> and GroES<sup>F5M</sup> in the “football” complex decreased (figure 5-6), which was caused by the replacement of labeled GroES<sup>F5M</sup> with the unlabeled GroES in solution, with a half-life of  $\sim 2.5 \pm 0.04$  seconds. Note that both GroES<sup>F5M</sup> were replaced in this experiment.

#### 5.4.2 The SP Encapsulated in “Football” is Exchanging with Others

The IAEDANS has a maximum excitation wavelength at 336 nm and maximum emission wavelength at 490 nm. The distance between the excitation and emission wavelength prevents the self-excitation and the similar unfolding

phenomena above. To see if  $\alpha$ -LA<sup>F5M</sup> and on GroEL<sup>IAEDANS</sup> can result in FRET without the self-quenching interference, a set of titration experiments were performed with different orders. If GroEL<sup>F5M</sup> was added before  $\alpha$ -LA<sup>IAEDANS</sup> (figure 5-7, A), the emission at 520 nM was enhanced which indicates the presence of FRET: the transfer of energy from IAEDANS on  $\alpha$ -LA to F5M on GroEL. If  $\alpha$ -LA<sup>IAEDANS</sup> was added first (figure 5-7, B), emission at 520 nM increased while the emission at 490 nM decreased. The increase of emission at 520 nM is due to the sum of both the background of fluorescein and FRET. The decrease at 490 nM indicates quenching of IAEDANS which confirms the FRET between  $\alpha$ -LA<sup>IAEDANS</sup> and GroEL<sup>F5M</sup>.

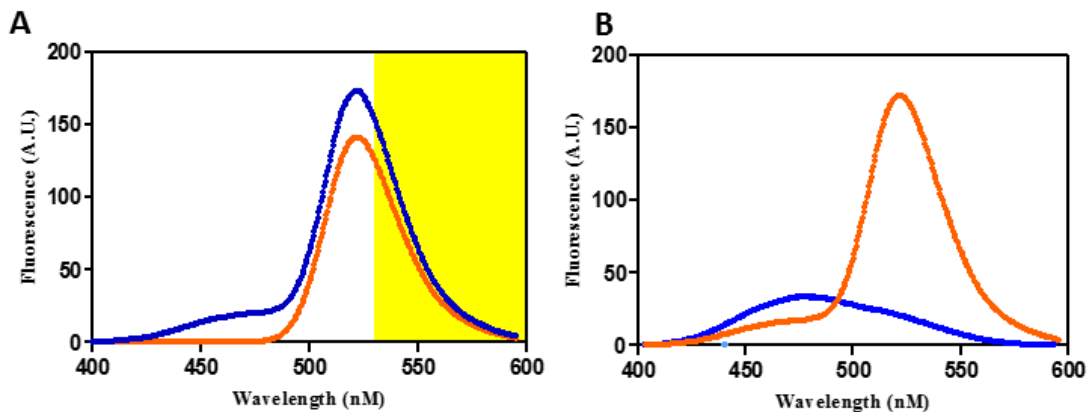


**Figure 5-7 FRET between  $\alpha$ -LA<sup>IAEDANS</sup> and GroEL<sup>F5M</sup>.** On the Perkin Elmer fluorescence spectrophotometer, the excitation wavelength was set to 336 nM, the excitation slit width was set to 15 nM and the emission slit width set to 20 nM. **A)** In a standard buffer, the GroEL<sup>F5M</sup> was added followed by the  $\alpha$ -LA<sup>IAEDANS</sup> was added later. After the addition of GroEL<sup>F5M</sup>, there was no emission at 470 nM (orange). Further addition of  $\alpha$ -LA<sup>IAEDANS</sup> brought the emission at 490 nM (blue) and an increase of emission at 520 nM due to the FRET. **B)**  $\alpha$ -LA<sup>IAEDANS</sup> was added first, there was only emission at 490 nM but no emission at 520 nM (blue). After the addition of GroEL<sup>F5M</sup>, the emission at 520 nM began to increase while the emission at 490 nM decreased (orange).

### 5.4.2.3 The Turning Over of $\alpha$ -LA<sup>IAEDANS</sup> in “Football” Cycle

To monitor the release of SP from the folding chamber of the “football” complex, the  $\alpha$ -LA<sup>IAEDANS</sup> was used with GroEL<sup>F5M</sup> to measure the decrease of the FRET signal as the  $\alpha$ -LA<sup>IAEDANS</sup> was exchanged with the unlabeled one. The decrease of the FRET signal upon mixing with unlabeled GroEL suggests the  $\alpha$ -LA<sup>IAEDANS</sup>, encapsulated in the “football” complex, is exchanging with the one in solution (figure 5-8). The result showed a FRET signal that decreased with a half-life of ~2.1 seconds.

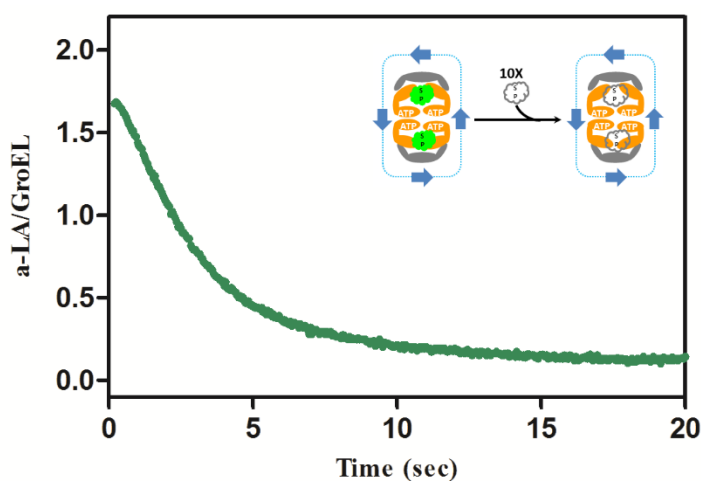


**Figure 5-8 Dynamics of SP in The “Football” Cycle.** In the stop flow instrument, a standard buffer containing final concentration of 4 $\mu$ M GroEL<sup>F5M</sup>, 8 $\mu$ M of unlabeled GroES, 1mM ATP with the regenerating system (1 mM PEP and 20 U/mL PK), and 10 fold of  $\alpha$ -LA<sup>IAEDANS</sup>, 1 mM DTT were loaded in syringe A. 57.1 $\mu$ M of unlabeled GroEL was loaded into syringe B. The excitation wavelength was set to 336 nm with the cutoff filter of 530 nm. Both syringes and the mixing cell were equilibrated at 37°C. The  $\alpha$ -LA<sup>IAEDANS</sup> on board was calculated with the  $\alpha$ -LA titration curve obtained under the same condition., the FRET emission between  $\alpha$ -LA<sup>IAEDANS</sup> and GroEL<sup>F5M</sup> was recorded as unlabeled  $\alpha$ -LA and GroEL was introduced into a turning over “football” system. The reaction was cycling in the “football” cycle and SP dissociated rapidly into the solution, exchanges with unlabeled ones as the “football” complex was turning over. The decrease of FRET signal indicated the rate of the SP dissociation from a turning over “football” complex.

GroEL is known as the heat shock protein since it rescues denatured/misfolded proteins mostly at the temperatures higher than the physiological temperature. To test whether the “football” complex turns over faster at higher temperatures, the same experiment was performed at different temperatures: 37°C, 40°C, 42°C and

45°C (figure 5-9, A). The circulating water bath was usually set at higher temperature than the actual needs since the heat loss in the tubing, and the final equilibrated temperature was read from the sensor installed in the stopped-flow instrument. As the temperature increased, the half-life of denatured  $\alpha$ -LA being released from the “football” complex decreased from  $2.13 \pm 0.06$  sec. to  $1.48 \pm 0.04$  sec (figure 5-9, B).

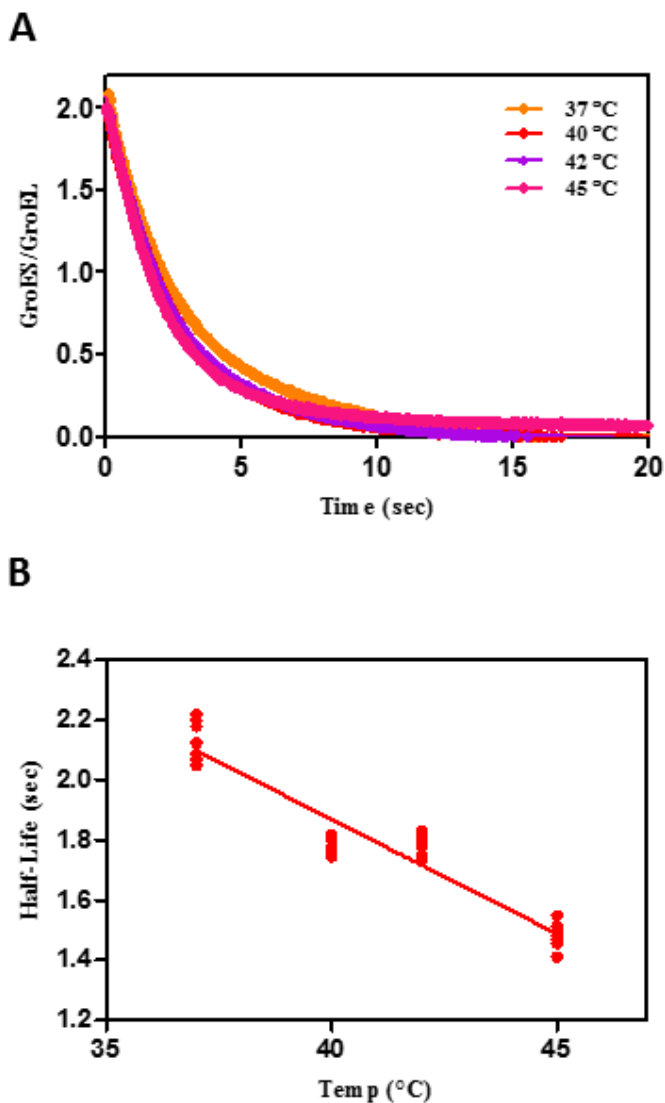


**Figure 5-9 SP Dissociation from The “Football” at Different Temperature.** In a stop flow instrument, the FRET emission between  $\alpha$ -LA<sup>IAEDANS</sup> and GroEL<sup>F5M</sup> was recorded as unlabeled  $\alpha$ -LA and GroEL was introduced into a turning over “football” system at different temperature. **A)** The reaction was incubated at 37 (orange), 40 (red), 42 (purple) and 45°C (pink) before the syringes were pushed together to initiate the reaction. **B)** The half-time of SP release from the “football” complex were plotted against the temperature the reaction took place.

At 37°C, SP and GroES exchanged from the turning over “football” complex at roughly the same rates. These sets of experiments directly showed that both of these allosteric ligands were actively turning over in the “football” cycle. As the temperature increased, less time was required for the SP to be encapsulated. The “football” complex was turning over at a higher speed to meet the requirements of folding in a harsher environment<sup>96</sup>.

In this chapter, we showed that the symmetric GroEL-GroES<sub>2</sub> “football” complex is the folding functional form of GroEL, the asymmetric GroEL-GroES<sub>1</sub> “bullet” complex is merely the resting complex of the chaperonin. Both chambers of GroEL are actively participating in the refolding of SP and the “football” complex is dynamic in nature. The ensemble population of “football” complex depends on the presence of denatured SP: increases as introducing more denatured SP into the system, or decreases as more SP get refolded. Individually GroES, on a “football” complex is turning over rapidly to release the SP encapsulated, maximizing the possibility a SP can be refolded<sup>55</sup>. This perfectly explains why nature created a double donut structure while in virtue both of the rings are utilized for folding: a parallel processing, iterative annealing machine.



## Chapter 6 The Role of Salt Bridges in The Formation of the “Football” Complex

Salt bridges play important roles not only stabilizing the structure of proteins but also in their allosteric regulation. As discussed in Chapter 3, double mutations D83A/R197A destabilized the **T** state of GroEL<sup>DM</sup> and favored its **R** state. This results a lower ATPase activity not because mutations changed the intrinsic ATPase activity but due to the slow release of ADP<sup>52</sup>. The conformational change, indicated by the dissociation of GroES from the acceptor state complex, from **R'** to **R** state is not hampered by these mutations. The next allosteric transition, from **R** state to **T** state, remains the only step affected by these mutations. Structural evidence shows apo-GroEL<sup>DM</sup> adopts a **T**-like state structure in the absence of nucleotide<sup>28</sup>. Thus, GroEL<sup>DM</sup> should still be able to visit **T** state even when it is destabilized.

Eliminating of these salt bridges, **T** state GroEL<sup>DM</sup> is no longer being favored although this does not prevent the formation of a **T**-like structure. GroEL<sup>DM</sup> is in an equilibrium between the **T** and **R** states at saturating amounts of ADP. The question remaining unanswered is: does the extremely slow release of ADP happen at the transition from **R** to **T** state in the absence of these salt bridges? If this is the case, what role do these salt bridges play in the chaperonin cycle?

### 6.1 The Failure of SP Induced “Football” Complex Formation

#### 6.1.1 Starting from apo- GroEL<sup>DM</sup>: EM Analysis

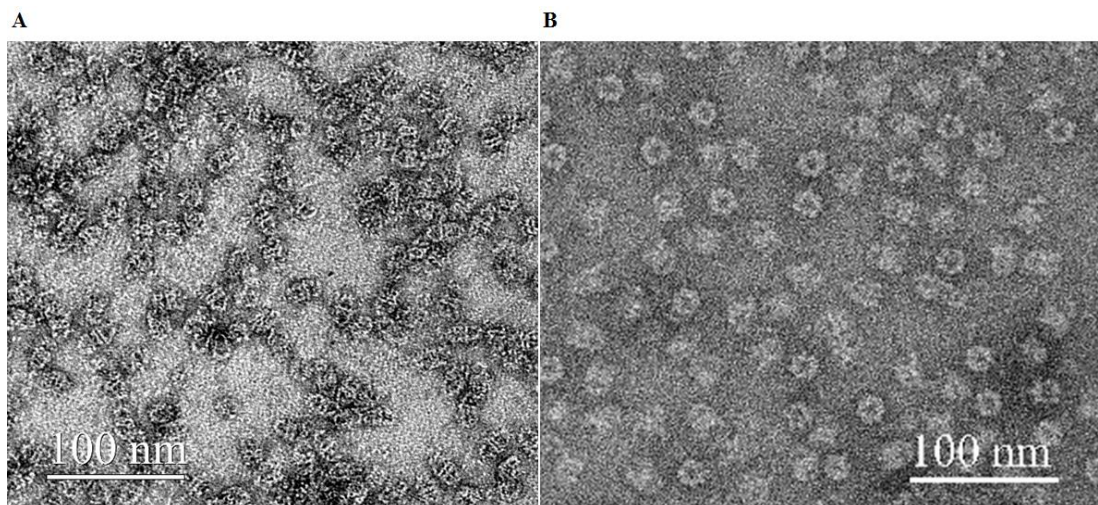


**Figure 6-1 Electron Microscopy of GroEL<sup>DM</sup>-GroES Complexes.** The electron microscope view of GroEL-GroES complex formed in the presence of **A**) ATP·BeF<sub>x</sub> (left), and most of the complex formed were GroEL<sup>DM</sup>-GroES<sub>2</sub> “football” complex and **B**) in the presence of ADP·BeF<sub>x</sub> (right) where the majority of complex formed were GroEL<sup>DM</sup>-GroES<sub>1</sub> “bullet” complex. The scale bar was of 100 nM.

To exam if these salt bridges affect the ability of GroEL<sup>DM</sup> to form the biologically, folding-active species, the “football” complex, the ATP·BeF<sub>x</sub> and ADP·BeF<sub>x</sub> method was employed. The GroEL particles formed under these conditions were examined via transmission electronic microscopy. The experiment was conducted the same as before for the GroEL<sup>WT</sup>, and the results obtained were similar. Under the ATP·BeF<sub>x</sub> conditions, the majority (>97%) of particles were the symmetric, GroEL<sup>DM</sup>-GroES<sub>2</sub> “football” complex (figure 6-1 A). Under ADP·BeF<sub>x</sub> condition, less than 0.3% of the particles were in the “football” complex while the rest were either asymmetric, GroEL<sup>DM</sup>-GroES<sub>1</sub> “bullet” complex or top views. This result was identical with that of GroEL<sup>WT</sup>, confirming the ability for GroEL<sup>DM</sup> to form the “football” complex was not affected by the removal of these salt bridges.

## 6.1.2 Analysis Starting from apo-GroEL<sup>DM</sup>:

### 6.1.2.1 Steady State Analysis

To determine the GroEL<sup>DM</sup>S stoichiometry biochemically, the FRET efficiency of IAEDANS labeled on K315C of GroEL<sup>DM</sup> (GroEL<sup>DM-IAEDANS</sup>) binding with GroES<sup>F5M</sup> was determined. This titration experiment was performed as it was on the GroEL<sup>WT</sup>. The absolute value of FRET efficiency was related to the labeling extent of the proteins. That was, the more dye that is on board of the GroEL or GroES rings, the higher the FRET efficiency after binding. GroEL<sup>DM-IAEDANS</sup> was labeled with average of 3.4 dyes per ring while GroEL<sup>WT-IAEDANS</sup> has only 2.7 dyes per ring. Thus, the formation of GroEL<sup>DM-IAEDANS</sup>-GroES<sub>2</sub> would yield a higher FRET efficiency than GroEL<sup>WT-IAEDANS</sup> to form the symmetrical complex.

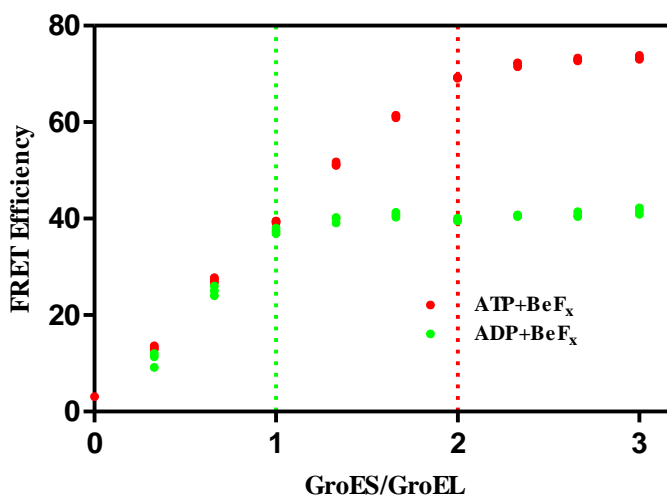


**Figure 6-2 Steady State FRET Titration of GroES<sup>F5M</sup> to GroEL<sup>DM-IAEDANS</sup>.** FRET efficiency was calculated as GroES<sup>F5M</sup> was titrated into a solution containing GroEL<sup>DM-IAEDANS</sup> in the presence of ATP·BeF<sub>x</sub> or ADP·BeF<sub>x</sub>. FRET efficiency increased as more and more GroES<sup>F5M</sup> was titrated and the plateau corresponded the stoichiometry of GroES binding to GroEL. Green circles were titration performed in the presence of ADP·BeF<sub>x</sub> and red circles were in the presence of ATP·BeF<sub>x</sub>.

In the presence of ADP·BeF<sub>x</sub>, as more GroES<sup>F5M</sup> was titrated into the solution, the FRET efficiency increased (figure 6-2, green) to a plateau of 37% at a

stoichiometry of GroES<sub>7</sub> to GroEL<sup>DM</sup><sub>14</sub> of 1.0. In the presence of ATP·BeF<sub>x</sub>, the FRET efficiency further increased (figure 6-2, red) to 73% at a stoichiometry of GroES<sub>7</sub> to GroEL<sup>DM</sup><sub>14</sub> of 2.0. For the GroEL<sup>DM</sup>, the conclusion was the same: in the ATP·BeF<sub>x</sub> conditions, there were two GroES bind with one GroEL<sup>DM</sup> in the steady state, and in the ADP·BeF<sub>x</sub> conditions, there was only one GroES bound with one GroEL<sup>DM</sup>.

#### 6.1.2.2 Pre-Steady State Analysis

To exam the process of “football” formation by GroEL<sup>DM</sup> in real time, the fluorescently labeled GroEL<sup>DM</sup> and GroES were employed to monitor the formation of FRET between dye pairs attached to each of the proteins.

The FRET signal generated by the binding of GroES<sup>F5M</sup> to GroEL<sup>DM-IAEDANS</sup> was observed (figure 6-3, A). For the association of GroES<sup>F5M</sup> to GroEL<sup>DM-IAEDANS</sup>, the GroEL-GroES<sub>2</sub> “football” complex was formed within the 1<sup>st</sup> second. Thereafter, as with GroEL<sup>WT</sup>, the GroEL<sup>DM</sup> underwent breakage of symmetry to form the GroEL-GroES<sub>1</sub> “bullet” complex. By the 5<sup>th</sup> second, the majority of the “football” complex had decayed into the “bullet” complex. Unlike GroEL<sup>WT-IAEDANS</sup>, which maintained the “football” formula in the presence of SP, GroEL<sup>DM-IAEDANS</sup> did not maintain the symmetric complex, even in the presence of same amount of SPs.

The hydrolysis of ATP during this process was monitored by the reporter protein PBP<sup>MDCC</sup> (figure 6-3, B). After two GroES became bound to one GroEL, one ATP molecule per GroEL monomer was hydrolyzed. In the presence of BeF<sub>x</sub>, the rate of the hydrolysis reaction approached zero. In both the presence and absence of SP, the release of Pi was not as fast as that of GroEL<sup>WT</sup> and it actually approaches zero.

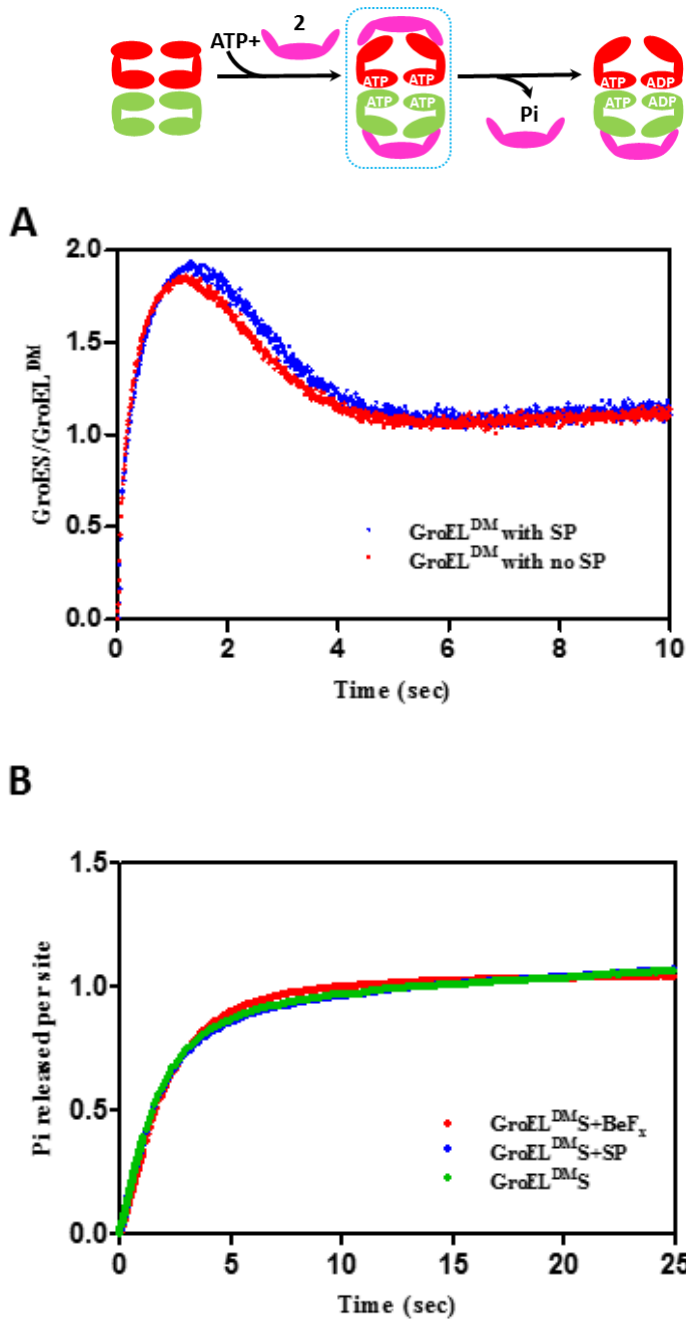


**Figure 6-3 Pre-Steady State GroEL<sup>DM</sup>-GroES Complex Formation and ATP Hydrolysis.** In syringe A, 2 $\mu$ M GroEL<sup>IAEDANS</sup> was loaded, and in syringe B, 2.5  $\mu$ M GroES<sup>F5M</sup> with the 1 mM ATP was loaded. As a control experiment, either 20 mM BeF<sub>x</sub> or 10 fold of denatured  $\alpha$ -LA was loaded into syringe B. The fluorescence excitation and detector is set the same as described previously. The standard buffer was used here and the instrument was equilibrated at 37°C. **A)** FRET emission was recorded upon mixture of GroEL<sup>DM-IAEDANS</sup> and GroES<sup>F5M</sup> in the presence (blue) and absence (red) of SP. In the presence of ATP • BeF<sub>x</sub> and ADP • BeF<sub>x</sub>, the magnitude of the FRET emission were set as two GroES per GroEL and one GroES per GroEL with which the Y axis was calibrated. **B)** The accompanying Pi release monitored by PBP<sup>MDCC</sup> in the presence (blue) and absence (green) of SP. The red trace was obtained in the presence of BeF<sub>x</sub>. The Y axis was calibrated with Pi standards as described in chapter 4.

Nonetheless, these results indicate a similar “football” formation mechanism exists for GroEL<sup>DM</sup>. That is, the binding of seven ATP to each ring is accompanied by GroES to each GroEL ring. The hydrolysis of ATP is not necessary. After the stochastic hydrolysis of ATP, the asymmetry of nucleotides promotes the transition to the asymmetric architecture of the “bullet” GroEL-GroES<sub>1</sub> complex. The difference between GroEL<sup>WT</sup> and GroEL<sup>DM</sup> lies in the response to SP. Even the presence of SP does not maintain the majority of GroEL in the “football” complex. This is consistent with the previous titration data that in the steady state SP does not promote the formation of “football” complex from GroEL<sup>DM</sup> as it does on GroEL<sup>WT</sup> (figure 4-3, yellow and orange trace).

### 6.1.3 Starting from GroEL<sup>DM</sup>-GroES<sub>1</sub> Complex

As shown in Chapter 4, SP does not stimulate “football” complex formation, either from the resting state complex (figure 4-8) or the acceptor state complex (figure 4-9, bottom panel). Notice that this failure of formation of GroEL-GroES<sub>2</sub> complex happens only after the presence of ADP on the *trans* ring. With the result in the previous section, GroEL<sup>DM</sup> is capable of forming the symmetric “football” complex starting from apo state but not after entering the chaperonin cycle, where it is bound with ADP.

As known that SP promotes the formation of “football” complex by catalyze the release of ADP on the *trans* ring, these results suggest a hindered catalysis mechanism by SP on GroEL<sup>DM</sup>. Thus it is helpful to investigate the interaction between SP and GroEL, especially in the presence of nucleotides.

## 6.2 The Decreased Binding towards SP

Much evidence showed that for GroEL<sup>DM</sup>, SP failed to stimulate the ATPase activity in both the steady state and pre-steady states, to catalyze the release of ADP, to speed up the release of the *cis* ring GroES and to promote the formation of the “football” complex. The reasons why this happens were not yet understood. A variety of efforts had been made to reveal the interaction between SPs and GroEL.

$\alpha$ -LA has three tryptophans encoded in its amino acid sequence and they are all buried in the hydrophobic cleft in the native state between helices. However, upon denaturation and the depletion of Ca<sup>2+</sup> ions,  $\alpha$ -LA remains unfolded in the presence of a reducing reagent (e.g. DTT) and the tryptophans are generally considered exposed to the bulky solvent. As described in Chapter 5, this enables us to utilize the tryptophan-IAEDANS FRET dye pairs to monitor the binding of denatured  $\alpha$ -LA to GroEL<sup>IAEDANS</sup>.

As illustrated in figure 6-4, when there was no IAEDANS GroEL<sup>WT</sup>, there was no emission at ~470 nM in either the presence or absence of denatured  $\alpha$ -LA (figure 6-4, A). However, when the GroEL<sup>WT-IAEDANS</sup> was mixed in the cuvette, there was a slight emission at 470 nM and this was intensified by the presence of denatured  $\alpha$ -LA (figure 6-4, B). The decreasing of emission at 336 nM also indicated the energy transfer from the donor-tryptophan on SP to the acceptor-IAEDANS on GroEL<sup>WT-IAEDANS</sup>. This titration was repeated, with either GroEL<sup>DM-IAEDANS</sup> or GroEL<sup>WT-IAEDANS</sup>, and using different concentrations of ADP. (Figure 6-5, A and B).

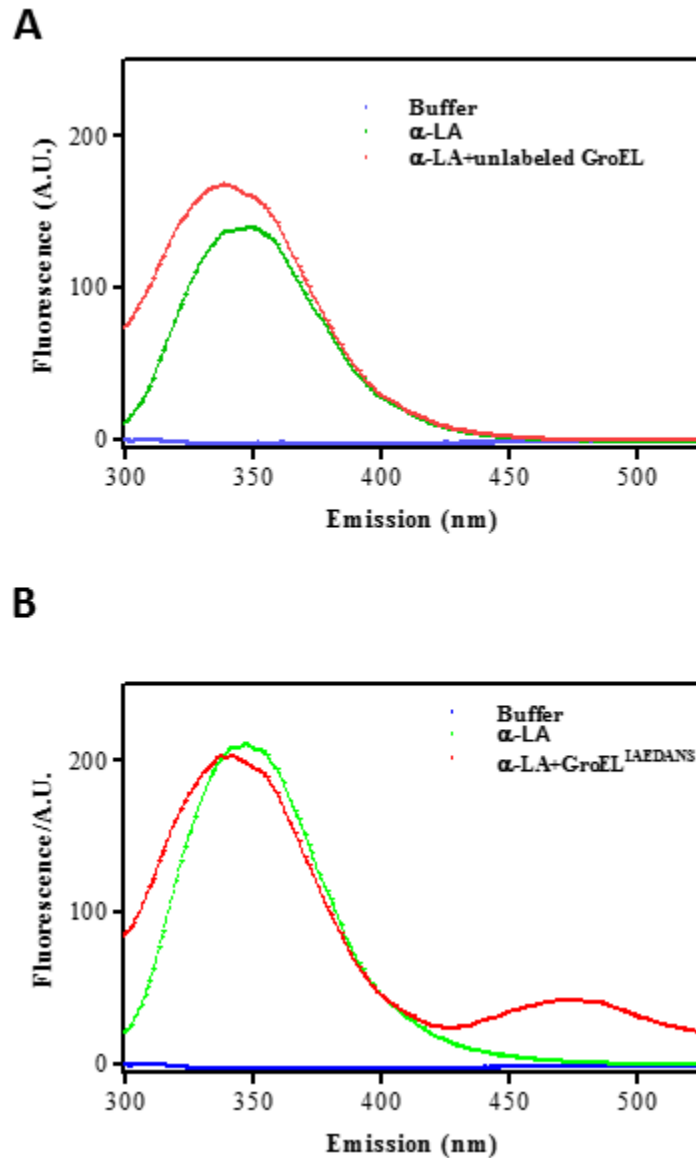


**Figure 6-4 FRET Spectrum between Trp on  $\alpha$ -LA and IAEDANS on GroEL.** The tryptophan on  $\alpha$ -LA was excited at 295 nM and emission spectrum from 300 to 550 nM was recorded. **A)** The green trace was only  $\alpha$ -LA was added in the solution and there was no emission at 470 nM. The red trace was recorded in the presence of both  $\alpha$ -LA and unlabeled GroEL where there was only emission at 330 nM but not at 470 nM. **B)** The blue and green trace was the same as in A) while the red trace was recorded in the presence GroEL<sup>IAEDANS</sup> where there was emission at both 330 and 475 nM.



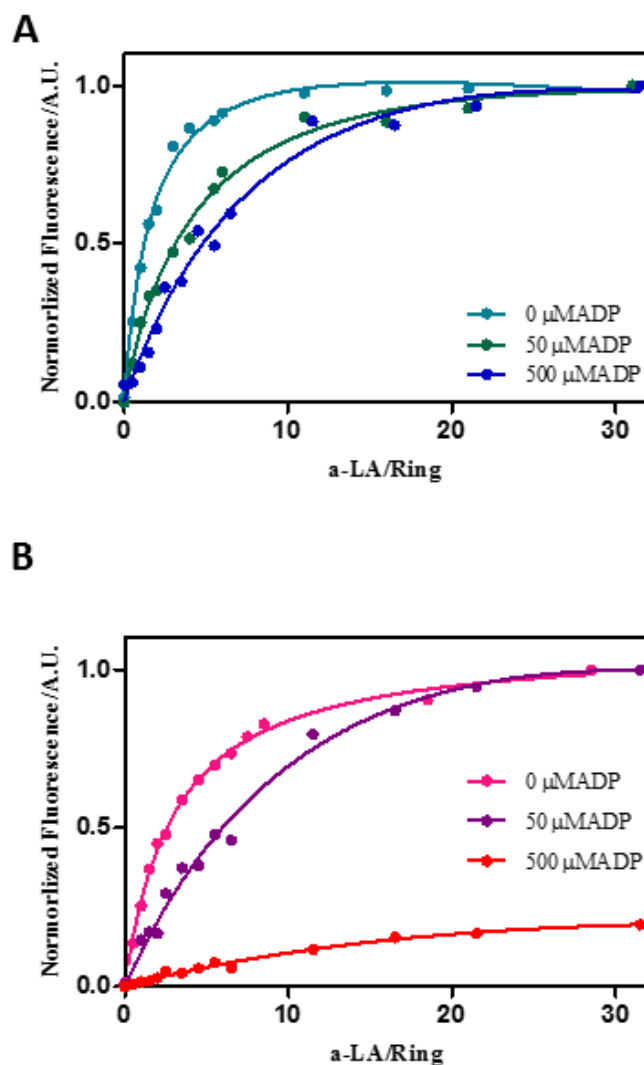


**Figure 6-5 FRET Titration of  $\alpha$ -LA to GroEL<sup>IAEDANS</sup> at Various ADP Concentration.** The experiment was performed under the standard conditions: 20 mM Tris pH7.5, 10 mM Mg<sup>2+</sup>, 200 mM K<sup>+</sup> and 37 °C. 2  $\mu$ M GroEL<sup>IAEDANS</sup> was incubated in the solution with 0, 50 and 500  $\mu$ M ADP. A small volume of concentrated, denatured  $\alpha$ -LA was added into the solution and pipetted up and down about 4-6 times before a brief incubation of 1 min. The excitation wavelength was set to 295 nM and the emission to 470 nM before data was recorded. The tryptophan on  $\alpha$ -LA was excited at 295 nM and emission spectrum from 300 to 550 nM was recorded. As more denatured  $\alpha$ -LA was added into the solution, the emission at 470 nM was recorded in the presence of GroEL<sup>WT-IAEDANS</sup> **A**) or **B**) GroEL<sup>DM-IAEDANS</sup>.

	0 $\mu$ M ADP	50 $\mu$ M ADP	500 $\mu$ M ADP
GroEL <sup>WT</sup> / $\mu$ M	0.49 $\pm$ 0.06	1.3 $\pm$ 0.3	3.5 $\pm$ 0.5
GroEL <sup>DM</sup> / $\mu$ M	0.8 $\pm$ 0.1	5.4 $\pm$ 0.7	N/D

**Table 6-1 The Binding Constant Derived of  $\alpha$ -LA to GroEL.** The fluorescence signal in figure 6-5 was normalized and fitted with one site binding model where the binding constant for each GroEL variant in the presence of different concentration of ADP were derived. N/D stands for not determined.

The fluorescence signal for each titration was normalized and fit into one site binding model (figure 6-5, A and B). The  $K_d$  value derived for each nucleotide concentration was determined (figure 6-5, C). The conclusion was apparent: as the nucleotide concentration increased, GroEL decreased its affinity towards its SP. For apo-GroEL<sup>DM</sup>, the affinity to the SP was almost the same as GroEL<sup>WT</sup> in the absence of ADP. This is consistent with the existence of a **T**-like state structure of apo-GroEL<sup>DM</sup> in the absence of nucleotide<sup>28</sup>. In the presence of 50  $\mu$ M ADP, the affinity of SP to apo-GroEL<sup>DM</sup> was much lower than GroEL<sup>WT</sup>. At physiological nucleotide concentrations (500  $\mu$ M ADP), there was almost no binding of denatured  $\alpha$ -LA to GroEL<sup>DM</sup>.

This conclusion is consistent with our previous model that GroEL binds SPs to both **T** and **R** state of GroEL but preferably to the **T** state. Since ADP promotes the transition from the **T** state to **R** state, the affinity of GroEL for the SP decreases as the nucleotides concentration increases. This also explains why the SP does not affect the behavior of GroEL<sup>DM</sup> as much as GroEL<sup>WT</sup> because at all ADP concentrations there is a great decline in the interaction with the SP.

### **6.3 The Decreased Rate of Refolding SP**

The ability of GroEL<sup>DM</sup> to fold denatured SP was tested here. MDH is an ideal substrate for this purpose for 1) it is easy to test its enzymatic activity and 2) it binds tightly to GroEL as compared to other SPs. The MDH activity during the course of refolding was measured the same as described in Chapter 5 except GroEL<sup>DM</sup> was used instead of GroEL<sup>WT</sup>. At different time points, an aliquot of the solution was

taken to measure the enzymatic activity of MDH either assisted by GroEL<sup>WT</sup>, GroEL<sup>DM</sup> or spontaneous refolding.

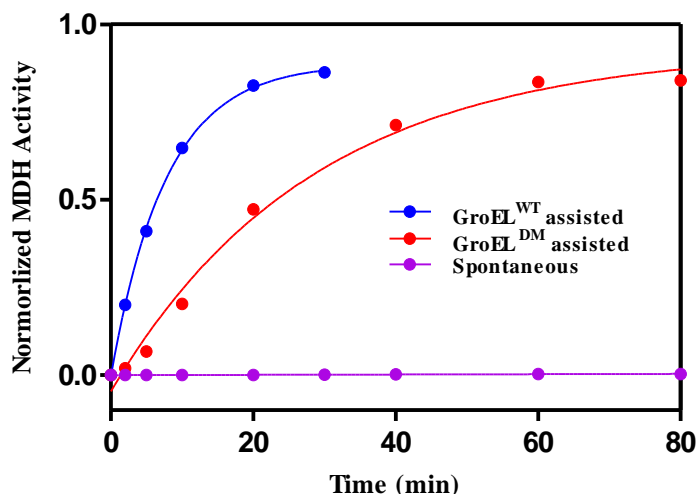


**Figure 6-6 MDH Activity during Its Refolding by GroEL<sup>DM</sup>.** The enzymatic activity of MDH to catalyze the oxidation of NADH was measured at different time point during its refolding by GroEL<sup>WT</sup> (blue), GroEL<sup>DM</sup> (red) or spontaneously (purple). Another aliquot of MDH without using urea denaturation was assayed as the fully active enzyme to calculate the percent recovery. The enzymatic activity as time was fitted with one phase exponential equation to derive the half-time of each refolding condition.

The half-time for GroEL<sup>WT</sup> to refold denatured MDH was ~5.4 min and that of GroEL<sup>DM</sup> was ~19.7 min (figure 6-6). Under these conditions where the temperature was 30 °C, it was called a non-permissive condition where the spontaneous folding did not occur and this was confirmed in the control experiment. The magnitude of percentage recovery after refolding did not differ significantly between two GroEL assisted MDH refolding, both of them yielded ~90% (88.7% and 92.9%) recovery. The only difference was the rate of refolding where GroEL<sup>WT</sup> was about three fold faster than GroEL<sup>DM</sup>.

## 6.4 The Decreased Encapsulation of SP

To determine why GroEL<sup>DM</sup> refolds SP at a slower rate than that of GroEL<sup>WT</sup>, the following experiment, which measures the MDH encapsulated at the course of refolding, was performed as described previously in Chapter 5.

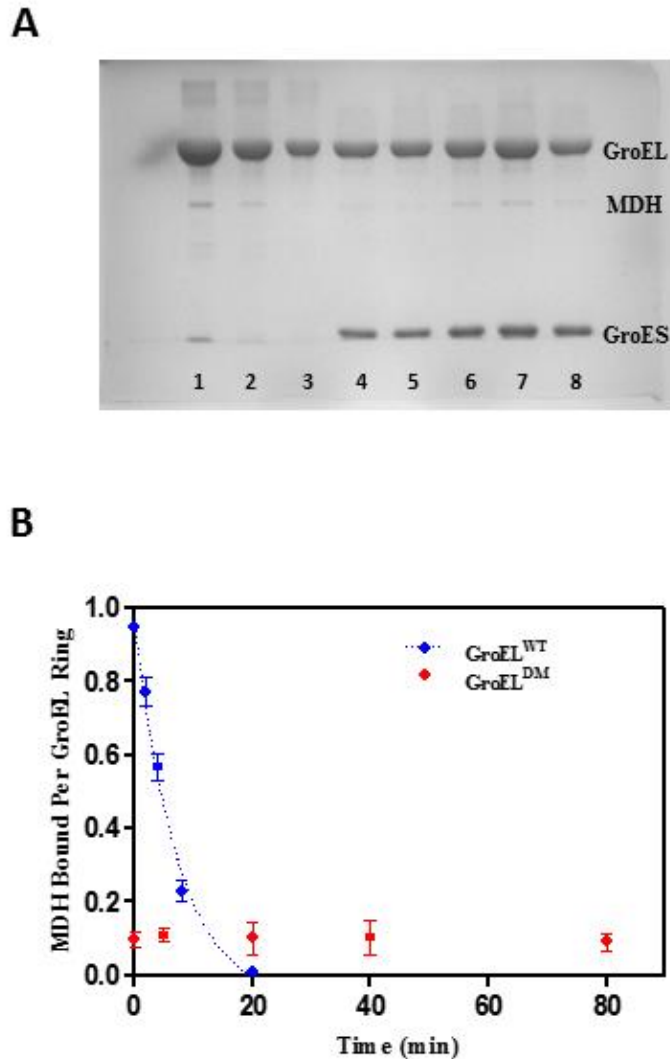


**Figure 6-7 Measurement of MDH Encapsulation during Its Refolding by GroEL<sup>DM</sup>.** **A)** The SDS-PAGE measurement of amounts of MDH bound by GroEL<sup>DM</sup> at different time points. The gel was stained with coomassie blue to view the GroEL<sup>DM</sup> bands and the same gel was destained before staining with silver to visualize the MDH bands. Lane 1, 2 and 3 were GroEL<sup>DM</sup> and MDH ladders with known concentration. Lane 4, 5, 6, 7 and 8 were the protein eluted from Ni column at 0, 5, 20, 40 and 80 min. **B)** The amounts of MDH encapsulated in GroEL<sup>WT</sup> (blue) and GroEL<sup>DM</sup> (red) were plotted at different time point.

The amount of GroEL and MDH in each elution was calculated using the standards (figure 6-7, A). The data analysis yielded an initial 1.9 MDH per GroEL tetradecamer at time 0, which was before the addition of ATP (figure 6-7, B). After addition of ATP the GroEL system began to fold the denatured MDH. As time passed, more MDH became refolded and less MDH was encapsulated in the central cavity. However, for GroEL<sup>DM</sup>, there was little initial capture of the denatured MDH: around 0.1 MDH bound per GroEL<sup>DM</sup> ring was found and there was not much fluctuation throughout the course of SP refolding (figure 6-7, B). This result was consistent with the previous SP titration data where GroEL yielded a lower affinity towards SP in the presence of nucleotides. Partially, this explained why GroEL<sup>DM</sup> refolded denatured MDH at a slower rate. That was, the inefficient encapsulation of MDH in the presence of nucleotide was responsible for the decreased rate.

### **6.5 The Altered Binding of ADP to GroEL**

As shown in many experiments here and chapter 4: GroEL<sup>DM</sup> releases ADP at a slower rate than GroEL<sup>WT</sup>. SP binds to GroEL<sup>DM</sup> with a much lower affinity in the presence of nucleotide. Since SP and ADP bind to GroEL in an allosteric state-competitive fashion, together this evidence suggests that the nucleotide binds to GroEL<sup>DM</sup> with a higher affinity than GroEL<sup>WT</sup>. Since there is no direct signal that can be coupled with the binding of ADP to GroEL, to measure the heat released by this process is a convenient way. ITC is a biophysical technique that is used to determine the thermodynamic parameters of interactions in solution, and was utilized

here to measure the binding affinity of ADP to GroEL<sup>WT</sup> and GroEL<sup>DM</sup>. The results are shown and interpreted as following:

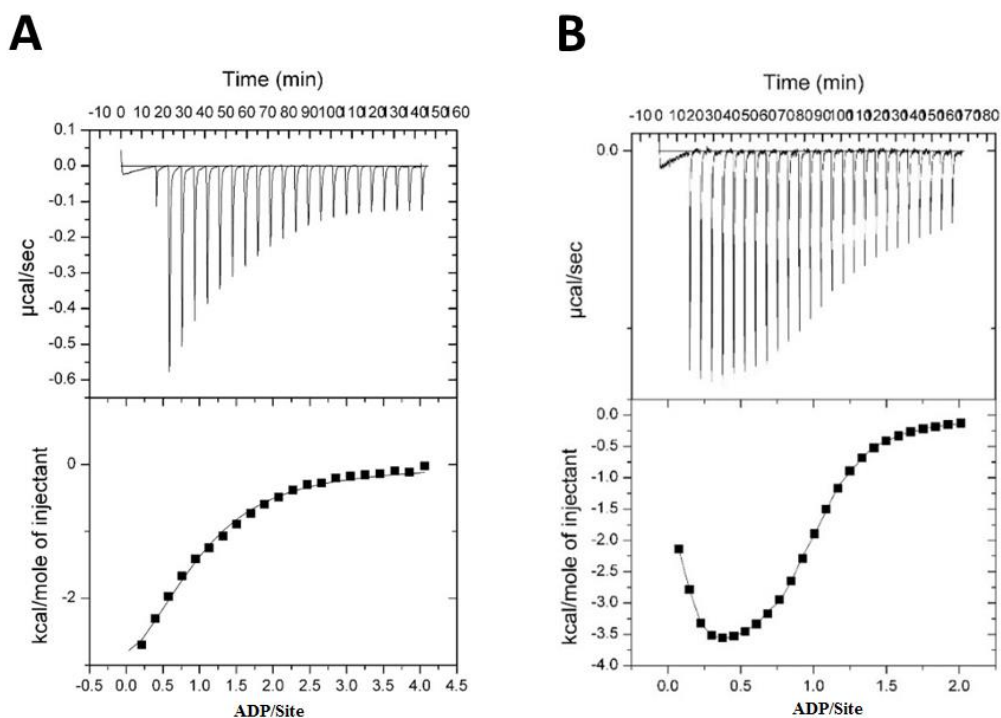


**Figure 6-8 ITC Measurement of ADP Binding to GroEL.** Binding isotherm of ADP titration to GroEL<sup>WT</sup> **A**) and GroEL<sup>DM</sup> **B**). The upper panels were the raw heat released as injections of ADP into the chamber and lower panels were the integrated heat as function of molar ratio of ADP over GroEL subunit. The solid line was the best fit of the data with one site binding model for GroEL<sup>WT</sup> and two sites binding model for GroEL<sup>DM</sup>.

	Model	N		K <sub>a</sub>		ΔH (kcal/mol)	
GroEL <sup>WT</sup>	Single site	1.09±0.07		(1.5±0.4) × 10 <sup>5</sup>		-4.2±0.3	
		0.91±0.05		(7.9±0.9) × 10 <sup>4</sup>			
GroEL <sup>DM</sup>	Two sites	N <sub>1</sub>	N <sub>2</sub>	K <sub>a1</sub>	K <sub>a2</sub>	ΔH <sub>1</sub>	ΔH <sub>2</sub>
		0.090±0.004	0.890±0.007	(7±3) × 10 <sup>8</sup>	(7.2±0.7) × 10 <sup>6</sup>	-	-
		0.120±0.004	0.880±0.004	(1.3±0.3) × 10 <sup>8</sup>	(3.27±0.09) × 10 <sup>6</sup>	1.1±0.3	4.78±0.05
						1.5±0.1	3.97±0.03

**Table 6-2 The Binding Constant of ADP to GroEL Derived from ITC.** With different models to fit the thermograms, the stoichiometry, association constants and enthalpy changes derived from the raw data were listed. ADP binding to GroEL<sup>WT</sup> was fit with one site model and ADP binding to GroEL<sup>DM</sup> was fit with two sites model. Two replicates of experiment results are listed and the K<sub>a</sub> value for GroEL<sup>WT</sup> is consistent with previously reported data<sup>43</sup>. It is worth noting for GroEL<sup>DM</sup>, six parameters were derived from one set of isotherm and the errors could be large.

The titration of ADP to GroEL<sup>DM</sup> showed two phases of binding isotherm (figure 6-8, B), similar to that of arginine repressor<sup>97</sup>. Various efforts had been made to ascribe the same behavior in GroEL<sup>DM</sup>: 1) Lower the K<sup>+</sup> concentration below our standard, physiological 200 mM; 2) Use different injection volume in the middle of the titration and 3) Lower titrant ADP concentration. These experiments confirmed the two phase binding isotherm did exist in GroEL<sup>DM</sup> rather than an artifact. As expected, GroEL<sup>DM</sup> had much higher affinity towards ADP. The tighter site had a K<sub>d</sub> in the nanomolar range and the other subunits had at least 50 fold higher affinity than GroEL<sup>WT</sup> (table 6-2). This was consistent with our theory that the mutation of these salt bridges destabilize the **T** state of GroEL and thus favoring its **R** state, which has a higher affinity towards nucleotides.

The stoichiometry of the higher affinity site in GroEL<sup>DM</sup> is ~0.11 corresponding to one subunit in GroEL<sup>DM</sup><sub>14</sub>. This indicates one subunit out of fourteen has unusual higher affinity towards ADP. It is consistent with the crystal structure of apo-GroEL<sup>DM</sup> where the electron density of the apical domain from one subunit is missing, suggesting a potential **R**-like state of that particular subunit in the absence of nucleotide.

In this chapter, we examined the ability of GroEL<sup>DM</sup> to form the folding functional, “football” complex. The mutations displaced this variant to its **R** side that has a higher affinity towards nucleotide. Further SP binding to the ADP bound GroEL<sup>DM</sup> is greatly compromised and thus the SP promoted GroEL-GroES<sub>2</sub> complex formation is hindered. This eventually leads to less efficient SP encapsulation and slower refolding by GroEL<sup>DM</sup>.

## Chapter 7 *In vivo* Study of GroEL in Supplementary Cell Growth

To study the function of GroEL in facilitated protein folding *in vivo*, the MGM100 cell were created. This cell was a variant of MG1655 (standard *E. coli* K12 strain) where the normal *groELS* promoter was replaced by pBAD-groELS on the chromosome<sup>98,99</sup>. Thus the genomic GroEL was not expressed on glucose plates as the pBAD promoter was tightly repressed, but grow normally on plates with arabinose which induced the pBAD promoter.

The ptrc99A vector was used as to introduce foreign GroEL and its mutant to the cell. Ptrc99A was a variant of pBR322 plasmid with amp resistant gene and a trc promoter under which the groES and groEL genes were sequentially linked after the EcoRI restriction site but before HindIII restriction site (see figure 7-1). With the original 4176 bp vector, the engineered ptrcESL plasmid was 6216 bp. The promoter of ptrc99A was quite leaky so that *groELS* gene and its mutants on the plasmid were expressed constantly regardless of the carbon source.

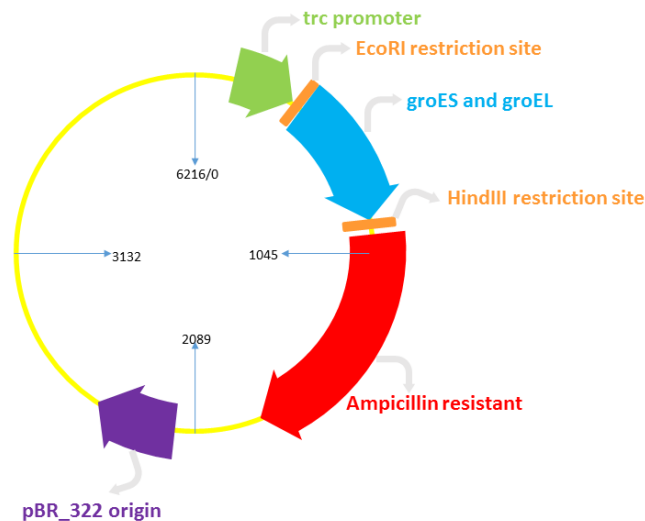


**Figure 7-1 Map of Plasmid pTrc99A.** The 4176 bp long plasmid pTrc99A was engineered that the groES and groEL genes were sequentially linked after the EcoRI restriction site and before HindIII restriction site (dark blue region) and the length increased to 6216 bp. This plasmid contains an Amp resistant gene that enables *E. coli* growing in medium with Amp.



## 7.1 The *in vivo* Study of GroEL<sup>DM</sup> and GroEL<sup>D398A</sup>

The experiment was performed as described in Chapter 2, the mutagenesis part was performed in our lab and the cell culturing part in this section was performed in Dr. Peter Lund's lab, University of Birmingham.

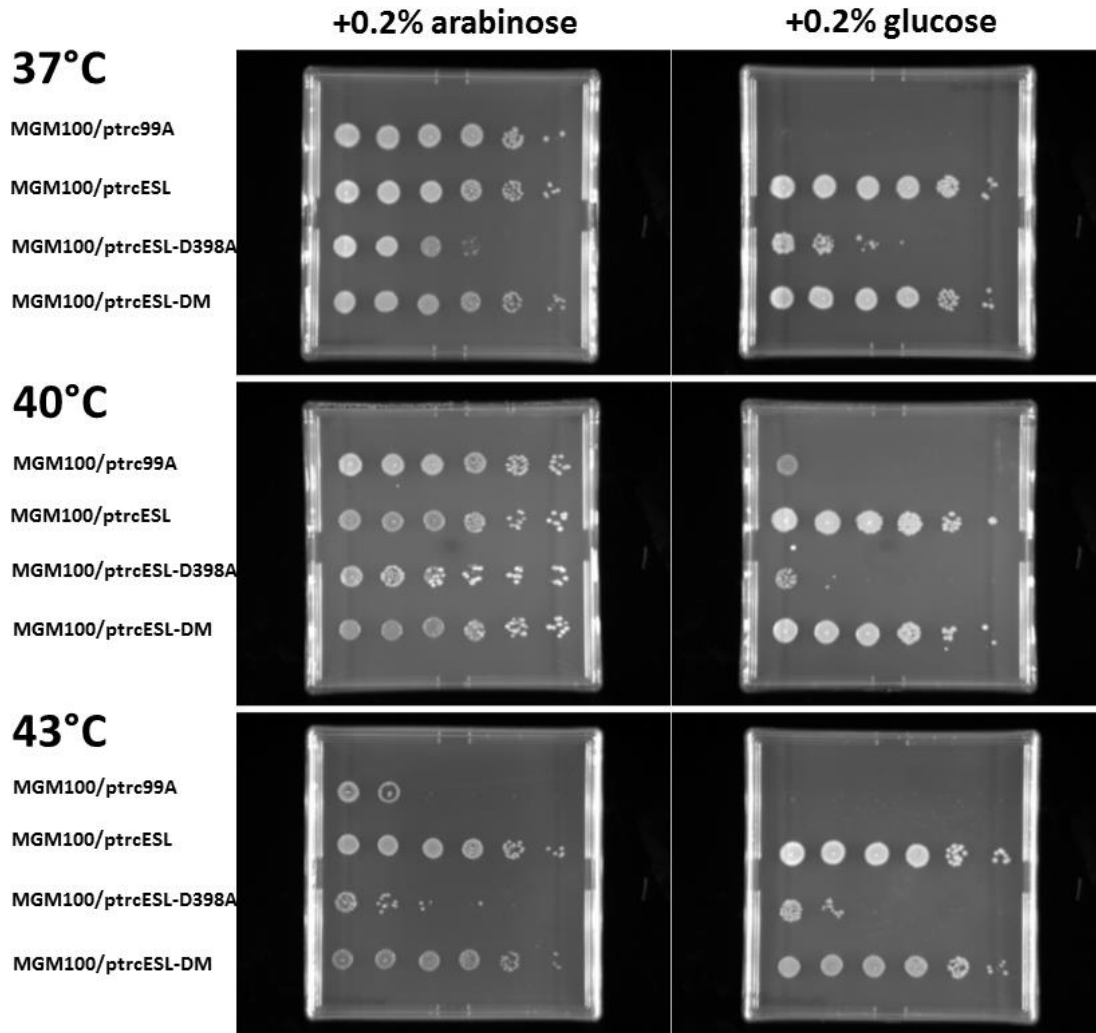


**Figure 7-2 Complementary Growth of GroEL Variant at Different Temperature.** MGM100 cells harboring ptrcESL, ptrcESL-D398A, ptrcESL-DM were cultured and spotted with series of 10 fold dilution on LB-Agar plates with either 2% arabinose or glucose. Plates were cultured at 37, 41, and 41°C for 12 hours to test the complementary support growth of different mutation on GroEL.

The results were fairly straight forward as shown in figure 7-2. The ptrc99A plasmid, when used as a template control, did not complement at any temperature just

as expected. Even in the presence of arabinose, the ptrc99A transformed GM100 cells did not grow well. This was probably due to the inability of *E. coli* to regulate *groELS* in response to the high temperature when it was under the pBAD control.

However, for the ptrcESL transformed MGM100 cells grew very well at 37°C, 41°C and 43 °C. One thing to notice was that at high temperature such as 43°C, wild type ptrcESL was still able to grow, demonstrating the ability of *groELS* to rescue the defective growth phenotype of MGM100 at 43°C.

For ptrcESL<sup>D389A</sup>, growth was barely supported at 37°C (figure 7-2), and did not support the growth at higher temperatures like 40°C or 43°C at all. This was because ATP hydrolysis was required for GroEL assisted protein folding. While D398A greatly hampered the hydrolysis of ATP, this mutant would have a compromised support of cell growth. On the other hand, ptrcELS<sup>DM</sup> supported the growth well at these temperatures. Even at 43°C it was able to rescue the defective growth phenotype of this strain on arabinose.

The plasmids were extracted from cultures grown from a single colony and sequenced again to confirm the mutants, and to exclude the possibility that recombination between chromosomal *groELS* and plasmid. The results showed that the mutations were correct in both cases. Here, *in vivo*, we tested the ability of GroEL<sup>DM</sup> to support the cell growth and the results showed no difference between GroEL<sup>WT</sup> and GroEL<sup>DM</sup> in supporting the cell growth *in vivo*, despite the inability of GroEL<sup>DM</sup> to support the folding of SP *in vitro*.

## 7.2 The *in vivo* Study of GroEL<sup>K105A</sup>

The K105 plays an essential role in the negative cooperativity of GroEL<sup>100</sup>. To test its significance in supporting bacterial growth *in vivo*, this mutation was also inserted on the ptrc99A-ESL plasmid and transformed into the MGM100 cells. This study was performed here in Maryland.

The same experiment was performed on K105A mutant as described above except the highest concentration in this experiment was of OD<sub>600</sub> equals to 0.1. Two parallel sets of plates were spotted under the same conditions and one set was incubated at 37°C overnight while the other was set at 42°C. The colonies grown on the plates were sequenced to confirm the mutations.

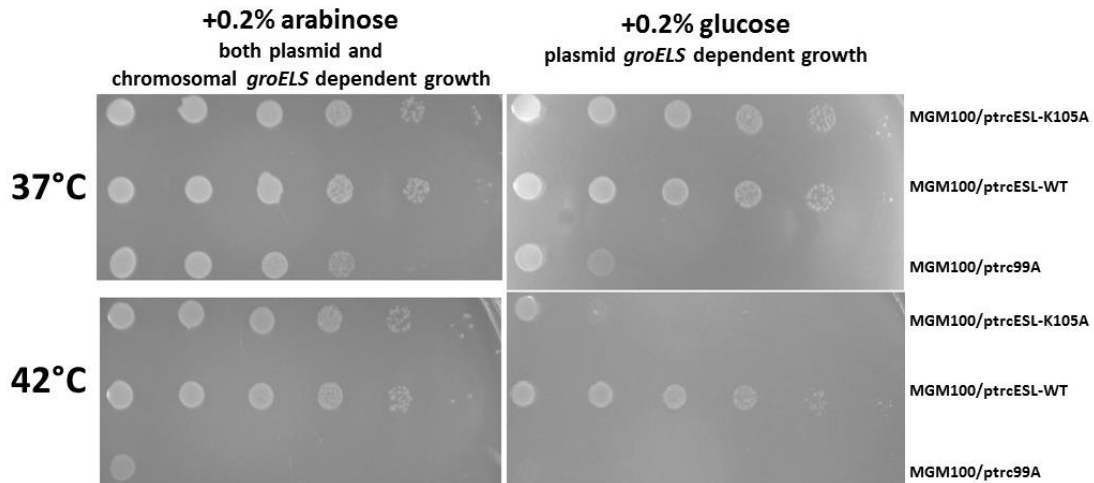


**Figure 7-3 Complementary Growth of GroEL<sup>K105A</sup> at Different Temperature.** MGM100 cells harboring ptrc99A, ptrcESL, ptrcESL-K105A were cultured and spotted with series of 10 fold dilution on LB-Agar plates with either 2% arabinose or glucose. Plates were cultured at 37 and 42°C for 12 hours to test the complementary support growth of this mutation on GroEL.

The results showed that ptrcESL-K105A mutant was able to support the growth of *E. coli*. at physiological conditions where the temperature was 37°C. However, when the temperature is raised to 42°C, this mutation in GroEL disabled

the cells ability to grow. This result indicated a temperature sensitivity for this mutant on its behavior regarding chaperonin assisted protein folding.

## Chapter 8 Summary

GroEL folds/refolds SPs with both of its rings operating almost in phase with each other. The current, dogmatic view of the GroELs chaperonin cycle lies largely on the asymmetrical cycling pathway<sup>65</sup>. There are many inconsistencies within this current model<sup>42,43,69-74</sup>. The shortcomings of the current chaperonin cycle model, are best understood after considering what the current model claims: 1) Binding of ATP to one ring of GroEL prevents the binding of ATP to the opposite ring. 2) Binding of GroES is dependent on the binding of ATP to the GroES-associated ring. 3) The chaperonin cycle starts with the SP binding to the ATP-bound ring of the asymmetric complex. 4) The GroEL-GroES nano-machine alternates back and forth with one ring and seven ATP bound to it at a time and discharges the previous one.

Nonetheless, evidence here shows that in the presence of GroES, each subunit in a GroEL molecule hydrolyzes ATP once within 5 seconds before it turns into the steady state ATP hydrolysis. Two GroES bind to one GroEL simultaneously, accompanying the binding and hydrolysis of ATP<sup>43</sup>. Of course, in the absence of BeF<sub>x</sub>, this “football” complex decays with a dependence on the amount of denatured SP in solution. Previous research shows that ATP promotes the formation of the “football” complex while ADP promotes the “bullet” complex formation. We further pushed the view that the symmetry of nucleotides supports the symmetry of GroES on GroEL. Once the hydrolysis of ATP on the GroEL rings reaches an extent that the symmetry of nucleotides no longer supports the formation of the symmetric “football” complex, the GroES on one of the GroEL ring begins to dissociate. That means, as long as there is ATP on both rings, the “football” complex will remain.

This was actually proved by mixing GroEL and GroES with a non-hydrolysable ATP analogue AMP-PNP and we saw the preservation of the “football” complex. Others results in our lab suggests that as long as ATP is not hydrolyzed, e.g. using the hydrolysis deficient mutant D398A, the “football” complex will maintain for a long time. In all, this suggests the remarkable role of that ATP occupancy has in both rings that it governs the status of GroES binding them.

These experiments provide an alternative explanation to the theory that strong, negative cooperativity exists such that the binding of ATP to the second ring is prevented by binding of ATP to the first ring. The origin of these incorrect views comes from the researcher’s selection of GroEL D398A mutant to study the negative cooperativity of GroEL<sup>54</sup>. After mixing with GroES and ATP, the researchers believe they had a “bullet” complex and tested the binding of a second GroES on it. The result showed no binding of any ligand, either SP or GroES. If, however, they had analyzed the complex they had, they would have seen the “football” complex where two ends of GroEL were both sealed with GroES. In this circumstance, there must be no binding of any ligand, SP or GroES, to this GroEL molecule. However, this lead these researchers to a misleading conclusion that the negative cooperativity is so strong that once one ring is bound with ATP the other ring is not capable of accepting any ligands. The research that followed from these results was apparently guided by this view and this lead to many more inaccurate conclusions being drawn.

We have proved that *in vivo*, the D398A mutant does not support the growth of *E. coli* as well as wild type in either physiological or higher temperatures. The SR1 also does not support the growth of *E. coli* with which many models have been built

on. While a mutant is not functional *in vivo*, its behavior *in vitro* certainly cannot be taken into consideration as cornerstones for theory to build up on.

The double ring structure of GroEL has evolved to chaperone the folding of SPs *in vivo* with both of its ring present. If nature only needs one ring to be functional to fold SPs, why is a two ring structure necessary? Another biological issue that remains unsolved by this dogmatic theory is that they propose ATP hydrolysis is the only rate limiting step in the chaperonin cycle regardless of the presence of the SP<sup>54,65</sup>. If this is the case, then the hydrolysis of ATP in the absence of SP will be a waste of energy and a regulatory mechanism where such consumption in vain is prevented does not exist.

### **8.1 GroEL-GroES<sub>2</sub> Symmetric “Football” Complex is the Folding Functional Form**

However, for the model we propose here, that GroEL cycles in between the symmetric and asymmetric cycles, we have proposed several points to make comparisons to the previous model: 1) In the absence of SP, ADP release is the rate limiting step of the cycle and GroEL is mainly in the asymmetrical “bullet” shape. 2) SP catalyzes the release of ADP from the *trans* ring by ~100 fold and promotes the binding of ATP and association of a second GroES<sup>43</sup>. 3) The population of the “football” complex is dependent on the needs of folding SPs<sup>42</sup>. In another words, the more SP present in the system, the more “football” complex forms. GroEL switches its cycling from the asymmetrical, “bullet” cycle, to the symmetrical, “football” cycle upon the introduction of SP and this switching of cycles takes less than a second. 4) The “football” complex is very dynamic itself and the dissociation of SP encapsulated

or GroES on board has an average half-life of ~2.1 sec at 37°C. 5) The ensemble population of “football” complexes, provided with enough ATP, only depends on the amount of denatured SP present. As more and more SPs get refolded and they are no longer recognizable by GroEL, the “football” population decays<sup>42</sup>.

It is well established that ligands affect the allosteric equilibrium of GroEL in the following ways: 1) SP binds, preferentially but not exclusively, to the **T** state of GroEL. 2) Nucleotides bind preferentially but not exclusively, to the **R** state of GroEL. 3) GroES binds exclusively to the **R** state of GroEL. 4) K<sup>+</sup>, enhances the affinity of nucleotides to both the **T** and **R** states<sup>51</sup>. However, since the **R** state has higher affinity towards nucleotides, increasing K<sup>+</sup> concentration usually favors the **R** state while decreasing K<sup>+</sup> concentration favors the **T** state of GroEL. Not only is there biochemical data to support these views but also structural data that shows the nucleotide binding pocket in **T** state is more open than that in the **R** state. Presence of SP pushes the equilibrium of GroEL to the **T** side where the nucleotide binding pocket is more open and nucleotides are freer to exchange. On the other hand, helix M latches the entrance of nucleotide binding pocket in the **R** state such that there is no free nucleotide exchange.

The nucleotide exchange is organically connected with the demand of SP folding in such way that when there is no denatured SP, the *trans* ring of GroEL is idling in its **R** state and ADP from previous cycle is stuck in the binding pocket that prevents the useless hydrolysis of ATP. However, when there is a need for SP folding, the *trans* ADP is released by catalysis of denatured SP itself<sup>43</sup>. Other evidence shows that titration of “football” complex as function of [K<sup>+</sup>] also indicates



that the population of “football” is directly related to the affinity of ATP to GroEL. More importantly, the folding functional form “football” is formed following ATP binding to the *trans* evacuated ring where both of the rings are processing the work with higher efficiency. This self-regulatory mechanism of GroEL action by the demand of its substrate is so delicately designed that it not only prevents a futile cycle where in vain ATP hydrolysis happens, but also ensures the maximum utilization of the rings when there is denatured SP present<sup>42</sup>.

Common wisdom would think that since both of the openings of GroEL are sealed in the “football”, there is no possibility of SP binding to such a symmetrical complex. The limitation of such thoughts arises from a static view of the “football” complexes as a stable architecture whereas in reality it is very dynamic both individually and ensemble. SPs bound to GroEL get captured and encapsulated for about 2 seconds before being ejected into the solution regardless if it is properly folded or not. This in turn supports the model that active folding of SP by GroEL through rounds of iterative unfolding and where encapsulation of SP in GroEL is less relevant to the refolding yield. The more dynamic the GroELs complex is, the more chances SPs have to be unfolded by GroEL in a certain amount of time and the more likely a substrate will be to reach its native state through multiple rounds of conformational searches<sup>96</sup>.

On the other hand, the decay of ensemble amounts of the “football” complexes as more SPs are refolded also decreases the consumption of ATP by placing the GroELs complex in the resting state. This process is achieved via the unrecognition of folded or partially folded SP by GroEL and efficiently modulate its

cycling mode. No matter how fast initiation of the “football” complex is or the comparatively slow decomposition of it, the whole process is solely dependent on the amount mis-folded or denatured SPs that are recognizable by GroEL, which unequivocally proves its role as the folding functional form of GroEL.

## **8.2 Salt Bridges as an Intrinsic Resetting Mechanism in the Chaperonin Cycle**

Allostery refers the conformational change upon binding of a ligand that either positively or negatively regulates the binding of consecutive ligands and/or activity of the biomolecule where there is no direct interaction between these ligands. This idea was first introduced by Monod and Jacob in 1961<sup>101</sup>. As for GroEL, the concerted binding of ATP is coupled with the rigid body movement where opening of the apical domain occurs for all seven subunits. SPs bound to GroEL, usually clamped by helix H and I between different subunits, are in their non-native state where non-native interaction within its secondary structure constrains them in a local minimum. To rescue these mis-folded structures, work has to be done on them to pull them out of the local minimum and the non-native interactions between residues have to be broken<sup>45,101,102</sup>. In order to do that, at least a pair of clamps have to move apart from each other during the apical domain movement and it reaches its maximum efficiency if all seven subunits are stretching the SP bound on it at the same time. This concerted stretching of the SP requires GroEL to overcome the free energy gap between **T** state and **R** state. The gap is increased by the cross linking force introduced by SP binding to the apical domain<sup>45</sup>. In turn this requires the binding of ATP to GroEL to occur in a cooperative manner so that this binding energy can fully fill the gap. That is, binding of ATP and its associated domain movement are

happening in a MWC type allosteric fashion to realize the biological function of GroEL described by the iterative annealing model.

The intrinsic mechanism that regulates such allosteric behavior between different subunits remains unclear. D83-K327 and R197-E386 are salt-bridges that form in the **T** state GroEL and break during the **T** to **R** transition. Mutations of D83 and R197 into alanine eliminated these salt bridges and thus destabilized the **T** state of GroEL and artificially favored the **R** state. The function of these salt bridges was confirmed in the steady state ATPase profile of GroEL<sup>DM</sup> that the **TT** to **TR** transition occurs at lower ATP concentration than that of GroEL<sup>WT</sup>. However, the crystal structure and other biochemical evidence indicates this variant is still capable of adopting a **T**-like state, but in the absence or at much lower nucleotide concentrations. Removal of a pair of these salt bridges produces two significant findings. First, this mutant favors the **R** state to such an extent that the SP does not return it to its **T** state. One thing to notice here is the removal of salt bridges did not eliminate the **T** state of GroEL as demonstrated by both biochemical and structural data. The SP preferentially binds to the **T** state and displaces the equilibrium to where ADP can more freely exchange so that ATP binding becomes possible. These mutations, where salt bridges that stabilize the **T** state are removed, decrease the population of GroEL ring in the **T** state where the SP has a chance to bind in the presence of nucleotides. This indicates the significance of these interactions to stabilize the **T** state to finish a complete chaperonin cycle.

Secondly, GroEL<sup>DM</sup> does not form the “football” complex that is stimulated by SPs. Again, the ability of the mutant to form the “football” complex was not

compromised and this is supported biochemically and structurally. The role of the symmetric, GroEL-GroES<sub>2</sub> “football” complex in chaperonin assisted protein folding has been demonstrated in research here and elsewhere in the literature<sup>42,69-74</sup>. SP directs GroEL cycling from the asymmetric cycle, where it is mostly idling in the resting state, to the symmetric cycle mainly by catalyzing the release of ADP that converting the **R** state *trans* ring to its **T** state since the SP has a higher affinity towards the **T** state of GroEL as illustrated here. Thus it is possible for the previous hydrolysis product, ADP, to be released from its binding pocket, and a new set of seven ATP can bind to the *ex-trans* ring followed by the association of the second GroES on the same GroEL. However, due to artificially destabilized **T** state on GroEL<sup>DM</sup>, even SP cannot displace the equilibrium to the SP acceptor-**T** state. Since GroEL does not form the “football” in the ADP conditions, not even when one ring is occupied with ATP (or some ATP) and another ring is occupied with ADP, the ADP remaining in the *trans* ring of GroEL<sup>DM</sup> blocked the entrance of this variant to the functioning symmetric “football” cycle. Together this suggests visiting **T** state in a cyclical basis is necessary for the completion of the chaperonin cycle.

As with many other machines, either natural or man-made, GroEL shares their characteristics (concerted, coordinated movements, cyclical operation and irreversible energy consumption) as well. Resetting of such a machine to where it begins its work is critical to complete its cycle. A network of salt bridges, including D83-K327 and R197-E386, brings GroEL from the **R** state to **T** state where it more favorably binds with SP and setting this protein machine to the beginning of the working cycle. Partial elimination of these salt bridges stalls the chaperonin at its resting state and

prevents the formation of the biologically folding active-“football” complex, indicating its role as an intrinsic resetting mechanism while SP as the extrinsic resetting allosteric ligand.

## REFERENCES

- 1 Anfinsen, C. B. Principles that govern the folding of protein chains. *Science* **181**, 223-230 (1973).
- 2 Deechongkit, S. *et al.* Context-dependent contributions of backbone hydrogen bonding to beta-sheet folding energetics. *Nature* **430**, 101-105 (2004).
- 3 Gruebele, M. Downhill protein folding: evolution meets physics. *C R Biol* **328**, 701-712 (2005).
- 4 Thirumalai, D. & Lorimer, G. H. Chaperonin-mediated protein folding. *Annu Rev Biophys Biomol Struct* **30**, 245-269 (2001).
- 5 Stan, G., Thirumalai, D., Lorimer, G. H. & Brooks, B. R. Annealing function of GroEL: structural and bioinformatic analysis. *Biophys Chem* **100**, 453-467 (2003).
- 6 Chang, H. C., Tang, Y. C., Hayer-Hartl, M. & Hartl, F. U. SnapShot: molecular chaperones, Part I. *Cell* **128**, 212 (2007).
- 7 Tang, Y. C., Chang, H. C., Hayer-Hartl, M. & Hartl, F. U. SnapShot: molecular chaperones, Part II. *Cell* **128**, 412 (2007).
- 8 Goloubinoff, P., Christeller, J. T., Gatenby, A. A. & Lorimer, G. H. Reconstitution of active dimeric ribulose biphosphate carboxylase from an unfolded state depends on two chaperonin proteins and Mg-ATP. *Nature* **342**, 884-889 (1989).
- 9 Goloubinoff, P., Gatenby, A. A. & Lorimer, G. H. GroE heat-shock proteins promote assembly of foreign prokaryotic ribulose biphosphate carboxylase oligomers in *Escherichia coli*. *Nature* **337**, 44-47 (1989).

- 10 Schmidt, M., Buchner, J., Todd, M. J., Lorimer, G. H. & Viitanen, P. V. On the role of groES in the chaperonin-assisted folding reaction. Three case studies. *J Biol Chem* **269**, 10304-10311 (1994).
- 11 Bhattacharyya, A. M. & Horowitz, P. M. Rhodanese can partially refold in its GroEL-GroES-ADP complex and can be released to give a homogeneous product. *Biochemistry* **41**, 2421-2428 (2002).
- 12 Horwich, A. L., Low, K. B., Fenton, W. A., Hirshfield, I. N. & Furtak, K. Folding *in vivo* of bacterial cytoplasmic proteins: role of GroEL. *Cell* **74**, 909-917 (1993).
- 13 Keresztessy, Z., Hughes, J., Kiss, L. & Hughes, M. A. Co-purification from *Escherichia coli* of a plant beta-glucosidase-glutathione S-transferase fusion protein and the bacterial chaperonin GroEL. *Biochem J* **314** ( Pt 1), 41-47 (1996).
- 14 Lubben, T. H., Donaldson, G. K., Viitanen, P. V. & Gatenby, A. A. Several proteins imported into chloroplasts form stable complexes with the GroEL-related chloroplast molecular chaperone. *Plant Cell* **1**, 1223-1230 (1989).
- 15 Dhar, A. *et al.* Structure, function, and folding of phosphoglycerate kinase are strongly perturbed by macromolecular crowding. *Proc Natl Acad Sci U S A* **107**, 17586-17591 (2010).
- 16 Gruebele, M. Protein folding: the free energy surface. *Curr Opin Struct Biol* **12**, 161-168 (2002).
- 17 Thomas, P. J., Ko, Y. H. & Pedersen, P. L. Altered protein folding may be the molecular basis of most cases of cystic fibrosis. *FEBS Lett* **312**, 7-9 (1992).

- 18 Rechsteiner, M. Ubiquitin-mediated pathways for intracellular proteolysis. *Annu Rev Cell Biol* **3**, 1-30 (1987).
- 19 Stan, G., Lorimer, G. H., Thirumalai, D. & Brooks, B. R. Coupling between allosteric transitions in GroEL and assisted folding of a substrate protein. *Proc Natl Acad Sci U S A* **104**, 8803-8808 (2007).
- 20 Todd, M. J., Lorimer, G. H. & Thirumalai, D. Chaperonin-facilitated protein folding: optimization of rate and yield by an iterative annealing mechanism. *Proc Natl Acad Sci U S A* **93**, 4030-4035 (1996).
- 21 Braig, K. *et al.* The crystal structure of the bacterial chaperonin GroEL at 2.8 Å. *Nature* **371**, 578-586 (1994).
- 22 Xu, Z., Horwich, A. L. & Sigler, P. B. The crystal structure of the asymmetric GroEL-GroES-(ADP)<sub>7</sub> chaperonin complex. *Nature* **388**, 741-750 (1997).
- 23 Thirumalai, D., Klimov, D. K. & Lorimer, G. H. Caging helps proteins fold. *Proc Natl Acad Sci U S A* **100**, 11195-11197 (2003).
- 24 Hyeon, C., Lorimer, G. H. & Thirumalai, D. Dynamics of allosteric transitions in GroEL. *Proc Natl Acad Sci U S A* **103**, 18939-18944 (2006).
- 25 Ranson, N. A. *et al.* Allosteric signaling of ATP hydrolysis in GroEL-GroES complexes. *Nat Struct Mol Biol* **13**, 147-152 (2006).
- 26 Aharoni, A. & Horovitz, A. Inter-ring communication is disrupted in the GroEL mutant Arg13→Gly; Ala126→Val with known crystal structure. *J Mol Biol* **258**, 732-735 (1996).



- 27 Horwich, A. L., Burston, S. G., Rye, H. S., Weissman, J. S. & Fenton, W. A. Construction of single-ring and two-ring hybrid versions of bacterial chaperonin GroEL. *Methods Enzymol* **290**, 141-146 (1998).
- 28 Fei, X. *PhD Thesis University of Maryland* (2014).
- 29 Stan, G., Brooks, B. R., Lorimer, G. H. & Thirumalai, D. Residues in substrate proteins that interact with GroEL in the capture process are buried in the native state. *Proc Natl Acad Sci U S A* **103**, 4433-4438 (2006).
- 30 Fenton, W. A., Kashi, Y., Furtak, K. & Horwich, A. L. Residues in chaperonin GroEL required for polypeptide binding and release. *Nature* **371**, 614-619 (1994).
- 31 Motojima, F., Chaudhry, C., Fenton, W. A., Farr, G. W. & Horwich, A. L. Substrate polypeptide presents a load on the apical domains of the chaperonin GroEL. *Proc Natl Acad Sci U S A* **101**, 15005-15012 (2004).
- 32 Chen, L. & Sigler, P. B. The crystal structure of a GroEL/peptide complex: plasticity as a basis for substrate diversity. *Cell* **99**, 757-768 (1999).
- 33 Stan, G., Brooks, B. R., Lorimer, G. H. & Thirumalai, D. Identifying natural substrates for chaperonins using a sequence-based approach. *Protein Sci* **14**, 193-201 (2005).
- 34 Ma, J., Sigler, P. B., Xu, Z. & Karplus, M. A dynamic model for the allosteric mechanism of GroEL. *J Mol Biol* **302**, 303-313 (2000).
- 35 Ma, J. & Karplus, M. The allosteric mechanism of the chaperonin GroEL: a dynamic analysis. *Proc Natl Acad Sci U S A* **95**, 8502-8507 (1998).

- 36 Martin, J. Role of the GroEL chaperonin intermediate domain in coupling ATP hydrolysis to polypeptide release. *J Biol Chem* **273**, 7351-7357 (1998).
- 37 Boisvert, D. C., Wang, J., Otwinowski, Z., Horwich, A. L. & Sigler, P. B. The 2.4 Å crystal structure of the bacterial chaperonin GroEL complexed with ATP gamma S. *Nat Struct Biol* **3**, 170-177 (1996).
- 38 Weissman, J. S. *et al.* Mechanism of GroEL action: productive release of polypeptide from a sequestered position under GroES. *Cell* **83**, 577-587 (1995).
- 39 Yifrach, O. & Horovitz, A. Nested cooperativity in the ATPase activity of the oligomeric chaperonin GroEL. *Biochemistry* **34**, 5303-5308 (1995).
- 40 Lorimer, G. Protein folding. Folding with a two-stroke motor. *Nature* **388**, 720-721, 723 (1997).
- 41 Yang, Z., Majek, P. & Bahar, I. Allosteric transitions of supramolecular systems explored by network models: application to chaperonin GroEL. *PLoS Comput Biol* **5**, e1000360 (2009).
- 42 Yang, D., Ye, X. & Lorimer, G. H. Symmetric GroEL:GroES<sub>2</sub> complexes are the protein-folding functional form of the chaperonin nanomachine. *Proc Natl Acad Sci U S A* **110**, E4298-4305 (2013).
- 43 Ye, X. & Lorimer, G. H. Substrate protein switches GroE chaperonins from asymmetric to symmetric cycling by catalyzing nucleotide exchange. *Proc Natl Acad Sci U S A* **110**, E4289-4297 (2013).
- 44 White, H. E. *et al.* Structural basis of allosteric changes in the GroEL mutant Arg197→Ala. *Nat Struct Biol* **4**, 690-694 (1997).

- 45 Corsepius, N. C. & Lorimer, G. H. Measuring how much work the chaperone GroEL can do. *Proc Natl Acad Sci U S A* **110**, E2451-2459 (2013).
- 46 Horovitz, A. Putting handcuffs on the chaperonin GroEL. *Proc Natl Acad Sci U S A* **110**, 10884-10885 (2013).
- 47 Fei, X., Yang, D., LaRonde-LeBlanc, N. & Lorimer, G. H. Crystal structure of a GroEL-ADP complex in the relaxed allosteric state at 2.7 Å resolution. *Proc Natl Acad Sci U S A* **110**, E2958-2966 (2013).
- 48 Monod, J., Wyman, J. & Changeux, J. P. On the Nature of Allosteric Transitions: A Plausible Model. *J Mol Biol* **12**, 88-118 (1965).
- 49 Koshland, D. E., Jr., Nemethy, G. & Filmer, D. Comparison of experimental binding data and theoretical models in proteins containing subunits. *Biochemistry* **5**, 365-385 (1966).
- 50 Yifrach, O. & Horovitz, A. Two lines of allosteric communication in the oligomeric chaperonin GroEL are revealed by the single mutation Arg196→Ala. *J Mol Biol* **243**, 397-401 (1994).
- 51 Grason, J. P., Gresham, J. S., Widjaja, L., Wehri, S. C. & Lorimer, G. H. Setting the chaperonin timer: the effects of K<sup>+</sup> and substrate protein on ATP hydrolysis. *Proc Natl Acad Sci U S A* **105**, 17334-17338 (2008).
- 52 Grason, J. P., Gresham, J. S. & Lorimer, G. H. Setting the chaperonin timer: a two-stroke, two-speed, protein machine. *Proc Natl Acad Sci U S A* **105**, 17339-17344 (2008).
- 53 Inobe, T., Makio, T., Takasu-Ishikawa, E., Terada, T. P. & Kuwajima, K. Nucleotide binding to the chaperonin GroEL: non-cooperative binding of ATP

- analogs and ADP, and cooperative effect of ATP. *Biochim Biophys Acta* **1545**, 160-173 (2001).
- 54 Rye, H. S. *et al.* GroEL-GroES cycling: ATP and nonnative polypeptide direct alternation of folding-active rings. *Cell* **97**, 325-338 (1999).
- 55 Todd, M. J., Viitanen, P. V. & Lorimer, G. H. Dynamics of the chaperonin ATPase cycle: implications for facilitated protein folding. *Science* **265**, 659-666 (1994).
- 56 Shtilerman, M., Lorimer, G. H. & Englander, S. W. Chaperonin function: folding by forced unfolding. *Science* **284**, 822-825 (1999).
- 57 Lin, Z. & Rye, H. S. Expansion and compression of a protein folding intermediate by GroEL. *Mol Cell* **16**, 23-34 (2004).
- 58 Lin, Z., Madan, D. & Rye, H. S. GroEL stimulates protein folding through forced unfolding. *Nat Struct Mol Biol* **15**, 303-311 (2008).
- 59 Madan, D., Lin, Z. & Rye, H. S. Triggering protein folding within the GroEL-GroES complex. *J Biol Chem* **283**, 32003-32013 (2008).
- 60 Lin, Z. & Rye, H. S. GroEL-mediated protein folding: making the impossible, possible. *Crit Rev Biochem Mol Biol* **41**, 211-239 (2006).
- 61 Grason, J. P. Allosterity in GroEL: Its Role in The Refolding of Protein Substrates. *PhD Thesis University of Maryland College Park* (2003).
- 62 Vinckier, A. *et al.* Atomic force microscopy detects changes in the interaction forces between GroEL and substrate proteins. *Biophys J* **74**, 3256-3263 (1998).

- 63 Horwich, A. L., Apetri, A. C. & Fenton, W. A. The GroEL/GroES *cis* cavity as a passive anti-aggregation device. *FEBS Lett* **583**, 2654-2662 (2009).
- 64 Horwich, A. L. & Fenton, W. A. Chaperonin-mediated protein folding: using a central cavity to kinetically assist polypeptide chain folding. *Q Rev Biophys* **42**, 83-116 (2009).
- 65 Horwich, A. L. Protein folding in the cell: an inside story. *Nat Med* **17**, 1211-1216 (2011).
- 66 Horwich, A. L. Chaperonin-mediated protein folding. *J Biol Chem* **288**, 23622-23632 (2013).
- 67 Schmidt, M. *et al.* Symmetric complexes of GroE chaperonins as part of the functional cycle. *Science* **265**, 656-659 (1994).
- 68 Horowitz, P. M., Lorimer, G. H. & Ybarra, J. GroES in the asymmetric GroEL<sub>14</sub>-GroES<sub>7</sub> complex exchanges via an associative mechanism. *Proc Natl Acad Sci U S A* **96**, 2682-2686 (1999).
- 69 Takei, Y., Iizuka, R., Ueno, T. & Funatsu, T. Single-molecule observation of protein folding in symmetric GroEL-(GroES)<sub>2</sub> complexes. *J Biol Chem* **287**, 41118-41125 (2012).
- 70 Sameshima, T. *et al.* Single-molecule study on the decay process of the football-shaped GroEL-GroES complex using zero-mode waveguides. *J Biol Chem* **285**, 23159-23164 (2010).
- 71 Sameshima, T., Iizuka, R., Ueno, T. & Funatsu, T. Denatured proteins facilitate the formation of the football-shaped GroEL-(GroES)<sub>2</sub> complex. *Biochem J* **427**, 247-254 (2010).

- 72 Nojima, T. & Yoshida, M. Probing open conformation of GroEL rings by cross-linking reveals single and double open ring structures of GroEL in ADP and ATP. *J Biol Chem* **284**, 22834-22839 (2009).
- 73 Sameshima, T. *et al.* Football- and bullet-shaped GroEL-GroES complexes coexist during the reaction cycle. *J Biol Chem* **283**, 23765-23773 (2008).
- 74 Koike-Takeshita, A., Yoshida, M. & Taguchi, H. Revisiting the GroEL-GroES reaction cycle via the symmetric intermediate implied by novel aspects of the GroEL(D398A) mutant. *J Biol Chem* **283**, 23774-23781 (2008).
- 75 Behlke, J., Ristau, O. & Schonfeld, H. J. Nucleotide-dependent complex formation between the Escherichia coli chaperonins GroEL and GroES studied under equilibrium conditions. *Biochemistry* **36**, 5149-5156 (1997).
- 76 Kovacs, E. *et al.* Characterisation of a GroEL single-ring mutant that supports growth of Escherichia coli and has GroES-dependent ATPase activity. *J Mol Biol* **396**, 1271-1283 (2010).
- 77 Frank, G. A. *et al.* Out-of-equilibrium conformational cycling of GroEL under saturating ATP concentrations. *Proc Natl Acad Sci U S A* **107**, 6270-6274 (2010).
- 78 Hirshberg, M. *et al.* Crystal structure of phosphate binding protein labeled with a coumarin fluorophore, a probe for inorganic phosphate. *Biochemistry* **37**, 10381-10385 (1998).
- 79 Brune, M., Hunter, J. L., Corrie, J. E. & Webb, M. R. Direct, real-time measurement of rapid inorganic phosphate release using a novel fluorescent

- probe and its application to actomyosin subfragment 1 ATPase. *Biochemistry* **33**, 8262-8271 (1994).
- 80 Brune, M. *et al.* Mechanism of inorganic phosphate interaction with phosphate binding protein from *Escherichia coli*. *Biochemistry* **37**, 10370-10380 (1998).
- 81 Rye, H. S. *et al.* Distinct actions of cis and trans ATP within the double ring of the chaperonin GroEL. *Nature* **388**, 792-798 (1997).
- 82 Gresham, J. S. Allostery and GroEL: Exploring The Tenets of Nested Cooperativity. *PhD Thesis University of Maryland College Park* (2004).
- 83 Johnson, M. L., Correia, J. J., Yphantis, D. A. & Halvorson, H. R. Analysis of data from the analytical ultracentrifuge by nonlinear least-squares techniques. *Biophys J* **36**, 575-588 (1981).
- 84 Schuck, P. Size-distribution analysis of macromolecules by sedimentation velocity ultracentrifugation and lamm equation modeling. *Biophys J* **78**, 1606-1619 (2000).
- 85 Lorimer, G. H. A quantitative assessment of the role of the chaperonin proteins in protein folding *in vivo*. *Faseb J* **10**, 5-9 (1996).
- 86 Conway, E. J. Nature and significance of concentration relations of potassium and sodium ions in skeletal muscle. *Physiol Rev* **37**, 84-132 (1957).
- 87 Kiser, P. D., Lorimer, G. H. & Palczewski, K. Use of thallium to identify monovalent cation binding sites in GroEL. *Acta Crystallogr Sect F Struct Biol Cryst Commun* **65**, 967-971 (2009).

- 88 Aoki, K. *et al.* Calorimetric observation of a GroEL-protein binding reaction with little contribution of hydrophobic interaction. *J Biol Chem* **272**, 32158-32162 (1997).
- 89 Tyagi, N. K., Fenton, W. A. & Horwich, A. L. ATP-triggered ADP release from the asymmetric chaperonin GroEL/GroES/ADP<sub>7</sub> is not the rate-limiting step of the GroEL/GroES reaction cycle. *FEBS Lett* **584**, 951-953 (2010).
- 90 Taguchi, H., Tsukuda, K., Motojima, F., Koike-Takeshita, A. & Yoshida, M. BeF(x) stops the chaperonin cycle of GroEL-GroES and generates a complex with double folding chambers. *J Biol Chem* **279**, 45737-45743 (2004).
- 91 Viitanen, P. V. *et al.* Chaperonin-facilitated refolding of ribulosebiphosphate carboxylase and ATP hydrolysis by chaperonin 60 (groEL) are K<sup>+</sup> dependent. *Biochemistry* **29**, 5665-5671 (1990).
- 92 Kuwajima, K. The molten globule state of alpha-lactalbumin. *Faseb J* **10**, 102-109 (1996).
- 93 Okazaki, A., Ikura, T., Nikaido, K. & Kuwajima, K. The chaperonin GroEL does not recognize apo-alpha-lactalbumin in the molten globule state. *Nat Struct Biol* **1**, 439-446 (1994).
- 94 Widjaja, L. Allosteric control of GroEL by ATP: effects of monovalent and divalent cations. *MS Thesis University of Maryland* (2002).
- 95 Hayer-Hartl, M. K., Ewalt, K. L. & Hartl, F. U. On the role of symmetrical and asymmetrical chaperonin complexes in assisted protein folding. *Biol Chem* **380**, 531-540 (1999).



- 96 Lin, Z., Puchalla, J., Shoup, D. & Rye, H. S. Repetitive protein unfolding by the trans ring of the GroEL-GroES chaperonin complex stimulates folding. *J Biol Chem* **288**, 30944-30955 (2013).
- 97 Jin, L. *et al.* Asymmetric allosteric activation of the symmetric ArgR hexamer. *J Mol Biol* **346**, 43-56 (2005).
- 98 Nielsen, K. L., McLennan, N., Masters, M. & Cowan, N. J. A single-ring mitochondrial chaperonin (Hsp60-Hsp10) can substitute for GroEL-GroES in vivo. *J Bacteriol* **181**, 5871-5875 (1999).
- 99 McLennan, N. & Masters, M. GroE is vital for cell-wall synthesis. *Nature* **392**, 139 (1998).
- 100 Ye, X. *PhD Thesis University of Maryland* (2014).
- 101 Monod, J. & Jacob, F. Teleonomic mechanisms in cellular metabolism, growth, and differentiation. *Cold Spring Harb Symp Quant Biol* **26**, 389-401 (1961).
- 102 Jacob, F. & Monod, J. Genetic regulatory mechanisms in the synthesis of proteins. *J Mol Biol* **3**, 318-356 (1961).